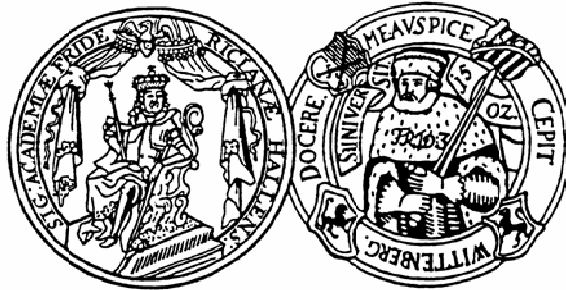


Predicting Crystal Growth Rates Using Molecular Modelling Techniques with Explicit Consideration of the Driving Force



DISSERTATION

Zur Erlangung der akademischen Grades

Doktor-Ingenieur (Dr.-Ing.)

eingereicht am

Zentrum für Ingenieurwissenschaften der Martin-Luther-Universität Halle-Wittenberg

als organisatorische Grundeinheit für Forschung und Lehre im Range einer Fakultät

(§75 Abs. 1 HSG LSA, §19 Abs. 1 Grundordnung)

von

Herrn MSc. Caner Yürüdü

Geboren am 07.09.1979, in Karaman, Türkei

Geschäftsführender Direktor des Zentrums für Ingenieurwissenschaften:

Prof. Dr.-Ing. habil. Dr. h.c. Holm Altenbach

Gutachter:

1. Prof. Dr.-Ing. Dr. h. c. Joachim Ulrich

2. Prof. Dr.-Ing. Günther Schulte

Tag der mündlichen Verteidigung: 23.07.2010

Acknowledgement

The work presented in this thesis corresponds to the results of my scientific researches which were performed during my doctoral education at the Chair of the Thermal Process Technology, Centre of Engineering Science of Martin Luther University Halle-Wittenberg.

This work represents to the most important stage of my journey. Everyone who I came across during last marvellous four years has unique contributions on the consequence of this work. Those people who joined my journey made my life easier and more meaningful. Now I would like to use this opportunity in order to express my gratitude to all those wonderful people one more time.

First of all, I would like to thank my supervisors Prof. Dr.-Ing. habil. Dr. h.c. Joachim Ulrich and Dr. Matthew J. Jones for giving me opportunity to work on the DFG project as well as their support and encouragement. Furthermore, I am also appreciated for giving me chance to represent my institute in several conferences, workshops, industrial projects and exchange programs. All the way through this period, I gained matchless experiences not only in my academic but also in my social life.

This work would not have been successful without the collaboration of valuable group members. I would like to signify my sincere appreciation to Dr. Anke Fiebig who introduced computer simulations, helped me about the theory and answered my endless questions with great patience during my learning progression. I am also appreciated to former PhD students, Dr. Ali Al-Atia, Dr. Nadine Pachulski and Dr. Isolde Trümper, who helped me while I was trying to adapt my new life.

I would like to separate another paragraph in order to express my sincere appreciation to my current colleagues who came into my life when I was close to lose my motivation for many things. I could not come to the point to write the acknowledgement for this work without the presence of the corners of my triangle: Robert Buchfink, Anke Schuster and Sandra Petersen. I cannot express my gratitude here to all of you who were with me whenever I need. Other important team members who should be named here are Anika Wachsmuth, Patrick Frohberg, Claudia Müller, other former and current members of TVT and every other friend who our way intersects somehow during last four years with. My students who accompanied me during my work deserve special thanks for excellent contributions of them. I would like to write a bit more for one of my students who is my colleague now: Christiane Schmidt has significant contribution on this thesis and she helped and sometimes forced me to regain my motivation for my work. Thank you for your helps and friendship.

Now, some more lines for my former colleagues who have contributions on my former work which assisted me to come to Germany. I would like to thank first to my former supervisor Prof. Dr. Nurfer Güngör who planted inspiration on me in order to carry out an academic work with great enthusiasm, my former team mates Dr. Sevim Isci and Dr. Ebru Günister who taught me how to perform scientific research, Prof. Dr. Nusret Bulutcu who advised and encouraged me to come to Germany, my lifetime friends Ilknur Bayrak and Selin Sunay who are other parts of me. Thank you all of you I could not do without you.

And, last but not least, my family who never give up believing me: Gecesini gündüzüne katip, Türkiyenin dört bir yanini dolasarak bizlere iyi bir gelecek hazirlamak icin usanmadan calisan babama, hayatini cocuklarına adayan ve bize bizden çok inanan anneme, agabey-kardes iliskisinden çok iki arkadaş iliskiskisine sahip olduğum ve her zaman yanımda olduğunu bildigim agabeyime ve aramiza sonradan katilmasina ragmen kısa surede ailemizin parçasi olan Özleme, bizleri kendi cocuklarından ayirmayan ve hayatim boyunca bana yol gösterip benim olmak istedigim kisi olan dayim Prof. Dr. Ekrem Ekinci ve ikinci annem Janet Ekinci'ye ve tüm sevdiklerime bu süreçteki desteklerinden ve sevgilerinden dolayı sonsuz minnetdarim. Hicbir zaman kelimeler sizlere olan sevgimi tanımlamaya yetmeyecek.

Halle (Saale), June 2010

Caner Yürüdü

1. Introduction	1
2. Crystal, Crystallization and Crystal Morphology	3
2.1 Crystal and Crystallization.....	3
2.2 Crystal Growth.....	4
2.2.1 Growth Mechanism and Morphology.....	6
2.3 Diffusion.....	15
2.4 Aim of work.....	17
3. Modelling	19
3.1 Computer Modelling in Crystallization.....	19
3.2 Molecular Modelling.....	19
3.3 Main methodology of molecular modelling in crystallization.....	29
3.3.1 Bravais-Friedel-Donnay-Harker (BFDH) Method.....	29
3.3.2 Hartman-Perdok Approach.....	30
4. Materials & Methods	34
4.1 Model Systems.....	34
4.1.1 Benzophenone [(C ₆ H ₅) ₂ CO].....	34
4.1.2 Hydroquinone [C ₆ H ₄ (OH) ₂].....	35
4.1.3 Benzoic Acid [C ₆ H ₅ COOH].....	36
4.2 Methodology of simulations.....	37
4.2.1 Computer Simulations.....	40
5. Results	42
5.1 A general look at the “results” chapter.....	42
5.2 Molecule structure optimization.....	42
5.2.1 Benzophenone.....	43
5.2.2 Hydroquinone.....	44
5.3 Morphologies of the substances.....	45
5.3.1 Benzophenone.....	46
5.3.2 Hydroquinone.....	49
5.3.3 Benzoic Acid.....	54
5.4 Diffusion coefficient calculations.....	58
5.4.1 Diffusion coefficient calculations for the pure solute system.....	59
5.4.2 Diffusion coefficient calculations for the solute-solvent system.....	63
5.4.3 Diffusion coefficient calculations for the solid-liquid system.....	70

6. Discussion	75
6.1 A general look at the “discussions” chapter.....	75
6.2 Molecule structure optimization.....	76
6.3 Morphologies of the substances.....	77
6.3.1 Benzophenone.....	78
6.3.2 Hydroquinone.....	81
6.3.3 Benzoic Acid.....	83
6.4 Diffusion coefficient calculations.....	84
6.4.1 Diffusion coefficient calculations for the pure solute system.....	85
6.4.2 Diffusion coefficient calculations for the solute-solvent system.....	89
6.4.3 Diffusion coefficient calculations for the solid-liquid system.....	93
6.5 Conclusions.....	102
6.6 Outlook.....	105
7. Summary	107
8. Zusammenfassung	110
List of Symbols	114
References	117

Selbständigkeitserklärung

Lebenslauf

Publikationsliste

1. Introduction

The rapid developments in the natural sciences in recent years necessitate a more fundamental approach to engineering sciences in order to translate the potential of physics, chemistry, materials science and biology to mass-produced goods and real-life applications. Industrial crystallization is a good example on how product properties drastically depend on small changes on fundamental data and the ambient situation of processing conditions. Computer based simulations can help finding fast development routes which nowadays are done dominantly as screening work in experimental studies – timely and costly – in the laboratory. The advantage of computer based simulations is also convincing for the habit prediction of crystals. This process is kinetically controlled and up to date not fully resolved. The crystal habit is a consequence of face growth rates of a crystal. The theoretical framework describing crystal growth was conceived by these simple computational methods which, however, only take into account the solid side of a crystal. These simple methods are not capable of describing the correct crystal habit in the presence of external factors such as different supersaturation solvent interactions or additives. Effects of crystal environments, however, cannot be ignored when it is the interest to obtain a more realistic crystal habit by calculation. Modified methods adopt in principle the findings of parameters that show a trend of regular changes in the presence of additives or external effects based on detailed crystallographic knowledge. Since crystal growth depends upon mass transport to the surface of the crystal whenever crystal growth occurs in solution, it is reasonable to assume that a quantitative description of the mass transport at the solid liquid interface can give useful insight concerning the calculation of face growth rates. If crystallization takes place in the melt, consideration should be focussed on heat transfer. Such approaches have to be incorporated into existing software program packages for the simulation of crystal habits which are up to date based only on simulations of the solid side of the growing crystal.

In this work it is the aim to adapt classical molecular dynamics simulations in order to access information on the molecular transport at the crystal liquid interface. Simulations involve the determination of effects of thermodynamics. Molecular dynamics simulations are employed to study diffusion coefficients. Molecular dynamical methods provide suitable tools in order to simulate the physical properties for a large group of systems. However, in this work the aim is to define only transport properties of organic systems and to perform the relevant calculations for it. Benzophenone and hydroquinone were selected as test systems because of their wide area of application and high number of literature data available. Computer

simulations are performed taking into consideration the characteristic physical properties of the materials, such as solubility, density, boiling and melting points.

A short overview of the crystallization theory is given in the second chapter. In third chapter earlier theories of the computational methods, their physical backgrounds and drawbacks are summarized. Definitions of the calculation method, physical and chemical properties of the materials are specified in chapter four. Findings of the simulations are presented in the “results” section. The starting geometries of the crystals or molecules were also investigated in some detail and the findings are given in the “results” chapter. It was found that geometry optimization of the molecule geometry has some effect on the results of the dynamic simulations are carried out. A one component system is considered a melt and computer experiments are performed on the system. Characteristic changes of the transport parameters depending upon variations in the external factors, such as temperature level, simulation time, number of molecules in the amorphous cell, and force fields used in the simulations. After acquiring enough simulation experience and eliminating unsuitable system conditions a solution (solute-solvent) was simulated and effects of changes of other system parameters such as supersaturation level were investigated. The data obtained from these simulations are used to calculate the transport properties of the molecules under the given conditions and are compared to the results of the empirical equations which are available in the literature.

After the determination of the transport properties of the selected systems the calculation of the transport properties in the presence of a crystal surface was investigated. The presence of crystal surface leads to small changes in the methodology of calculation because in the presence of a crystal surface the symmetry of all the systems breaks down. Data obtained from these simulations producing diffusion coefficient values are used to correlate to the calculations of face growth rates by considering the ambient system conditions. Finally, depending upon the values of the mass transfer coefficients, the process controlling solution growth is defined and face growth rates are calculated depending upon the process which limits the face growth.

Evaluation and compatibilities of the results are given in the “discussions” chapter. For the limited conditions the growth rate of single crystal faces is calculated by considering the transport properties of the solute molecules to the solid surface. Drawbacks of the theory are addressed and in order to cover larger applications further possibilities are indicated in the “discussions” chapter.

2. Crystal, Crystallization and Crystal Morphology

2.1 Crystal and Crystallization

A *crystal* is a form of matter wherein its atoms and/or molecules are regularly arranged in a definite structure. The external form of the solid is symmetrically arranged by plane faces. The crystals have the same faces present and the same initial structure, however, the relative areas of the faces might be different, thus resulting in a different external habit. It means the relative area of the crystal faces have a major impact on the external habit, even though the internal structure is the same. It is possible to give a clear description with the characteristic geometrical properties such as the lengths of the axes in the three directions, the angles between the faces or the shape factor of the crystal. Those faces present might not even be the same for two crystals of the same substance with the same internal structure. Such differences are due to the fact that the external habit of a crystal is controlled not only by its internal structure, but also by conditions at which the crystal grows. This interesting fact attracts attention of researches for years. The rate of growth is dominantly affected by external factors such as supersaturation, temperature, fluid flow conditions and solvents or impurities.

Understanding crystallization requires the knowledge of both the internal structure of the crystals, that is, how the atoms and molecules are arranged within their lattice structure and the external appearance of the crystals which is referred as the *crystal habit* or *crystal morphology*. Crystal morphology defines the interactions between a molecule or an ion and their neighbours in the crystal and indicates the changes of crystal structure considering these conditions. The morphology of organic crystals is particularly important in industrial applications. It plays a major role in their storage, handling, drying and end-use properties because it affects the efficiency of down-stream processes and influences the material properties. The whole process of crystal formation is called *crystallization*.

Theoretically, crystallization starts when the concentration of a compound in a solvent is higher than the solubility of this compound. Crystallization is often kinetically hindered and crystals grow only from sufficiently high supersaturated solutions. *Supersaturation* is defined as the presence of more solute in solution than would exist at equilibrium and it is the driving force for the crystallization process. A supersaturated solution is not at equilibrium and there are several ways to achieve supersaturation. According to thermodynamics supersaturation can be reached by the changes of temperature, pressure or concentration. In order to relieve the supersaturation and move towards to equilibrium, the solution crystallizes. It means,

supersaturation in a solution with seeds or by forming nuclei causes the mass transfer of solute from the solution onto the surfaces of individual crystals or nuclei. Once crystallization starts, however, the supersaturation is reduced by nucleation or crystal growth, respectively.

2.2 Crystal Growth

When a nucleus is formed, by the nucleation procedure, it is the smallest sized crystalline entity that can exist under a given set of conditions. However, immediately after the formation of nuclei, they begin to grow. The growth takes place larger through the addition of solute molecules to the crystal lattice. This part of the crystallization process is known as *crystal growth*. Crystal growth theories differentiate in terms of growth mechanism according to the different operation conditions. Therefore, many possibilities have to be considered such as the nature of the fluid phase (melt, solution, vapour), the stable or unstable nature of the growth process, the growth mode (layer by layer, continuous, step flow, spiral), the growth rate (linear versus non-linear in the disequilibrium chemical potential difference), etc.

When crystal growth is viewed from a mechanistic point of view, it is necessary to look at the growth of a particular crystal face. The crystal growth process involves the incorporation of growth units into the crystal lattice. These growth units can be molecules, atoms, or ions, depending upon the type of substance and type of crystal being grown. The growth can be carried out by solidification from an undercooled melt, growth from supersaturated solution, or condensation from a vapour phase [Lan06]. The molecules in the melt, solution or vapour state require a driving force for transport, through convection or diffusion, from the liquid phase to the crystal surface. The major difference between the industrial (mass) crystal growth and single crystal growth is the requirement concerning the growth environment where the crystals grow.

Depending upon the magnitude of the driving force, the amount of impurities and the growth environment, the growing crystal surface can become different in nature (rough or smooth). In addition temperature, pressure and concentration gradients can play a significant role on final crystal morphology. The important factors for the crystal growth differ according to the media in which a crystal grows. Whenever the expression “solution” is used the mass transfer effects should dominate a process. Whenever the heat transfer is dominating a process of liquid solid phase change it should be called “melt” crystallization. The choice of words is a historical issue. If the phase diagrams are carefully examined, it can be concluded that in the case of a two component system, there is no difference between a solution and a melt. Solubility

diagrams from the field of solution crystallization are always a part of the complete phase diagram.

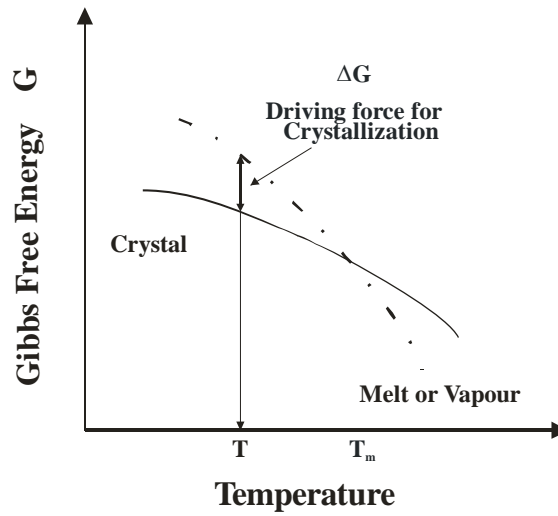


Figure 2.1: The Gibbs free energies as a function of temperature for solid and fluid phases [Lan06].

The growth mechanism also needs to be examined from the viewpoint of thermodynamics and kinetics in order to apprehend how the crystal growth can proceed and which form will develop.

An excess Gibbs free energy, ΔG , in other words a supersaturation, σ , is required to reach a first order transition from the liquid phase into a solid phase.

$$f = -\frac{\Delta G}{V} = \frac{kT \ln(1+\sigma)}{V} \sim \left(\frac{kT}{V}\right)\sigma \quad (2.1)$$

Where f is the driving force per unit area, V is the volume per molecule, k is the Boltzmann constant, T is the absolute temperature and σ is the dimensionless supersaturation defined as $\sigma = P / P^{sat} - 1$ for the gas phase and $C / C^{sat} - 1$ for the solution phase; P is the partial pressure and C the solution concentration. For nucleation and growth to take place the driving force needs to be larger than the minimum *activation energy* which is the energy value in order to enable the process to proceed according to the thermodynamics. The activation energy consists of the surface energy for forming a new surface and the barrier for diffusion and surface integration. For the growth of a single crystal, the supersaturation is usually kept small to avoid parasitic nucleation. Therefore, $\ln(1+\sigma)$ approaches σ and the driving force is proportional to supersaturation as shown in equation 2.1. In order to grow a single crystal often an oriented seed is used. Self seeding could also be used but then the control of the numbers of nuclei is impossible. Furthermore, the environment should be carefully controlled

so that the supersaturation or supercooling is kept small and exists only around the growing crystal. With a given driving force the growth rate depends upon the growth mechanisms and properties of the growing interface. The crystal morphology is determined by the interfacial energies and growth kinetics.

2.2.1 Growth Mechanism and Morphology

As crystal growth proceeds through the transport of the solute molecules to the crystal surface the newly formed surface could be smooth or rough depending upon the growth conditions. At absolute zero temperature a surface at equilibrium does not have growth steps. At higher temperature, there are adatoms owing to thermal energy, and the adatom density, ρ_a , can be described by the Gibbs formula (eq. 2.2):

$$\rho = \exp\left(-\frac{\Delta G}{kT}\right) \quad (2.2)$$

Where ΔG is the Gibbs free energy needed to extract an atom from making it an adatom. In order to estimate the transition from a different point of view, Jackson [Jac58] introduced the α factor that takes the contact nature of the solution and the surface into account:

$$\alpha = \left(\frac{\Delta H}{kT}\right) f_k \quad (2.3)$$

Where ΔH is, the latent heat, the amount of the energy released or absorbed by a substance during a change of state which occurs without changing its temperature. f_k is a crystallographic factor representing the fraction of all neighbours lying in parallel to the crystal surface. At a large α factor ($\alpha > 2$) the surface is almost smooth owing to the strong bonding energy as compared to the thermal fluctuation. There are also other advanced computational approaches to predict the surface roughness. Nevertheless, Jackson's α factor provides estimations on surface quality. Growth kinetics changes depending upon the newly formed surface structure:

When the *surface is smooth*, the crystal faces or singular surfaces are corresponding to a minimum surface energy which determines the final form of a growing crystal. The criterion for crystal shape according to Gibbs's method for a crystal containing faces is given by:

$$\min \sum_i \gamma(n_i) A(n_i) \quad (2.4)$$

Where $\gamma(n_i)$ is the surface energy and $A(n_i)$ the area of a crystal face of the orientation n_i . The geometry features the shape of the crystal that minimizes the surface free energy. According

to the Wulff theorem [Ben93] the length of a vector l_i drawn normal to a crystal face A_i will be proportional to its surface energy:

$$\gamma_i \cdot l_i = \lambda \gamma_i \quad (2.5)$$

Then, the smallest polyhedral bounded by the tangent planes having the smallest volume at $\sum_i l_i A(n_i)/3$ is the equilibrium shape of the crystal. Unfortunately, the nature is not so simple, because crystal grows at nonequilibrium conditions. The driving force is inversely proportional to l_i , when the crystal is small, the driving force back to the equilibrium is high. Therefore, the equilibrium shape of a small crystal could be maintained:

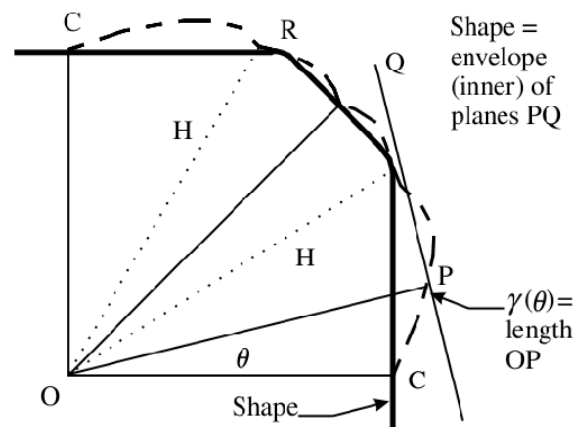


Figure 2.2: *Equilibrium shape of a crystal and competition of the faces. Singular faces OC always present in equilibrium; higher energy faces (OH) may not be present [Kla09].*

Due to the non-equilibrium nature of crystal growth the Wulff form is usually not produced. However, Wulff's method is one of the fundamental bases for the calculation of morphology with computer simulations and it gives a rough idea on the possible habit of a crystal. A crystal which is stored in a saturated solution for a long period of time will, however, transform into the equilibrium form with time through solvent mediated dissolution and re-growth of the crystal faces. This is known as *aging process* and has been reported by a number of investigators (e.g. [Mye99]). For smooth faces another common method of describing the crystal shape is using a shape factor. Area and shape factors are defined as:

$$V = \alpha L^3 \quad (2.6)$$

$$A = \beta L^2 \quad (2.7)$$

Where L is the characteristic dimension of a crystal, V is the volume and A is the total surface area. Shape factors for common geometrical systems can be found in literature [Nyv85].

Shape factors are employed in the analysis of crystal size distribution data because measurement methods measure a characteristic dimension of a crystal and must be related to the actual crystal shape in order to produce an accurate representation of the distribution that can be used in modelling of industrial systems.

Crystal habit can change dramatically as a function of the rate of crystal growth and its growth environments. Identical substances might have different crystal habits under different conditions. This can be explained by the fact that the smallest faces on a grown crystal are the fastest growing faces, while the largest faces are the slowest growing. The fast growing faces grow so rapidly that they effectively disappear on the final morphology of the crystal. Impurities might change the habit of crystals through specific interactions with particular crystal faces, thus retarding the growth rate of these faces. This can result in faces appearing or disappearing.

Solvents might have similar effects as impurities on the crystal habit. Changing solvents can therefore also result in a change in the crystal habit because the specific solute-solvent interactions might not be similar with different solvents. The role of solvents on the crystal habit was thermodynamically analysed by Jackson [Jac58] who defined a surface entropy factor that could be related to the growth mechanism.

When the *surface is rough* the growth kinetics is usually simple because the growth sites are randomly distributed. For such a case, the growth rate is, in general, proportional to the local driving force. However, in reality the crystal surface consists of steps, with terraces and kinks, as well as growth units and vacancies. This can be visualized by a Kossel type of crystal, Figure 2.3 [Kos34, Oha73, Str28]. A growth unit can be incorporated into the crystal with one of the surface sites. The first type of site is a flat surface which is atomically smooth. If a growth unit (Figure 2.3) attempts to become incorporated at this site, it can bond in only one contact side. A step provides two contact sides for the growth unit to bond the crystal, while kink site provides three contact sides in which the growth unit can bond. From an energetic point of view, kink sites are the most favourable sites since there is additional volume of the crystal created without creating new surface. The step sites are the next favourable positions. This is translated into a crystal growth mechanism by which molecules is absorbed by the surface and diffuse along the surface until they are incorporated into the lattice at step or kink site.

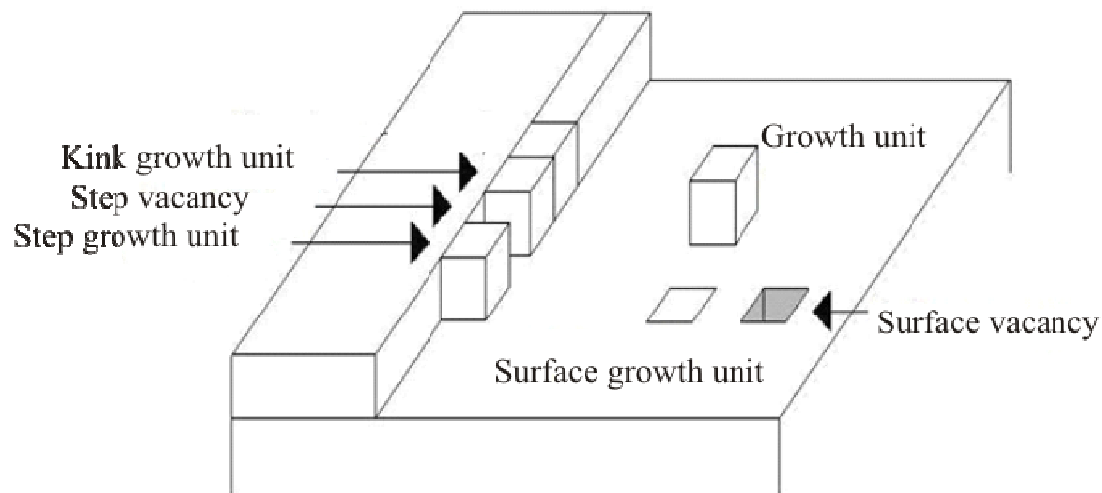


Figure 2.3: *Surface structure of a growing crystal, Kossel type of surface.*

The simple step model with the surface diffusion could lead to a simple linear law for growth, i.e., the growth rate is linearly proportional to the supersaturation and similar to the one in the rough surface formed by kinks. However, when the surface is almost smooth, the kinetics depends on the growth mechanisms. As soon as step growth is completed, almost the smooth surface requires a new two-dimensional nucleation for the next layer growth. The major problem with all these models of this type is that surface nucleation is the rate determining step. Hence, a surface nucleus must form in order for crystal growth to occur. Since there is a free energy barrier for the formation of the surface nucleus which requires significant supersaturation these models all predict that crystals will not grow at low supersaturations. Details of methods and drawbacks were described thoroughly in several references (e.g. [Oha73, Mye02]).

Drawbacks of the theories were mentioned above caused new efforts in order to explain growth mechanisms. Based on the spiral growth of the screw dislocation, Burton, Cabrera and Frank proposed a model (BCF) [Bur51] considering the transport of solute molecules from the bulk solution to surface, and then surface diffusion to the kinks of the spiral generated steps from a screw dislocation (Figure 2.4).

Molecules absorb on the crystal surface and diffuse to the top step of the two planes of the screw dislocation. The surface becomes a spiral staircase. After a layer is complete, the dislocation is still present, it is just a layer higher. Using this idea surface nucleation is not required for growth. The BCF theory also predicts a quadratic kinetics at low supersaturations on the contrary to other growth mechanisms such as two dimensional nucleation theories. Derivations of this theory can also be found in several references (e.g. [Oha73, Che84, Nyv85]).

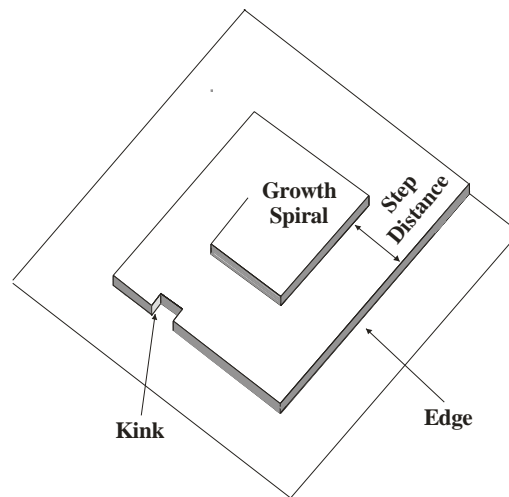


Figure 2.4: *Spiral growth on a macroscopically flat face [Win00].*

The BCF theory has been quite successful in comparison with experimental observations and measurements [Ben73]. The typical growth rate curves based on different growth models are shown in Figure 2.5.

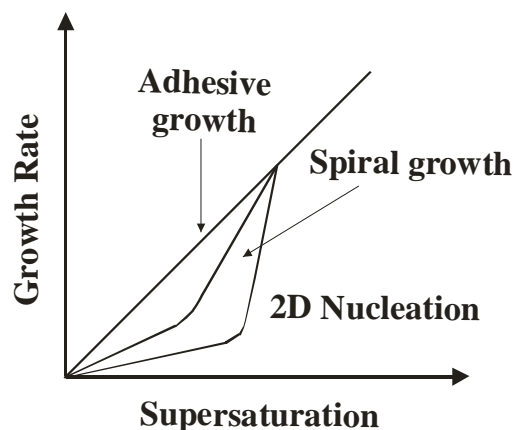


Figure 2.5: *Growth rate dependence on the supersaturation for various growth models.*

The growth on the kinks or rough surfaces is referred as adhesion growth. With the consideration of multiple screws it can be come out a more complicated kinetic behaviour. The BCF model was derived for the case in which surface diffusion is the rate determining step in the crystal growth process. This is true in growth from the vapour phase. However, in solution growth, diffusion of the solute from the bulk liquid phase to the crystal liquid interface can often be the rate determining step. Chernov [Che61] developed a model employing the screw dislocation of the BCF model with bulk diffusion consideration. In this model, diffusion of solute molecules through a boundary layer is the rate determining step. The results predicted by Chernov's method are similar to the results by the BCF model with the added condition that the growth rate is a function of the boundary layer thickness, which

is a function of the fluid dynamic conditions. This theory showed that growth rate decreases with an increase in boundary layer thickness. This is an important result since the boundary layer thickness is directly related to fluid dynamic conditions and stirring rates. The Chernov bulk diffusion model provides an important link between the crystal growth theories and the practical world of industrial crystallization where fluid flow and agitation are important.

Other more complex models based on the BCF theory in which surface and bulk diffusion limitations are treated in series and in parallel, have also been developed (e.g. [Gil71]). These models are mathematically complex and are described in detail in the literature (e.g. [Gil71, Ben69]). One important result of these models is that if the relative velocity between a crystal and the solution is increased, the growth rate will increase to a maximum value and then will remain constant. The maximum value is obtained when only surface diffusion limits growth. In the literature, this is known as a growth *limited by interfacial attachment kinetics*. When the crystal growth rate can be changed by changing fluid dynamics conditions, it is known as a *mass transfer limited growth* [Mye02].

Chernov showed in bulk diffusion models that the diffusion of the solute in the boundary layer and the boundary layer thickness can play a significant role in controlling crystal growth rate. A simple method which focuses on the diffusion of solute through the boundary layer is known as the *diffusion layer model*. Generally this method is used to correlate the data for industrial crystallization processes. The definition of the boundary layer is currently difficult to model by computer simulations. However, in order to highlight the importance of diffusion on the crystallization mechanism in industrial applications the theory is briefly described here.

When a crystal is growing from a supersaturated solution solute molecules leave the solution at the bulk and become a part of the crystal. This will deplete the solute concentration in the region next to the crystal liquid interface. In other words, since the concentration of the solute at the bulk is higher than at the surface, solute will diffuse to the crystal surface. The concentration of the solute continuously increases from the value at the interface to the value in the bulk solution. The region where the concentration is changing is called the *concentration boundary layer* (there is also a momentum and thermal boundary layer). The distance from the crystal surface to the region where the concentration of the bulk is called the *boundary layer thickness*.

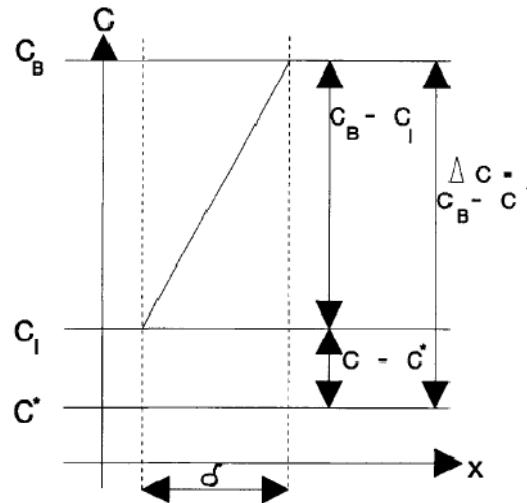


Figure 2.6: A schematic representation of the concentration profile near a growing crystal according to Myerson [Mye02].

For the single one dimensional case shown in Figure 2.6 the rate of mass increase of the crystal can be equated to the diffusion rate through the boundary layer through the expression:

$$\frac{dm_c}{dt} = DA \left(\frac{dC}{dx} \right) \quad (2.8)$$

Where A is the surface area of the crystal and D is the diffusion coefficient. The concentration versus position in the boundary layer can be written as:

$$\frac{dC}{dx} = \frac{C - C_i}{\delta} \quad (2.9)$$

Where δ is the boundary layer thickness, C and C_i are the bulk and interfacial concentrations, respectively. The rate of solute integration into crystal surface can be approximated by:

$$\frac{dm_c}{dt} = k_i A (C - C_i) \quad (2.10)$$

Where k_i is the rate constant. For example: $k_d = D/\delta$ is the diffusion rate constant.

$$\frac{dm_c}{dt} = K_G A \Delta C \quad (2.11)$$

Where K_G is defined as:

$$\frac{1}{K_G} = \frac{1}{k_d} + \frac{1}{k_i} \quad (2.12)$$

When $k_d \ll k_i$, the crystal growth rate will be diffusion controlled and $K_G = k_d$. When $k_i \ll k_d$, the crystal growth rate will be controlled by the rate of solute incorporation into crystal. Constants in these equations are obtained from experimental data.

According to the thickness of the boundary layer, growth rate can be diversified by considering mass transport controlled growth [Kar02]. Considering Fick's law, it will be a linear growth rate:

$$R_G = \frac{4D}{\rho_c} \left(\frac{1}{L} + \frac{1}{2\delta} \right) (C - C_i) \quad (2.13)$$

Where L is the crystal size (edge length or diameter).

When the diffusion layer thickness is large compared to the crystal size ($2\delta \gg L$), eq 2.13 can be reduced to:

$$R_G = \frac{4D}{\rho_c L} (C - C_i) \quad (2.14)$$

When the diffusion layer thickness is small compared to the crystal size ($2\delta \ll L$), eq. 2.13 can be reduced to:

$$R_G = \frac{2D}{\rho_c \delta} (C - C_i) \quad (2.15)$$

In order to avoid the uncertainty in determining the diffusion layer thickness, the following semi empirical engineering model is often used:

$$R_G = \frac{2k_d}{\rho_c} (C - C_i) \quad (2.16)$$

For mass transport associated with suspended crystals in an agitated solution, bulk diffusion often involves molecular diffusion and convective transport. For spheres and other simple geometric shapes, k_d can be correlated by the Frössling equation [Fro38]:

$$Sh = 2 + 1.10 Re^{1/2} Sc^{1/3} \quad (2.17)$$

Where $Sh = k_d / D$ is the Sherwood number, $Re = u_s L \rho / \mu$ is the Reynolds number, u_s is the particle slip velocity, ρ is the solution density, μ is the solution viscosity, and $Sc = \mu / \rho D$ is the Schmidt number.

The first term on the right hand side of eq. 2.17 represents the contribution of molecular diffusion, and the second term represents the contribution of convective transport. For the very small particle sizes associated with the sparingly soluble precipitates, the suspended phase tends to move with no slip along with the circulating fluid (i.e., $u_s = 0$). In this case, the effect of convective transport is negligible and bulk diffusion occurs mainly by molecular diffusion.

$$Sh = k_a L / D = 2 \quad (2.18)$$

Substitution of eq. 2.18 into eq. 2.16 gives eq. 2.14 which describes diffusion controlled growth in an infinite diffusion field. Such a relationship is appropriate to describe growth of very small crystals such as those produced during a precipitation process. It should be emphasized that eq. 2.14 is applicable only if the diffusion fields around separate crystals do not influence each other and may be taken to be infinite in extent. This will be the case if the distance between the crystals is greater than about 20 particle diameters. When the distance between the crystals is less than 20 particle diameters, the diffusion fields around the individual crystals begin to influence each other [Kar02].

Both the bulk diffusion process and the surface integration process influence crystal growth depending upon the process conditions. When bulk diffusion dominantly effects the growth mechanism eq. 2.14 defines the growth rate. When surface integration dominantly affects the growth mechanism well known screw dislocation mechanism defines the growth rate (eq. 2.19).

$$R_G = k_i (C_i - C_{eq})^m \quad (2.19)$$

In order to manifest a general way of growth rate mechanism these two equations were combined [Liu71] in order to eliminate the interface solute concentration. For high supersaturation the surface integration process was assumed first order ($m=1$). A growth rate expression which involves both bulk diffusion and surface integration can be given by:

$$R_G = \frac{g}{1 + \xi L} \quad (2.20)$$

Where

$$g = K_G (C - C_{eq}) \quad (2.21)$$

and

$$\xi = \rho_c K_G / 4D \quad (2.22)$$

Eq. 2.21 represents a size dependent growth rate which is not existed in reality [Ulr90], but can describe many experimental results quite good when surface integration is dominating. The parameter ξ represents the ratio of the relative resistance of bulk diffusion to surface integration so that when $\xi L \ll 1$ growth is controlled by surface integration and when $\xi L \gg 1$ by bulk diffusion [Mye02].

2.3 Diffusion

As it can be seen from the fundamental crystal growth theories, the diffusion mechanism is rather important to understand the real mechanism of not only crystal growth but also many chemical engineering processes. Diffusion models are still lacking accuracy, while highly sophisticated models have been derived for the other physical properties. Even though, there are already a few sophisticated methods existing [Fic55, Max52, Wil55], the development of diffusion models only recently have increased attention.

At molecular level *diffusion* is the relative motion of individual molecules in mixtures and their random, irregular movements which can be induced by thermal energy, temperature gradients, pressure gradients, concentration gradients. In an ideal case a diffusive particle is considered to travel with a constant velocity along a straight line until it collides with another molecule and this result in a change of its velocity and direction. This kind of collisions causes the molecules to move in a cursory path. Since the number of collisions is a function of the density diffusion rates in liquids are much smaller than in gases. Right along with density, pressure and temperature changes effect the molecule movement, hence, it results changes at diffusion rate.

At first, the diffusion coefficient was described by Fick [Fic55] as the diffusion flux of a species to be proportional to its concentration gradient times a proportionality constant. At similar time, Maxwell and Stefan [Max52] described the diffusion flux in terms of gradients in activities from the kinetic gas theory, and later extended it to liquid systems. It is called the Maxwell-Stefan diffusion coefficient. For a binary mixture the two models, Fick diffusion gradient and Maxwell-Stefan diffusion gradient, can be correlated with a correction factor. Hence, modelling of diffusion fluxes is shifted towards the accurate determination of diffusion coefficients. Detailed information on diffusion gradients can be found in related articles and well structured reviews (e.g. [Bos05, Rut92]).

Diffusion coefficients can be determined either experimental or by empirical methods. In this work, using empirical diffusion coefficient values the determination of organic molecule diffusion coefficient is aimed by using computer simulations. As the number of diffusion coefficient data published in literature is limited, the development of diffusivity models is highly desirable. A comparison between the Fick's law and the Maxwell-Stefan equation reveals that expressions for the Maxwell-Stefan approach are to be preferred because of its simplistic nature. For example, the Maxwell-Stefan approach separates thermodynamics and mass transfer while the Fick diffusivity accounts for both effects in one coefficient. Many other important diffusion coefficient calculation methods are the optimized version of the Maxwell-Stefan approach [Li01, Rut92]. They employ additional parameters and physical properties in order to improve the accuracy of prediction such as fluid dynamic theories, kinetic theory, statistical mechanics, and absolute reaction theory. The majority of the models are founded based on the Stokes-Einstein equation. Within this approach, the diffusivity is related to the solute size and viscosity. One of the most representative modifications is Wilke-Chang equation [Wil55]:

$$D_{AB} = (7.4 \cdot 10^{-8}) \frac{(\varphi \cdot M_B)^{1/2}}{\eta_B \cdot V_A^{0.6}} \quad (2.23)$$

Here, φ is a factor accounting for association of the solvent and V is the molar volume of the solute. The other parameters take their usual meaning.

Even though, widely accepted, it must be stressed here that this model is, in its original form, not suitable for diffusivity predictions if water is the solute component [Bos05]. However, this situation was improved by simply applying a different constant for the water as correction factor [Koo02].

Another method to calculate empirical diffusion coefficient is the method of the Dullien (eq. 2.24, [Dul63, Ert73]).

$$D_{AB} = (0.107 \cdot 10^{-16}) \frac{V_c^{2/3} RT}{\mu \cdot V} \quad (2.24)$$

Here, V_c is the critical volume, μ the liquid viscosity, V the molecular volume, R is the gas constant, and T is the liquid temperature. The value of the critical volume is calculated by the critical property estimation method, of Joback *et al.* [Job87]. A current overview on empirical diffusion coefficient methods can be found in the literature [Igl07].

Diffusion is a kind of parameter which is rather important for different disciplines such as crystallization. Since current crystal growth theories are based on the diffusion of growth elements to the crystal surface and their diffusion, migration, on the crystal surface. Hence, understanding the diffusion behaviour of the growth elements in every different zone has quite an importance in order to understand the nature of the crystal growth. Even some researchers tried to find out relations between surface diffusion and molecular diffusion experimentally [Miy01]. Current computer technologies have considerably powerful calculation tools. Hence, benefits of computational methods to new model developments with the aid of computers are reasonably increased.

2.4 Aim of work

Considering the entire crystallization process there are still many facts and problems need to be answered. In order to uncover the crucial answers intensive researches, either theoretical or experimental, have to be done. Therefore, this study aims to clarify a part of these unanswered questions according to the centre of attention. Main important items can be aligned as:

- A large number of studies have already been implemented in order to determine factors that control the morphology and purity of crystals grown from solution or melt. Particularly, crystallization kinetics has to be measured, especially, those in the presence of additives or impurities. This lowers the time consumption and high laboratory costs.
- Computer simulations can help to explain the effects of impurities and to find the right additives in order to get the desired crystal habit. Time and cost consumption for the laboratory work can be reduced.
- A lot of models are already developed in order to find relations between the crystal lattice and the crystal morphology. Nevertheless, none of these approaches explains fully the detailed mechanism by which a crystal grows. Up to date, computer simulations – in the commercially available form – generally only consider the solid side of the crystal growth process. Since the liquid side in the crystal growth process has great importance, the existing computer simulation tools for crystal growth have to be enlarged by considering the liquid side and its effects.
- Diffusion is one of the deterministic steps of crystal growth mechanism. Understanding diffusion by calculation of diffusion coefficient for different system conditions, aids to be informative on the possible role of a molecule in growth mechanism. For instance, the growth mechanism can be more understandable by

determination of the contribution of a molecule to the growth mechanism by its importance in diffusion to the crystal surface (diffusion controlled crystal growth) or on the crystal surface (surface integration controlled crystal growth). For this purpose computation of the diffusion coefficient of organic molecules in the presence of solvent molecules and determination of changes on the diffusion in the amorphous cell by using modern computer techniques is aimed for.

- Designing correct simulation conditions for specific organic molecules lead to a simulation of the diffusion properties of the molecules according to the structural properties. Results can be evaluated with empirical equations in the absence of experimental results.
- Even though, the role of diffusion on growth mechanism was already defined theoretically, growth conditions which limit the growth mechanism and growth rate of the solid surface have to be visualized by computer simulations.
- Useful theoretical investigations have to be linked with real life applications. For this purpose, associations of theoretical results have to be implemented with existing engineering approaches.
- A road map to find the way from the chemistry of a compound to the crystal growth purely by simulation is still missing.
- An example to demonstrate that it is possible to follow such a road map is also missing in literature up to date.

3. Modelling

3.1 Computer Modelling in Crystallization

Many problems in the field of solid state can be solved by using computer simulation methods. The most important areas of investigation are crystal growth and crystal habit calculations and the study of crystal structures. Computer simulation methods which simulate crystal structure and habit can be classified into two main methods: quantum mechanics methods and classical molecular modelling methods (also called molecular mechanics methods or Force Field methods). Both methods get assistance from different codes of theoretical physics. While quantum mechanical methods deal with laws of quantum mechanics, molecular mechanical methods employ laws of classical mechanics. Quantum mechanical methods deal with the electrons in the system, so that even if some of the electronic interactions are ignored a large number of particles must still be considered, and the calculations might be time consuming in some cases. Molecular mechanical methods ignore the electronic motions and calculate the energy of a system as a function of the nuclear positions only. Thus, it is generally used to perform calculations on systems containing significant numbers of atoms and using transferability properties of molecular mechanical computer simulation methods can be applied to a much wider range of problems. Moreover, parameters developed from data on small molecules can be used to study much larger molecule systems. In some cases molecular mechanics methods can provide answers that are almost as accurate as even the quantum mechanical methods, in a fraction of the computer time. However, molecular mechanical methods cannot provide properties that depend on the electronic distribution in a molecule [Lea01]. Therefore, charge calculation is one of the most important procedures in molecular mechanical methods.

3.2 Molecular Modelling

A principal tool in the theoretical study of molecules is the method of molecular dynamics simulations (MD). This computational method calculates the time dependent behaviour of molecular systems and it is routinely used to investigate the structure, dynamics and thermodynamics of the wide range of molecule types. The molecular dynamics methods were firstly introduced by Alder and Wainwright [Ald57] in the late 1950's in order to study the interactions of hard spheres. The first molecular dynamics simulation of a realistic system was performed by Stillinger and Rahman [Sti74] in their simulation of liquid water. The number of simulation techniques has greatly expanded, now many specialized techniques for

particular problems exist in literature including mixed quantum – classical mechanical simulations such as semi-empirical methods *AM1*, *PM3*, *PM5* and full quantum mechanical such as *ab initio*, *Density functional theory (DFT)*, *Hartee-Fock (HF)* [For06].

Molecular dynamics simulations generate information at the microscopic level, including atomic positions and velocities. The conversion of microscopic information to macroscopic observables such as pressure, energy, heat capacities, etc., requires statistical mechanics. Statistical mechanics is one of the fundamental disciplines which investigate the properties of the molecular systems and the most updated tool to perform is molecular dynamics. In order to apprehend the theory behind the molecular dynamics, statistical mechanical grounds are given here very briefly. Detailed information on the statistical mechanics is not aimed in this study and can be found in an excellent book [Lan80].

Statistical mechanics is one of the branches of physical sciences which studies macroscopic systems from a molecular point of view. The main aim of statistical mechanics is to understand and predict macroscopic phenomena from the properties of individual molecules which create the system. In a molecular dynamics simulation, it is desired to explore the macroscopic properties of a system through microscopic simulations, for example, to calculate the changes in the binding free energy of a particular candidate, or to examine the energetic and mechanisms of conformational change. Statistical mechanics which provides the mathematical expressions that relate macroscopic properties to the distribution and motion of the atoms and molecules of the N-body system. Molecular dynamics simulations provide the means to solve the equation of motion of the particles and evaluate these mathematical formulas. With molecular dynamics simulations, it is possible to study both thermodynamic properties and time dependent (kinetic) phenomenon. In order to correlate the macroscopic system to the microscopic system, time independent statistical averages are often introduced. Before introducing the way of correlation between macroscopic and microscopic level information with the help of statistical mechanics, a few fundamental definitions have to be introduced here [Har99].

The *thermodynamic state* of a system is usually defined by a small set of parameters, for example, the pressure, P , and the number of particles, N . Other thermodynamic properties can be derived from the equations of state and other fundamental thermodynamic equations.

The *mechanical* or *microscopic state* of a system is defined by the atomic positions, q , and momenta, p , these can also be considered as coordinates in a multidimensional *phase space*.

For a system of N particles, this space has $6N$ dimensions. A single point in phase space, denoted by G , describes the state of the system. An *ensemble* is a collection of points in phase space satisfying the conditions of a particular thermodynamic state. In other words, an ensemble is a collection of all possible systems which have different microscopic states but have an identical macroscopic or thermodynamic state. A molecular dynamics simulation generates a sequence of points in phase space as a function of time; these points belong to the same ensemble, and they correspond to the different conformations of the system and their respective momenta. Several different ensembles which are used for molecular dynamics simulations are described below.

Micro-Canonical Ensemble (NVE): The thermodynamic state characterized by a fixed number of atoms, N , a fixed volume, V , and a fixed energy, E . This ensemble corresponds to an isolated system.

Canonical Ensemble (NVT): A collection of all systems whose thermodynamic states are characterized by a fixed number of atoms, N , a fixed volume, V , and a fixed temperature, T .

Grand-Canonical Ensemble (μ PT): The thermodynamic state for this ensemble is characterised by a fixed chemical potential, μ , a fixed volume, V , and a fixed temperature, T .

Isobaric-Isothermal Ensemble (NPT): This ensemble is characterized by a fixed number of atoms, N , a fixed pressure, P , and a fixed temperature, T .

It is possible to explain functional form of the molecular dynamics considering the fundamental information which was given above. Molecular mechanics is based on the interactions within the system with contributions from process as such as the stretching of bonds, the opening and closing of angles and rotations about single bonds. Even when simple functions, such as Hooke's law, are used to describe these contributions a force field can perform quite acceptably. Molecular mechanical methods are set up from energy calculations in classical mechanics above potential energy functions. One of the easiest way to do these calculations is considering a group of atoms which are connected by bonds (springs) with different elasticities. Movements, hence potential energy, of these can be described by a parabolic equation. The energies obtained are similar to the real potential energy provided. The distances between atoms are not unrealistically large.

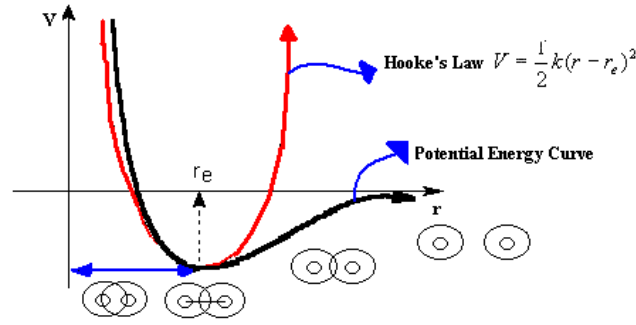


Figure 3.1: Potential Energy Curve and Hooke's Law.

The harmonic part of the potential energy curve is important for molecular mechanic simulations, because this part of the curve represents the bond interactions of atoms and the Hooke law which provides a good approach for this interaction (Figure 3.1). Similar interactions between atoms and molecules can be defined using *force fields* in molecular dynamics. Force fields use a set of empirical methods to model the interactions. Atoms in different environments are classified into different atom types. Generally, potential energies of the interactions can be calculated by splitting intra- and inter- molecular forces.

$$E_{Interaction\ Potential} = E_{Bonded} + E_{Non-Bonded} \quad (3.1)$$

Valence (bonded) interactions include bond-stretch, bond-angle, torsion and inversion terms. More sophisticated force fields may have additional terms, but they invariably contain these four components. The non-bonded interactions between atoms are normally considered to consist of simple coulomb energy interactions which are needed for correct definitions of the distribution of charges and van der Waals attractive and repulsive interactions. According to their reference or equilibrium values, there is a function that defines how the energy changes as bonds are rotated. Finally the force field contains terms that describe the interaction between the non-bonded parts of the system.

$$v(r^N) = \sum_{bonds} \frac{k_i}{2} (l_i - l_{i,0})^2 + \sum_{angles} \frac{k_i}{2} (\theta_i - \theta_{i,0})^2 + \sum_{torsions} \frac{V_n}{2} (1 + \cos(n\omega - \gamma)) \\ + \sum_{i=1}^N \sum_{j=i+1}^N (4\epsilon_{ij} \left[\left(\frac{\sigma_{ij}}{r_{ij}} \right)^{12} - \left(\frac{\sigma_{ij}}{r_{ij}} \right)^6 \right] + \frac{q_i q_j}{4\pi\epsilon_0 r_{ij}}) \quad (3.2)$$

Eq. 3.2 is the open form of eq. 3.1. The first term in eq. 3.2 refers to the interaction between pairs of bonded atoms, modelled here by a harmonic potential that gives the changes when the bond length l_i deviates from the reference value $l_{i,0}$. The second term refers to the summation

over all valence angles in the molecule, again modelled using a harmonic potential. The third term represents the torsion potential that models how the energy changes when a bond rotates. The fourth term represents the non-bond interactions, calculates between all pairs of atoms (i and j) that are in different molecules or that are in the same molecules. In all simple force fields, the non-bonded terms are usually modelled using coulomb potential for electrostatic interaction and a Lennard-Jones potential for van der Waals interactions [Lea01].

Bond-Stretch: This part of the potential function determines the interactions between two bonded atoms during the changes of distance between these two atoms. Many of the force fields use a simple Hooke's law expression to define it as in eq. 3.2, where the energy varies with the square of the displacement from the reference bond length. It is necessary to define the reference bond length here: It is the value that the bond adopts when all other terms in the force fields are set to zero. The equilibrium bond length is on the other hand the value adopted in a minimum energy structure, when all other terms in the force field contribute. Even if the true bond-stretching potential is not harmonic which gives quite similar responses with a harmonic potential which means that the 'average' length of the bond vibrating molecule deviate from the equilibrium value for the hypothetical motionless state [Lea01]. Some force fields use the Morse potential instead of a harmonic potential, such as DREIDING/M. Even if this function seems to be more adequate, starting geometry and long distances make a harmonic potential more efficient.

Angle-Bend: When the two bonds share a common atom, the deviation from their reference values is also generally identified by a harmonic potential or Hooke's law, as in eq. 3.2. θ_i is the angle between the bonds and equilibrium angle $\theta_{i,0}$ are assumed independent of these bonds. The accuracy of the force field can be improved by the incorporation of higher order terms.

Torsion: The torsion interaction for two bonds connected via a common bond is taken by this part of the potential function as in eq. 3.2. Where γ is the dihedral angle and V_n is the barrier for rotation, n periodicity and ω is the torsion angle.

Inversion: Even if most force fields do not include this term, some of the important force fields, such as DREIDING, contains this term in their functional form. When an atom is bonded to exactly three other atom, it is necessary to include a term which identifies how difficult it is to force all three bonds into the same plane (inversion) or how favourable it is to

keep the bond in the same plane [May90]. This term is generally suitable for force fields which were produced for biological simulation aims.

$$E_{inv}(\psi) = \frac{1}{2} K_{inv} (\psi - \psi_0) \quad (3.3)$$

Where ψ denotes the angle between bond and plane, K_{inv} is the force constant.

In order to include inversion interaction calculations to the total interaction energy calculations, eq. 3.3 should be added to the functional form of the potential energy term of the sophisticated force field (for this specific case to eq. 3.2).

Some of the force fields use an inversion term where the inversion is treated as if it was an improper torsion, such as CHARMM or AMBER, but earlier methods are preferred, because of their close correspondence to chemical concepts.

Van der Waals interaction: Deviations from the ideal gas behaviour are quantified by van der Waals forces. The Lennard-Jones 12-6 (LJ/12-6) function describes the van der Waals interaction as in eq. 3.2, where ϵ_{ij} is the well depth of the potential energy curve and σ_{ij} is the collision diameter and r_{ij} is the bond length. Even if the (LJ/12-6) potential is a simple and fast method to calculate the interactions, in order to model the short range interactions some force fields prefer an exponential form (Buckingham potential) for the van der Waals interactions. According to the systems different Lennard-Jones potentials can be written in different powers.

Electrostatic interactions: Electrostatic interactions between two molecules are calculated as a sum of interactions between pairs of point charges. In order to do this almost all force fields use Coulomb's law as in eq. 3.2, where q_i and q_j are charges, r_{ij} is the distance between these two charges and ϵ_0 is the permittivity of free space. The key point for calculating the electrostatic interactions is defining the charges. For this calculation a few methods have already been improved such as Gasteiger, semi empirical and quantum mechanics based methods and according to the size of the molecules charges can be fixed.

Hydrogen Bonding: Some of the force fields (e.g. DREIDING) use a special hydrogen bond term to identify the interactions involving a hydrogen atom on the very electronegative atom associated with hydrogen bonds. This function is used to model the interaction between the donor hydrogen atom and the heteroatom (it is any atom that is not Carbon or Hydrogen)

acceptor atom. Its use is intended to improve the accuracy with which the geometry of hydrogen-bonding systems is predicted. A general form for this part of the potential is:

$$v(r) = \frac{A}{r^{12}} - \frac{C}{r^{10}} \quad (3.4)$$

Even if some force fields use the same functional forms, they might provide different results. The functional forms employed in molecular mechanics force fields are often a compromise between accuracy and computational efficiency. Force fields mainly can parameterise in two different ways: *Ab initio* parameterisation and empirical parameterisation. Nevertheless, *ab initio* methods are the more direct ways to derivation of force fields, empirical adjustments are often required because of the some limitations of *ab initio* methods.

In order to include the effect of hydrogen bonding interaction calculations to the total interaction energy calculations, eq. 3.4 should be added to the functional form of potential energy term of the sophisticated force field (for this specific case to eq. 3.2).

Parameterisation of a force field can be performed by changing the equations which determine the forces between atoms and molecules, changing the parameters in the equations, changing the internal coordinates, compatibility and transferability parameters, cut-off distances according to the chemical and physical structure of the chemical group.

In order to control non-bonded interactions, summation method difference might be important depending on the system which is simulated. Choosing how to treat long-range non-bond interactions is an important factor in determining the accuracy and the time taken to perform an energy calculation. Summation methods can be classified according to the periodicity of the system under investigation.

Atom based cut offs is based on all atoms within the sum of the cutoff and buffer-width distances of an atom. A simple approach to the calculation of long-range non-bond interactions is the direct method, where non-bond interactions are simply calculated to a cutoff distance and interactions beyond this distance are ignored. However, the direct method can lead to discontinuities in the energy and its derivatives. Good reviews on atom and group based cut-offs can be found in literature (e.g. [Bro85]).

Table 3.1: *According to the periodicity of the system summation methods.*

System	Summation Method
Periodic and Non-periodic systems	Atom based cutoff
	Group based cutoff
	Cell multipole
Periodic systems only	Cell based
	Ewald
Non-periodic systems only	No cutoff

Group based calculation methods are based on the charge groups within the sum of the cutoff and buffer-width distances of a charge group. The advantage of this method is that dipoles are not broken at the cutoff. This method requires specification of charge groups.

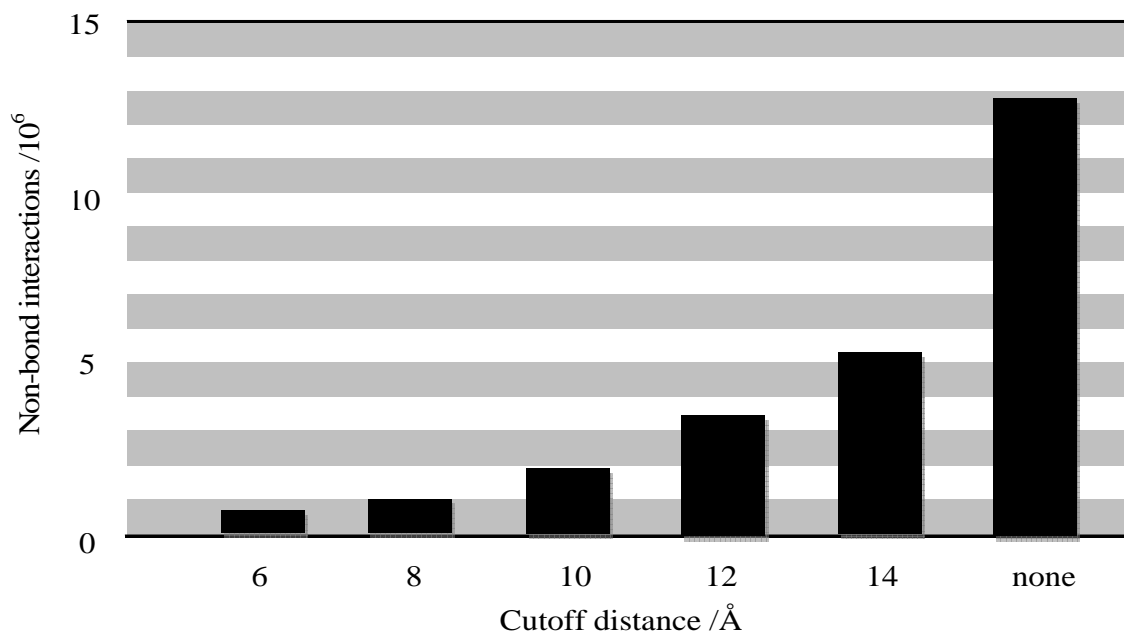


Figure 3.2: *Number of non-bond interactions as a function of cutoff distance. The number of non-bond pair-wise interactions (in millions) expected for a 5000-atom system as a function of cutoff distance. The time required to evaluate the total energy of this system is approximately proportional to the number of non-bond interactions [Acc06].*

The cell multipole method is a way of handling non-bond interactions in both non-periodic and periodic systems that are more rigorous and efficient than cutoffs. This method [Gre87, Sch91] is a hierarchical approach that allows the accuracy of the non-bond calculation to be controlled. Cell based methods can be applied to the systems, based on a specified number of cell layers surrounding the central cell.

The Ewald technique [Ewa21] is a method for the computation of non-bond energies in periodic systems. Crystalline solids are the most appropriate candidates for Ewald summation, partly because the error associated with using cutoff methods is much greater in an infinite lattice. However, the technique can also be applied to amorphous solids and solutions. Due to this property the Ewald method, this summation algorithm, is used in this thesis's result part.

In no-cutoff method, all non-bond terms in the system are determined. No-cutoff methods are not recommended for systems larger than 200 atoms.

In the past, force fields were widely used for predictive studies, calculating vibration frequencies and conformational properties for molecules in isolation. Today, with the fast progress of computer hardware and calculation algorithms (in particular, the density functional theory), quantum mechanical methods have been increasingly used for applications but still for large molecular systems and molecules in condensed phases that the force field methods has an incomparable advantage over *ab initio* methods. This is not only because the force field methods are several orders of magnitude faster than any *ab-initio* methods, but also fundamentally, an *ab-initio* method is often not necessary for the applications. The properties of interest in large scale simulations are usually relevant to the statistics of atomic motion in a much longer time scale than the rapid electron motion that *ab-initio* methods describe and also one of the most important interaction terms in the condensed phase simulations, the non-bond (dispersion in particular) forces, are extremely difficult to describe using *ab-initio* methods [Sun98].

One of the other important procedures of the molecular mechanics computer simulations is minimization. It supplies the possibility of the adjustment of atomic coordinates and unit cells in order to reduce the molecular energy and get a more stable crystal structure. X-ray diffraction can be used to determine the exact position of the atoms in the unit cell [Lu04]. The accuracy of the measurement increases with the increment of the number of electrons in the atom [Kin91]. This means that the positions of the hydrogen atoms are determined with a low accuracy. In order to define the exact positions of hydrogen atoms, every other atom,

which can easily be defined by X-ray measurements such as carbon atoms, should be fixed. Therefore, only hydrogen atoms are movable and with a minimization algorithm the right positions of hydrogen atoms can be determined. Charge calculations of the structure should be repeated after every minimization steps because charge calculations of the structure strongly depend on the geometric positions of the atoms.

As it was stated before, one of the most significant differences between the quantum mechanical based computer simulations and classical mechanical based computer simulations, molecular dynamics, is the charge calculation during the dynamics calculations. Molecular dynamics simulations do not consider charge calculation during the dynamics simulations. Hence, molecular dynamics has significant advantageous in computation expense compared to the quantum mechanical methods. However, charge is a kind of natural quantity which is undeniable. Known current physical facts indicate that charge interactions have tremendous effects on all other physical properties. Molecular dynamics simulations handle with this fact by finding the most appropriate charge distribution for the working system before dynamics calculations. Thereby, obtaining the most convenient charge distribution without performing charge calculations during the dynamics simulations causes computationally cheaper simulations and sometimes, according to the working conditions, relatively more reliable results. Molecular dynamics simulations mainly use definite algorithms in order to find appropriate charge algorithms. *Charge Equilibration* (QEq) [Rap91] takes into account the geometry and the electronegativities of the various atoms. Molecular conformation, as well as connectivity, affects the charge calculation. The calculation is iterative for structures that contain hydrogen. Another method is called *Gasteiger method* [Gas80] in which atoms are characterised by their orbital electronegativities. Only the connectivity of the atoms are considered, so only the topology of a molecule is important. Through an iterative procedure, partial equalization of orbital electronegativity is obtained.

After minimization the interaction energies, the main procedure of the molecular dynamics method is dynamic calculations of the cell. Dynamic calculations enable to compute the forces and movement of atoms in response to the forces by using laws of classical mechanics.

Dynamic simulations allow examining the motions of the molecules under different conditions, such as temperature, constant volume, energy, pressure, etc. By all molecular dynamic simulation methods a trajectory is obtained by solving the differential equations embodied in Newton's second law of motion:

$$m_i \frac{d^2 x_i}{dt^2} = F_i \quad (3.5)$$

Dynamics simulations can be performed on periodic and non-periodic systems. Unlike the minimization calculations, dynamics simulations enable to investigate the behaviour and the physical properties of systems at non-zero temperatures. Natural state can be represented by working with elevated temperatures.

3.3 Main methodology of molecular modelling in crystallization

Due to the different surface chemistries of the various crystal faces, the growth and development of a crystal is anisotropic and depending upon the relative growth rates of the crystal faces in the three dimensions, the particle morphology can be variable. Thus, the crystal habit is defined by the changes of the crystallographically independent faces. Nearly all crystal growth theories were established on this basis.

The equilibrium shape of a crystal is that of its minimum energy. Such situation is called Wulff condition which indicates that the area of all faces present will be those to minimize the Gibbs free energy of the crystal and point out that a crystal face grows laterally and along to perpendicular to it. Generally observed crystal habits grown from solutions are different from the prediction by the Wulff condition which was explained in detail in chapter 2.

In the past, some traditional methods have been published to predict the growth morphology of crystals. Among these, BFDH and Hartman-Perdok methods are used quite frequently. The BFDH method defines the possible important faces of a crystal during the growth and according to the Hartman-Perdok method the relative growth rate of the crystal faces $\{hkl\}$ is taken to be in direct proportion to the attachment energy of the faces [Liu95].

3.3.1 Bravais-Friedel-Donnay-Harker (BFDH) Method

Some of the earlier investigations of crystal science led to interest in the relation of crystal morphology with only the internal structure. This approach is called Bravais-Friedel-Donnay-Harker (BFDH) law and makes first estimates for determining the important faces on a grown crystal. This method finds relation between interplanar spacing of a crystallographic plane, d_{hkl} , and its area on an average crystal. Since the area of a plane is proportional to the inverse of its linear growth rate, R_G , BFDH law states that $R_G \sim 1/d_{hkl}$. It means that the larger a face's interplanar spacing (d_{hkl}), the slower its growth and the larger its size. This corresponds

to the kinetic models that faces with larger d_{hkl} have higher densities of molecules and therefore more nearest neighbours, more stable edges, larger edge free energy and slower growth [Win98]. However, BFDH law does not take into account the chemical nature of the bonding between atoms and molecules in the crystal. Therefore, it has no high accuracy compared to the real crystal shape.

3.3.2 Hartman-Perdok Approach

Due to the quite simplified nature and low accuracy of the BFDH theory compared to the real states, early observers made efforts to find more sensible models for a correct description of the crystal morphology. Hartman and Perdok [Har55a, b, c] developed a model that relates crystal morphology to its internal structure on the basis of energy consideration. Their approach was built in two different concepts: Periodic Bond Chain (PBC) theory and Attachment Energy (AE) theory.

According to PBC theory, it is possible to derive the habit of a crystal from the crystal structure. Hartman and Perdok [Har55b] concluded that the morphology of a crystal is governed by a chain of strong bonds which run through the surface and they classified the crystal faces into three types:

1. F-Faces (flat) each of which is parallel to at least two PBC vectors
2. S-Faces (stepped) parallel to at least one PBC vector
3. K-Faces (kinked) not parallel to any PBC vector

This approach assumes that strong bonds should form more easily and faster than weaker bonds and that a crystal can only grow in a given direction when an uninterrupted chain of strong bonds exist in the structure. According to structural properties of PBC vectors have different growth mechanisms. F faces grow by a layer mechanism and therefore grow slower than other kinds of faces. S faces grow according to one dimensional nucleation, this kind of face grows faster than F faces but slower than K faces. K faces do not need nucleation at all and hence grow the fastest compare to other kinds of faces. The *attachment energy* (E_{att}) of a crystal face is defined as the energy released on the addition of a slice to the surface of the growing crystal and it is a measure of the growth rate normal to that face. Faces with higher attachment energy grow faster. For F faces the attachment energy can also be expressed as the energy of bonds belong to the PBCs that are not parallel to the face. The attachment energy of a S face will require the formation of at least one stronger bond than a F face and a K face requires at least one stronger bond than a S face.

$$E_K^{att} > E_S^{att} > E_L^{att} \Leftrightarrow R_G^K > R_G^S > R_G^L \quad (3.6)$$

Hartman and Perdok [Har55b] defined PBC vectors as the first nearest neighbour interactions in the crystal, the “strong bonds”, for some materials such as metallic and ionic solids. However, they did not define PBCs strictly for organic molecules, they suggested that there is a coordination sphere round a central molecule that encompassed all the molecules with which it made strong bonds but they did not provide an exact definition of this sphere. As a result, the PBC theory is not as widely employed for ranking morphologically important forms and there is a need of a new and clearer definition. This method defines the important faces which have high possibilities of growing towards their normal direction of the crystals, in the end this model needs attachment energy values to predict the crystal morphology. As a further development of the PBC theory, Attachment Energy is defined as the difference between the Crystallization Energy (E_{cr}) and Slice Energy (E_{sl}).

$$E_{cr} = E_{att}^{hkl} + E_{sl}^{hkl} \quad (3.7)$$

Where E_{cr} is the energy required to dissociate a crystal into its constituent molecules and E_{sl} is the energy released upon the formation of a slice of thickness d_{hkl} .

The role of the attachment energy in controlling the growth and shape of crystals was analysed according to various growth mechanisms. These results showed that the *attachment energy model can be used as the standard methodology to calculate the morphology of pure organic molecular crystals* in agreement with experimental observations. A major weakness in the calculations is that they can only be used to represent the morphology of the vapour grown crystals. In crystals grown from solution, the solvent can strongly influence the crystal habit as small amounts of impurities can. Several researchers have observed that the crystal habit and the obtained attachment energies by assuming preferential solvent or impurity adsorption on crystal faces can slow down the growth of a face by hindering the attachment of additional molecules [Har55a, b, c].

In recent years, in order to define the correct morphology considering the effect of the crystal environment some methods had been offered such as the “tailor-made” additives approach [Cly94a,b], “build-in” [Nie97] and “surface docking” approach [Sch04, Mat99, Lu04], the approach of Bennema’s group [Liu96], approach of Doherty’s group [Win98]. All these models based on similar physical principles.

The methodology of theory which was proposed by Liu and Bennema [Liu96] based on the application the methods of statistical mechanics to examine solvent and supersaturation effects at the crystal-solution interface and combining these formulations with detailed growth kinetics (BCF method) as a means of predicting crystal shape from solution. Their model requires solvent-crystal physical properties that are estimated from detailed experiments or molecular dynamics simulations. Their method needs lengthy simulations or experiments for process engineering applications [Win98].

The method of Winn and Doherty [Win98] is based on similar physical principles to those proposed by Liu and Bennema [Liu96] but requires only the knowledge of the pure components properties that, for many systems, are readily available. It is the crystal structure and the internal energy of the solid which can be calculated by attachment energy calculations, and the pure components surface energy of the solvent. Solid-solvent interface properties are estimated using a classical approach. One of the limitations of the Winn and Doherty's approach [Win98] is that it applies to cases where there are many dispersive forces between the solvent and crystal at kinks and steps, or where there are known to be very specific electrostatic interactions. The method of Winn and Doherty [Win98] cannot handle situations where the forces are mostly columbic (such as for inorganic materials) or where there are electrostatic induced interactions between the solvent and the crystal. Another drawback is that it cannot predict the absolute or relative growth rate of faces undergoing rough, transport limited growth. However, these fast growing sections are the most susceptible to mechanical abrasion and breakage, and therefore, even a fully detailed transport model might not result in quantitatively accurate predictions. One of their criteria for nearest neighbour bonds and stable edges has not been proposed. It is one of the critical assumptions of their technique, eliminating many edge directions and faces from the consideration, and is by itself a useful tool for determining crystal faces [Win98].

In recent years a generalized approach to predict the morphology of crystals in the presence of so called "tailor-made" auxiliaries has been presented and described [Ber85]. Additive molecules affect the growth rate of crystal surfaces either by blocking the movement of surface step/kink terraces (referred as blocking modifiers) or by incorporating in the solid state and disrupting networks (disrupting modifiers) [Ber85].

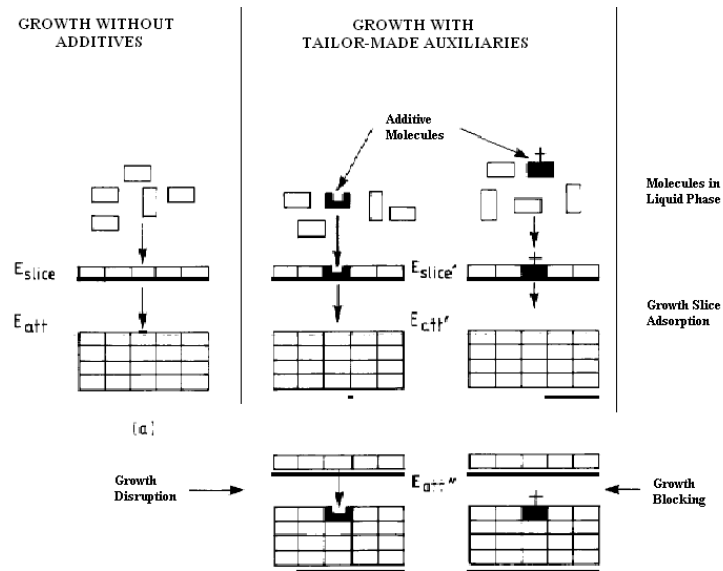


Figure 3.3: Sketch showing the definition of the energy terms E_{att} , E'_{att} , E''_{att} , E_{sb} , E'_{sl} used in morphological modelling for (a) pure system and systems have (b) disruptive-type (c) blocker-type tailor-made additives [Cly94b].

The main idea of the tailor-made additive method is that additives are blocking and disrupting modifiers have enough molecular coherence with the host system to incorporate onto the surface of the growing crystal and modify the energetic situation of the growing surface.

Other approaches to simulate crystal growth morphology for non-pure system are “surface docking” and “build-in” approaches which were improved by Niehörster [Nie97], Mattos [Mat99] and Lu [Lu04]. The approaches are based on the attachment energy model and the main idea is to find a suitable parameter that describes a trend of regular changes in the presence of additives. In the build-in approach host molecules are substituted by an additive on each specific symmetry position in the unit cell successively. After calculation of the incorporation energies of the pure crystal and the crystal with additives, the modified attachment energy is calculated from their differences. Therefore, the AE method is applied. In the surface docking approach [Mat99], analysing the energetic effect of additives on the individual crystal faces which are cleaved from a pure crystal is the main idea. The binding energy is defined as the interaction energy between an additive molecule and a specific crystal face and the aim of this model is to calculate a binding energy of an additive and to combine this value with the attachment energy model. It is thought that the magnitude of the binding energy is related to an effective reduction in the attachment energy, hence, the growth rate of a crystal face [Lu04].

4. Materials and Methods

4.1 Model Systems

The selection of model substances was governed by the intention to find different crystal habits depending upon the crystallization conditions of the main compound. Also there should be a number of literature studies accessible in order to have data for the verification of the finding from simulation.

4.1.1 Benzophenone

Benzophenone (*diphenylmethanone*, *phenyl ketone*, *diphenyl ketone*, *benzoylbenzene*) is an important compound in organic photochemistry and perfumery as well as in organic synthesis. It was investigated to reveal morphological differences depending upon the presence of different impurities [Wan01, Lu04, Fie07].

Table 4.1: Summary of thermodynamical data of benzophenone.

Type of Physical Property			
Melting point	$T_m / ^\circ\text{C}$	48.0	[Chi02]
Boiling point	$T_b / ^\circ\text{C}$	305	[Ola64]
Formation enthalpy	$\Delta H_{form} / \text{kJ} \cdot \text{mol}^{-1}$	32.9	[Par50]
Fusion enthalpy	$\Delta H_{fus} / \text{kJ} \cdot \text{mol}^{-1}$	18.8	[Chi02]
Latent heat of sublimation	$\Delta H_{sub} / \text{kcal} \cdot \text{mol}^{-1}$	94.7	[Kru83]
Latent heat of evaporation	$\Delta H_{vap} / \text{kcal} \cdot \text{mol}^{-1}$	16.7	[Sch60]

In order to perform molecular modelling calculations the crystal structure data, published by Lobanova *et al.* [Lob68], was extracted from the *Cambridge structural database* [Csd07]. Cell parameters were given as orthorhombic unit cell, P2₁2₁2₁ space group, unit cell diameters: a = 10.26 Å, b = 12.09 Å, c = 7.88 Å, Volume is 977.46 Å³, Z: 4.

The intensive research [Wan01], particularly concerning tailor-made additives on benzophenone molecules indicate that benzophenone has an immense potential for morphology changes in the presence of different kinds of additives.

4.1.2 Hydroquinone

Hydroquinone (*quinol*, *1,4- benzenediol*, *benzoquinol*) is an aromatic organic compound which is used as depigmentor, a photographic reducer and developer, a reagent in determination of small quantities of phosphates and an antioxidant in oils and greases. Investigations on hydroquinone molecule indicate that hydroquinone has greater potential than benzophenone concerning crystal morphology changes in the presence of additives [Che05, Kun09, Yür08, Yür09].

Table 4.2: Summary of thermodynamical data of hydroquinone

Type of Physical Property			
Melting point	$T_m / ^\circ\text{C}$	172	[And26]
Boiling point	$T_b / ^\circ\text{C}$	287	[Mer06]
Formation enthalpy	$\Delta H_{form} / \text{kJ} \cdot \text{mol}^{-1}$	27.9	[Ako00]
Fusion enthalpy	$\Delta H_{fus} / \text{kJ} \cdot \text{mol}^{-1}$	27.1	[And26]
Latent heat of sublimation	$\Delta H_{sub} / \text{kcal} \cdot \text{mol}^{-1}$	21-25	[Ver08]
Latent heat of evaporation	$\Delta H_{vap} / \text{kcal} \cdot \text{mol}^{-1}$	13.1	[Sci08]

In order to perform molecular modelling calculations the crystal structure three different polymorphs of hydroquinone was extracted from the *Cambridge structural database* [Csd07].

α - *polymorph* of hydroquinone, was published by Wallwork *et al.* [Wal80] cell parameters were given as rhombohedral unit cell, $R\bar{3}$ space group, unit cell diameters: $a = b = 38.4599 \text{ \AA}$, $c = 5.65 \text{ \AA}$ (hexagonal axes), $\alpha = \beta = 90^\circ$, $\gamma = 120^\circ$, density is $1.364 \text{ g} \cdot \text{cm}^{-3}$, Z : 54. α – polymorph is the most stable form within the extracted forms at room temperature. Calculated and measured densities are $d_c = 1.325 \text{ g} \cdot \text{cm}^{-3}$ and $d_m = 1.380 \text{ g} \cdot \text{cm}^{-3}$, respectively.

β - *polymorph* of hydroquinone, was published by Lindeman *et al.* [Lin81] cell parameters were given as rhombohedral unit cell, $R\bar{3}$ space group, unit cell diameters: $a = b = 16.613 \text{ \AA}$, $c = 5.4746 \text{ \AA}$, $\alpha = \beta = 90^\circ$, $\gamma = 120^\circ$, density is $1.258 \text{ g} \cdot \text{cm}^{-3}$, Z : 9. Transition of the β - polymorph to the α -form was observed spontaneously. The β -hydroquinone can become stabile when gas molecules are introduced into its lattice [Rya90]. Furthermore, it has a rather

close packaging than the α - and γ -modification. Calculated and measured densities are $d_c = 1.258 \text{ g}\cdot\text{cm}^{-3}$ and $d_m = 1.250 \text{ g}\cdot\text{cm}^{-3}$, respectively [Lin81]. The β -form has the same ability to build inclusion components into its lattice cavities as the α -polymorph. Containing these clathrates the density of β -hydroquinone is increased to the values of density given for the closer packed polymorphs. Lindeman *et al.* [Lin81] indicate that excluding the host molecules from density calculations will significantly decrease the packaging and leads to the assumption that the cavities of the β -polymorph are larger than those of the α -form. In addition, the β -polymorph is likely to form two interpenetrating interdependent molecules which together enclose one molecule of second component [Pal48]. Hence, this polymorph has the same behavior as it was found at the α -form.

γ - polymorph of hydroquinone was published by Maartmann-moe [Maa66], cell parameters were given as monoclinic unit cell, $P2_1/c$ space group, unit cell diameters: $a = 8.07 \text{ \AA}$, $b = 5.20 \text{ \AA}$, $c = 13.20 \text{ \AA}$, $\beta = 107^\circ$, density is $1.380 \text{ g}\cdot\text{cm}^{-3}$, $Z: 4$. The γ -polymorph is one of two which is not stable but changes spontaneously into the α -form of hydroquinone. This monoclinic form can be obtained by sublimation. It crystallizes at room temperature from an ether solution which evaporates rapidly [Maa66].

In order to define physical properties of mentioned organic molecules in the presence of external environments, ethanol, acetone and methanol molecules were used in relevant simulations.

4.1.3 Benzoic Acid

Benzoic acid (*carboxybenzene*, *benzenecarboxylic acid*, *benzeneformic acid*) is the simplistic aromatic carboxylic acid containing carboxyl group bonded directly to benzene ring. It is slightly soluble in water, soluble in ethanol, very slightly soluble in benzene and acetone. The most of commercial benzoic acid is produced by the reaction of toluene with oxygen at temperatures around $200 \text{ }^\circ\text{C}$ in the liquid phase and in the presence of cobalt and manganese salts as catalysts. Benzoic acid is converted to its salts and esters for the use of preservative application in foods, drugs and personal products.

Table 4.3: Summary of thermodynamical data of benzoic acid.

Type of Physical Property			
Melting point	$T_m / ^\circ\text{C}$	121.5	[Kae64]
Boiling point	$T_b / ^\circ\text{C}$	249.2	[Kop55]
Formation enthalpy	$\Delta H_{form} / \text{kJ} \cdot \text{mol}^{-1}$	390.2	[Bon35]
Fusion enthalpy	$\Delta H_{fus} / \text{kJ} \cdot \text{mol}^{-1}$	17.3	[Bon35]
Latent heat of sublimation	$\Delta H_{sub} / \text{kcal} \cdot \text{mol}^{-1}$	85.8	[Hir34]
Latent heat of evaporation	$\Delta H_{vap} / \text{kcal} \cdot \text{mol}^{-1}$	65.4	[Mor72]

4.2 Methodology of simulations

The use of the attachment energy model as a method for the calculation of the crystal morphology was developed by Hartman and Perdok [Har55a, b, c] and has become the standard method to calculate the morphology of organic crystals. The basic method, which is used by most investigators as well as the method used in most software packages (such as Cerius²), is the identification of the important crystallographic faces of crystal with the BFDH method. The attachment energy of these faces is then calculated using inter-atomic potential functions. The morphology of the crystal is calculated by assuming the relative rate of the face is directly proportional to the attachment energy. In order to incorporate the effect of crystal environment into the simulations, the change at the attachment energy value in the presence of the additive or solvent has to be considered and the related growth rate has to be recalculated.

In order to observe the changes on the crystal structure and simulate the morphology, the transport properties with respect to the crystal should be clearly resolved. Transport refers usually to a non-equilibrium case, however, molecular dynamic studies are usually built up for the equilibrium state. It is, however, possible to simulate the non-equilibrium phenomena by considering microscopic equilibrium cases, this is one of the fundamental results of statistical mechanics, every non-equilibrium case contains. This can be achieved by considering the microscopic local fluctuations that occur even in systems at the equilibrium.

Fick's law mentioned in the diffusion layer model is required for definitions of important parameters. Some physical parameters can be calculated, such as the diffusion coefficient (D) which is important in simulation of crystal growth by means of computational methods.

There are plenty of reasons to choose diffusion coefficient as physical parameter. One important reason is that diffusion coefficient is one of the fundamental physical parameters of the transport phenomena. Depending upon the diffusion coefficient the mass increase of the crystal can be examined. In some specific cases, it is rather difficult to observe by experiments other physical properties which would be necessary to compare them to the computational results. This is another important reason to prefer using the diffusion coefficient which avoids such problems.

Some experimental methods such as neutron scattering or isotopic tracing enable to measure diffusion coefficients but these diffusion coefficient values may not be informative about the diffusion at the point of interest the crystal-liquid interface. For example, a crystal is growing in a supersaturated solution and solute molecules are leaving the solution and becoming part of the crystal. As defined in the diffusion layer model (bulk diffusion) in order to do a correct analysis, the diffusion from the solid-liquid interface in crystal-solution system should be clearly resolved because this part of the system plays an efficient role in crystal growth. Many results indicate that the structure and macroscopic quantities such as density and potential energy in the regions adjacent to the surface are quite different from those of the bulk phase. This can be seen from the fact that in solid-liquid interfacial systems, the interfacial profile shows oscillations of density on the solid side that extend to the fluid side and gradually vanishes going from the solid surface to the bulk fluid. Correspondingly, it follows that potential energies (or interaction energies) of the fluids in the interfacial phase differ from those in the bulk phase [Liu96]. Experimental methods do not allow defining the motion of molecules during a definite time interval in the crystal-liquid system. Therefore, experimentally differentiation between the diffusion coefficients according to the location where diffusion takes place within the crystal-liquid system is problematic. However, molecular dynamic simulation methods represent sensible tools to study and visualize the growth mechanism. With correct algorithms, it is relatively easy to define the required values for desired parts of the structure by using computer methods. This is one of the main reasons to use computers for crystal growth investigations.

The diffusion coefficient is related to the mean square displacement and it can be determined by recording the motion of molecules during the molecular dynamics calculation. This result

immediately suggests an explanation how to measure the diffusion coefficient, D , in a computer simulation. For every particle the distance travelled at time t is measured and plotted the mean square of these distances as function of time the mean square displacement (MSD) of the diffusing molecules:

$$MSD = \frac{1}{n} \sum_{i=1}^n \langle |r_n(t) - r_n(0)|^2 \rangle \quad (4.1)$$

Once the MSD is calculated, the diffusion coefficient can be determined from the *Einstein relationship* [All87]:

$$2D = \frac{1}{d} \frac{\partial}{\partial t} (MSD) \quad (4.2)$$

Where d is the dimension of the system. Therefore, the diffusion coefficient can be determined from the slope of a plot of MSD versus time.

$$D = \frac{1}{2d} \lim_{t \rightarrow \infty} \frac{d \langle |r(t) - r(0)|^2 \rangle}{dt} \quad (4.3)$$

The Einstein relationship considers the displacement as the time integral of the rate of the target particles. It is also possible to calculate the diffusion coefficient using another calculation method which is called the *Green-Kubo relation* [Lea01]. This method calculates diffusion coefficients as the integral of the *velocity auto correlation function* (VACF) which is an equilibrium property of the system, because it describes correlations between rates at different times along an equilibrium trajectory. For classical systems, the Green-Kubo relation for D and the Einstein relation are strictly equivalent. There might be practical reasons to prefer one approach over the other, but a distinction is never fundamental. Dealing with rate instead of velocity auto correlation function is easier. Therefore, using the Einstein relation is more feasible compare to the Green-Kubo relation.

The diffusion coefficient values are obtained for the bulk liquid and they can be compared to empirical results. An old but still widely used correlation for diffusion coefficient is the *Wilke-Chang* (eq. 2.23) method an empirical modification of the Stokes-Einstein relation [Wil55].

4. 2. 1 Computer Simulations

Equilibrium morphologies were calculated based upon known crystal structures using both BFDH and attachment energy calculations.

Simulations are carried out using different partial charge sets, force fields, simulation durations and system sizes. Charge distributions were derived from geometry optimizations on isolated molecules using semi-empirical, *ab-initio* and DFT techniques implemented in the CAChe (FQS, Poland) and Gaussian03 (Gaussian Inc., USA) software packages. Growth from solutions of these molecules with phase-field Monte-Carlo hybrid algorithm simulations are presented elsewhere [Kun09]. MD simulations were carried out on assemblies of benzophenone and hydroquinone with the aid of the Cerius² modules (Accelrys Inc., USA), on an SGI Tezro visual workstation and IRIX64 Release 6.5 operating system. Assemblies of randomly positioned molecules were generated using the amorphous cell module in MaterialsStudio (Accelrys Software Inc., USA), and varied in size from 100 to 500 molecules.

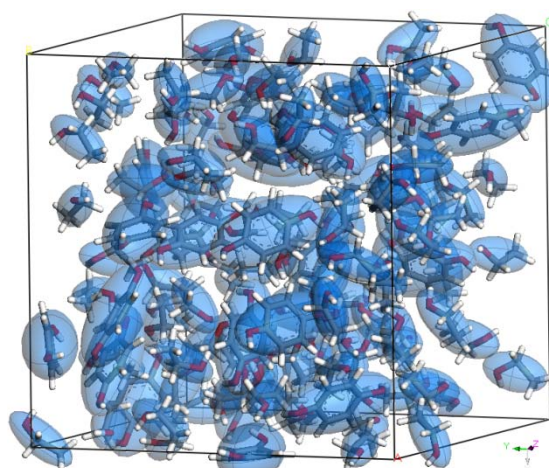


Figure 4.1: *A simulation box example containing 25 hydroquinone and 106 ethanol molecules. Molecules are showed on ellipsoidal representation. Light blue molecules are hydroquinone and dark blue molecules are ethanol molecules.*

The volume of the system was selected in such a way that the calculated density matches the experimental values [Wil55]. Production run durations are varied between 20 and 200 ps. In addition, different thermostats, force fields and temperatures were considered. Temperatures above the melting points of the respective compounds were selected. Simulations were performed with the COMPASS, PCFF and CVFF force fields. The Nosé, Andersen, Velocity Scale (only for equilibration runs) and Berendsen thermostats were considered in order to

control temperature during simulations. The initial configuration generated is equilibrated using the microcanonical ensemble (NVE, constant particle number, volume and energy) for a total of 10 ps with a time step 1 fs. Production runs employ the canonical ensemble (NVT, constant particle number, volume and temperature) using the same time step of 1 fs. The main simulation scheme of the thesis is given in Figure 4.2.

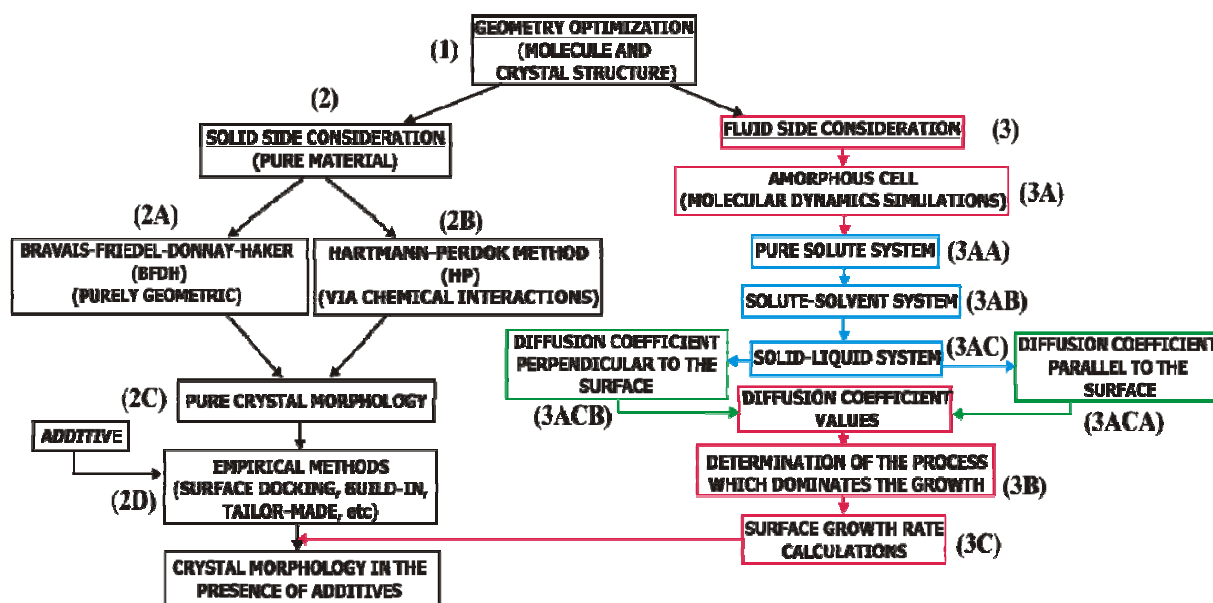


Figure 4.2: Flow chart for the simulation process. The left side represents the existing habit calculation method based only on the solid side. The right side represents the approaches described in this work including the section numbers.

5. Results

5.1 A general look at the “results” chapter

In order to proceed to the computer simulations within the aims of this work, useful codes of previous works [Nie97, Mat99, Sch04, Lu04, Fie07] are used for the beginning part of this work. Benzophenone and hydroquinone were selected as model substances, as they are known to exhibit different crystal habits depending upon the crystallization conditions.

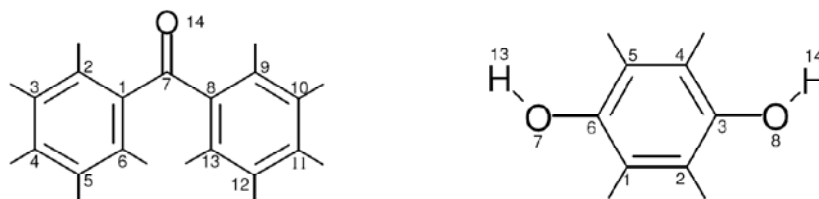


Figure 5.1: Simple molecule structures of benzophenone (left) and hydroquinone (right).

The “results” chapter has a deductive structure. It means that the results chapter starts with a single molecule construction and goes into the detail of molecular transport behaviour of a group of molecules within large systems and every section uses the results of the previous sections. A general scheme which indicates the structure of this work is given in Figure 4.2.

5.2 Molecule structure optimization (Figure 4.2, 1)

The first step of the simulation is to construct the molecule. The correct molecule structure has a great importance for the results of the entire work because of the deductive structure of this work. In order to find the optimum geometry a standard procedure is used. The energy of the molecule was minimised using the force field by employing the following the MD simulations.

For the substances benzophenone and hydroquinone (Figure 5.1) the conformation of the molecules was determined computationally using the Force Fields Dreiding, CFF_300_1.01, CVFF_300_1.01 and Compass (implemented in the software *Cerius²*) and the force fields MM2, MM3 and the three semi-empirical Methods AM1, PM3, PM5 (all implemented in the software *CAChe*).

In *Cerius²*, charge equilibration and minimization cycle were carried out until the structure reaches the constant minimum potential energy, and thus to optimize the molecule geometry, until a constant energy value was reached.

5.2.1 Benzophenone [(C₆H₅)₂CO]

CAChe offers a routine optimization cycle. To ensure that the minimizer finds the global – and not only a local – minimum conformation, the minimization was applied to five different start-conformations in each Force Field [Gal01]:

Start-conformations (<i>benzophenone</i>):	1	2-D plane, sketched and cleaned
	2	plane, but different angle 1-7-8
	3	different torsion 6-1-7-O14
	4	different torsion 1-7-8-13
	5	plane, but different distance 7-8

Each molecular mechanical and semi-empirical method finds only one end-conformation no matter which one of the start conformations are used. However, the calculated end-conformations vary depending upon the force field.

Table 5.1 shows the average deviations of the calculated benzophenone molecules from the molecule based in the database [Csd07]. The highest average deviation of the distances is observed as 3.4% (CVFF_300_1.01), the angles deviate between 0.3% (Dreiding) and 7.2% (PM5) from the database molecule. The torsion deviates between 1.1% (Compass) and 7.4% (PM3). Table 5.1 shows that the benzophenone molecule calculated by the Force Field Dreiding has the highest similarity to the one from the *Cambridge Structural Database* [Csd07].

The average deviations of simulated geometrical values from theoretical values for all sets of parameters are calculated by:

$$\Delta X_i [\%] = (X_i - X_{Database}) / X_{Database} \quad (5.1)$$

Table 5.1: Average deviations of the calculated benzophenone molecule according to the different optimization algorithm.

Model		Average Deviation [%] from the molecules extracted from the CSD [Csd07]		
		Δ Distance [\AA]	Δ Angle [$^\circ$]	Δ Torsion [$^\circ$]
Molecular Mechanical	Dreiding	1.0	0.3	1.6
	PCFF	2.7	1.8	3.9
	CVFF	3.4	1.7	5.8
	Compass	2.1	6.9	1.1
Semi-Empirical	MM2	0.3	3.6	2.6
	MM3	1.9	5.6	3.0
	AM1	1.6	5.4	3.9
	PM3	2.0	5.9	7.4
	PM5	2.4	7.2	3.1

5.2.2 Hydroquinone [$\text{C}_6\text{H}_4(\text{OH})_2$]

Similar optimization procedure is repeated for the hydroquinone molecule with either molecular mechanical or semi-empirical methods.

Start-conformations (<i>hydroquinone</i>):	1	2-D plane, sketched and cleaned
	2	different torsion 5-6-O7-H13
	3	torsion 5-6-O7-H13 90° and torsion 4-3-O8-H14 -90°
	4	plane, but both torsions 180°
	5	plane, but different distance 3-O8

Table 5.2: Average deviations of the calculated γ -hydroquinone [Maa66] molecule compared to the molecules extracted from the crystal structure database [Csd07] according to the different optimization algorithms.

Model		Average Deviation [%] from the molecules extracted from the CSD [Csd07]			
		Δ Distance [Å]	Δ Angle [°]	Δ Torsion [°]	
Molecular Mechanical	Dreiding	1.9	0.9	0	
	PCFF	1.1	0.9	0	
	CVFF	1.2	0.9	0	
	Compass	1.1	0.8	0	
	MM2	1.3	1.7	0	
Semi-Empirical	MM3	1.0	0.9	0	
	AM1	0.8	0.8	0	
	PM3	0.8	1.0	0	
	PM5	1.2	0.8	0	

The distance deviations fluctuate between 0.8% (AM1 and PM3) and 1.9% (Dreiding) from the database molecule [Csd07]. The maximum deviation of the angles is 1.7% (MM2). The torsions angles indicate same value for all optimization models. Table 5.2 indicates that the force fields PCFF_300_1.01 and Compass calculate the hydroquinone molecule close to the molecule based on the database. For further steps of this work these two force fields are used intensively within the force field index.

5.3 Morphologies of the substances (Figure 4.2, 2A, 2B and 2C)

When the entire simulation process of this thesis is considered, the optimization of the molecules should be followed by the fundamental morphology simulations. Here, some basic results are confirmed, morphologies of the working samples are given in the order of a possible simplistic situation to the most complex one. At first, pure material morphologies of

the working systems are given. At the second part of this section, experimental and simulated habits of the materials in the presence of solvent molecules are given.

The computer simulations for the pure substances were performed employing the Attachment Energy (AE) method. The AE method is able to model the habit of pure substances in the absence of any external factors with good accuracy. However, the AE cannot reproduce the effect of additives since these are not considered by the method. When a specific additive or solvent has no significant effect on the morphology of a crystallizing material, the AE method may provide an accurate representation of the observed morphology. However, additive molecules may interact with the solute or crystal surfaces. Hence, they may change the growth rates and lead to changes in the crystal morphology. Other methods have to be used to calculate the morphology in the presence of additives. The *surface docking method* [Mat99] which was developed in house is used to calculate the habit of a given substance in the presence of additives or solvents.

5.3.1 Benzophenone

Experimental mean aspect ratio of a grown morphology of the benzophenone from pure melt at an undercoolings of 0.2 K is 1.44 [Fie07], grown from stirred suspensions at an undercooling of 0.1K is 1.72 [Wan01] and at an undercooling of 0.4 K is 1.64 [Wan01].

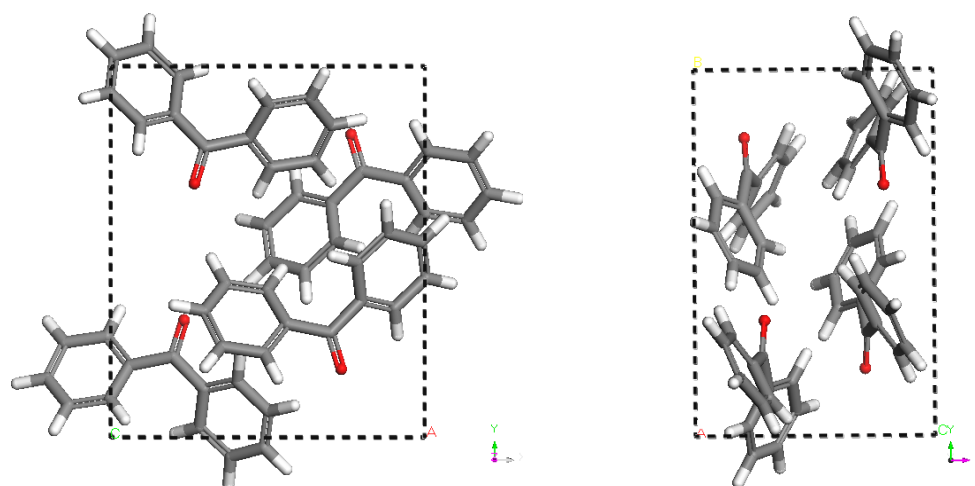


Figure 5.2: *Lattice structure of benzophenone [Lob69].*

In order to find the morphology of benzophenone in the presence of additives, investigations should be started with the habit of pure benzophenone molecules first. The properties of pure materials are defined according to the BFDH and attachment energy approaches.

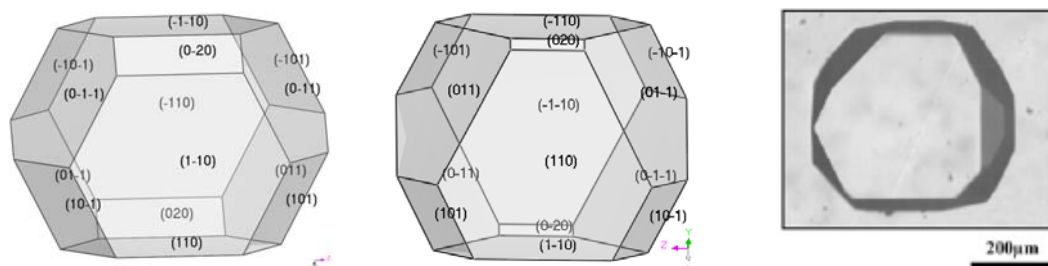


Figure 5.3: *Pure habits of benzophenone BFDH morphology (left), AE morphology (centre) and experimental [Lu04].*

A difference between BFDH and AE calculation is that the BFDH model is a pure geometrical calculation method, however, AE considers atomic interactions within the crystal structure. Both methods are simplified methods compared to the reality and they do not consider external environment effects.

Even though, small differences can be seen between the habits of different methods (Figure 5.3), these two methods generate similar final habits and the results are in good agreement with the experimental habit of benzophenone in the absence of a solvent.

General properties of the habit pure benzophenone molecule are extracted from the results of the attachment energy calculations. The habit aspect ratio (ratio between the longest and the shortest diameter of the habit) is 1.51 which is in the range of experimental results. The relative surface / volume ratio (comparison the surface area of the habit with that of a sphere of the same volume) is 1.131. The total surface area is $4.96 \cdot 10^4 \text{ \AA}^2$ and volume is $8.64 \cdot 10^5 \text{ \AA}^3$. Attachment energy values and corresponding surface area ratios are given in Table 5.3.

Table 5.3: *Results of the Attachment Energy calculation of pure benzophenone.*

Surface	Attachment Energy / $\text{kcal} \cdot \text{mol}^{-1}$	Total Face Area / $10^3 \cdot \text{\AA}^2$
(110)	-49.07	25.7
(011)	-52.97	18.1
(101)	-63.14	5.50
(020)	-72.29	0.38
(111)	-67.79	0.00
($11\bar{1}$)	-67.79	0.00

Here are the important questions: What is the habit of benzophenone in the presence of external environment and how can this habit be generated with computational methods? In order to define the effect of the solvent on the crystal morphology the surface docking approach [Nie97] is used.

Benzophenone habit in the presence of additives

The growth morphology of benzophenone crystals in the presence of different kinds of additive molecules was already presented in earlier works [Lu04, Fie07]. Results of earlier works indicate that selected additive molecules do not change the morphology of benzophenone molecules significantly. These results were confirmed experimentally. Here, benzophenone habits in the presence of different additive molecules are recalculated by the use of the surface docking method. Hence, results of earlier works are confirmed and the methodology of this work is successfully tested.

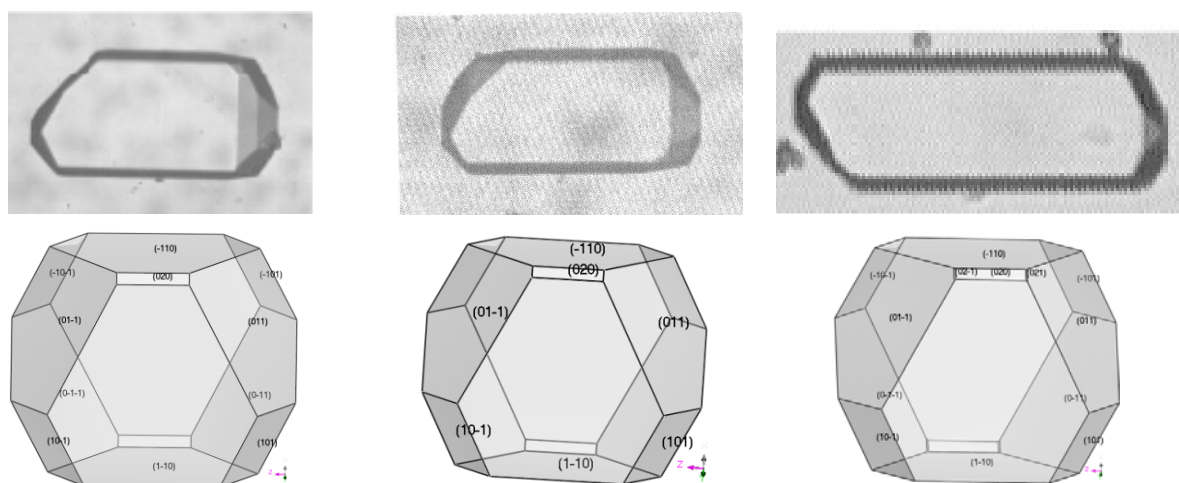


Figure 5.4: Results of the experimental (above) [Lu04] and simulated (below) habits of benzophenone in the presence of ethanol, acetone and benzoic acid, respectively.

All here used different additive molecules show no significant effects on final morphology of benzophenone. All additive molecules lead to similar morphologies with minor differences such as a new small face in benzoic acid case ((021) face in Figure 5.4). In the same time, very similar results were obtained in earlier works [Lu04, Sch04]. Habit aspect ratio values are 1.51 for all simulations which were performed with different kinds of additives.

Attachment energy values of benzophenone in the presence of different additives are compared with the pure attachment energy values (Figure 5.5). Here, it can be distinguished that none of the additives create a significant difference within the attachment energy values

and for all faces additives showed similar interaction tendency with the applied crystal surfaces.

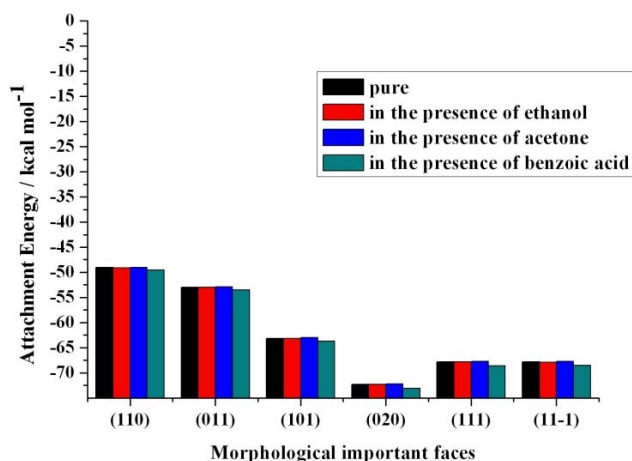


Figure 5.5: Attachment energy values of the morphologically important faces of benzophenone in the presence of different kinds of additives.

5.3.2 Hydroquinone

Puel *et al.* [Pue97] analyzed the transient behaviour of hydroquinone. They characterized each individual crystal as parallelepiped with length, width and depth. Using experimental analysis, they showed that the habit expressed as a shape factor did not remain constant. For different polymorphs of hydroquinone different habit aspect ratios are observed [Chi03]. A hydroquinone crystal generally shows a long rodlike shape.

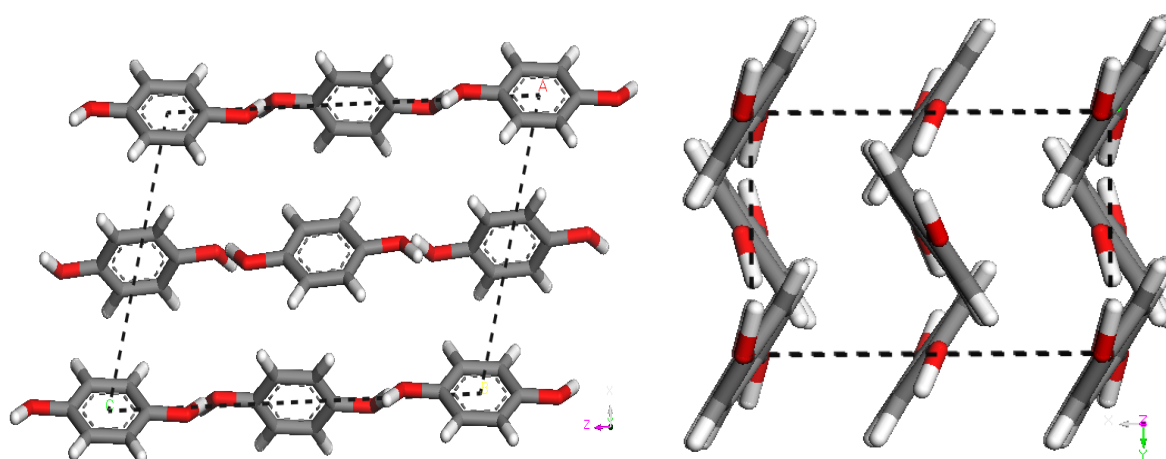


Figure 5.6: Lattice structure of the γ -polymorph of hydroquinone.

Within the obtained hydroquinone polymorphs the γ -polymorph is focused, because of its unstable and spontaneously changeability to the α -polymorph. In order to be able to differentiate the changes which the transport mechanism creates, only results of the γ –

polymorph is focused for the further stages of this work. However, also the AE morphologies of the other polymorphs are given here.

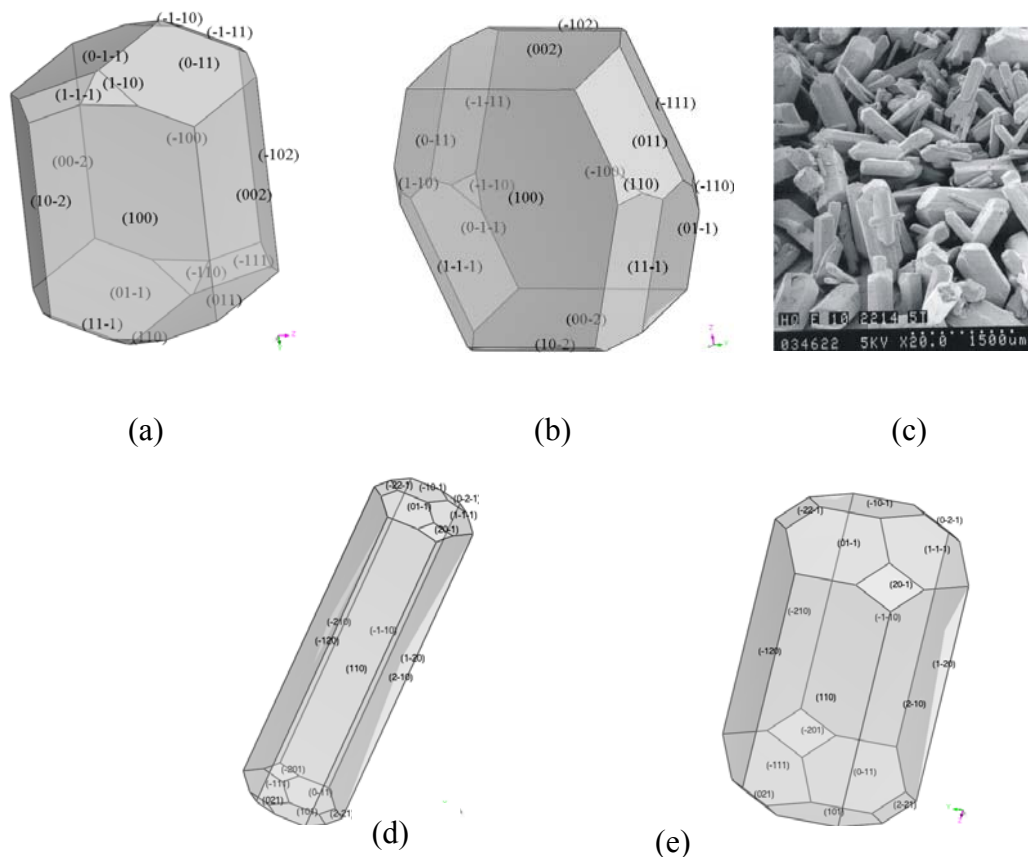


Figure 5.7: *Pure habits of hydroquinone. (a) BFDH morphology of γ -polymorph, (b) AE morphology of γ -polymorph, (c) experimental rod like habit [Pue03], (d) AE morphology of α -polymorph and (e) AE morphology of β -polymorph.*

Even though, a small difference appears between the calculated habit of the pure α - and β -polymorphs, the final habit tendencies are similar to the general experimental rod like habit (Figure 5.7). Here, it can be concluded that the pure habits of α - and β -polymorphs may be hardly affected by the external environment such as additives and solvents. On the other hand, the morphology of the pure γ -polymorph exhibits a completely different habit structure than the other polymorphs. Therefore, γ -polymorph is rather suitable to be affected by external environments. As a result, in the later stages of this work the focus will be mainly on the diffusion properties of the γ -polymorph.

Table 5.4: Results of the Attachment Energy calculation of pure γ -hydroquinone.

Surface	Attachment Energy / kcal · mol ⁻¹	Total Face Area / 10 ³ · Å ²
(100)	-31.12	31.9
(002)	-66.11	12.5
(10 $\bar{2}$)	-79.88	1.03
(011)	-75.45	10.8
(11 $\bar{1}$)	-72.43	0.00
(110)	-75.64	0.00
(102)	-86.09	8.14

Hydroquinone habit in the presence of ethanol

In order to find the effect of ethanol and acetone molecules on the final morphology of hydroquinone the surface docking method is also used for this substance. During simulations a single additive molecule is docked onto the morphologically important faces depending upon the hydrogen bonding interactions between the surface and the additive. Throughout the dynamic simulations in order to obtain continuous molecular interaction between the surface and additive molecule, surfaces are produced relatively large. Therefore, an additive finds a minimum energy point on the crystal surface without leaving the surface.

The final crystal habit of hydroquinone in the presence of ethanol is obtained by simulation and experiment (Figure 5.8). Both methods generate a similar final habit for the hydroquinone crystal in contrast of the benzophenone case. Employed force fields and the crystal form have a significant effect on final morphology calculations.

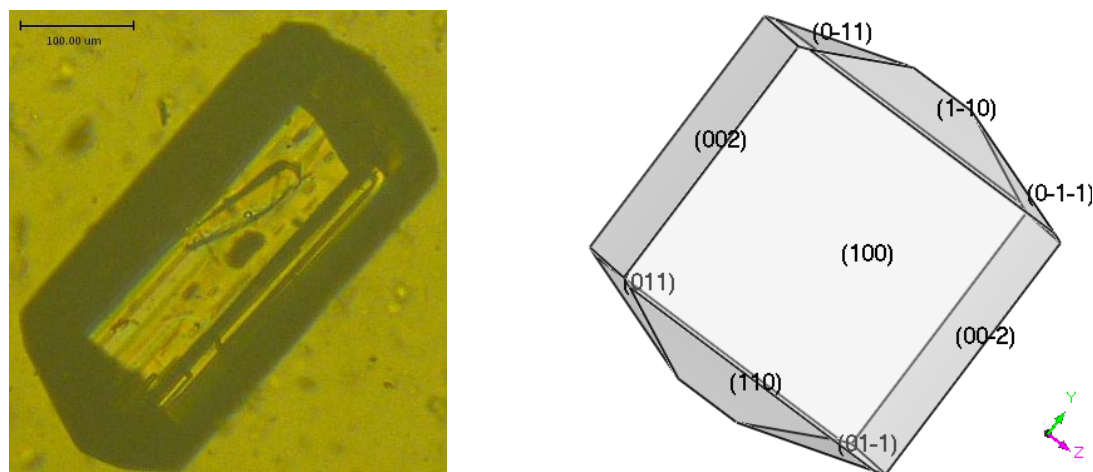


Figure 5.8: Experiment (left) and simulated (right) habits of the hydroquinone in the presence of ethanol.

Differences on the attachment energy values are given in Figure 5.9. The presence of ethanol molecules creates deviations of the attachment energy values and every single face is affected distinctly by an ethanol molecule. The most noticeable differences can be seen on the $(11\bar{1})$ and $(10\bar{2})$ faces (Figure 5.9). These faces lose their morphological importance and they are not visible in the final morphology of the hydroquinone crystal in the presence of ethanol.

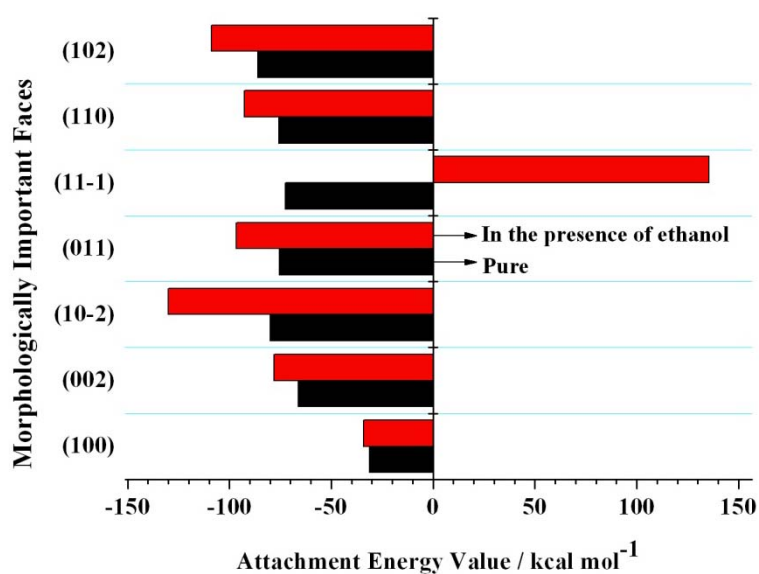


Figure 5.9: Attachment energy values of the morphologically important faces of the hydroquinone. Pure hydroquinone attachment energy values are given in black and attachment energy values of hydroquinone in the presence of ethanol are given in red.

Hydroquinone habit in the presence of acetone

A similar simulation procedure is applied to the same morphological important faces in the presence of acetone molecules. However, the experiments defining the habit of hydroquinone in the presence of acetone have to be different than in the case of ethanol because acetone easily evaporates under normal experimental conditions. Experimental morphologies of hydroquinone in the presence of acetone were achieved in a petri-dish growth cell. The saturated solution was injected into the special growth cell and the acetone evaporated controlled at room temperature. Within 24 hours various γ -modification crystals could be observed in the petri dish.

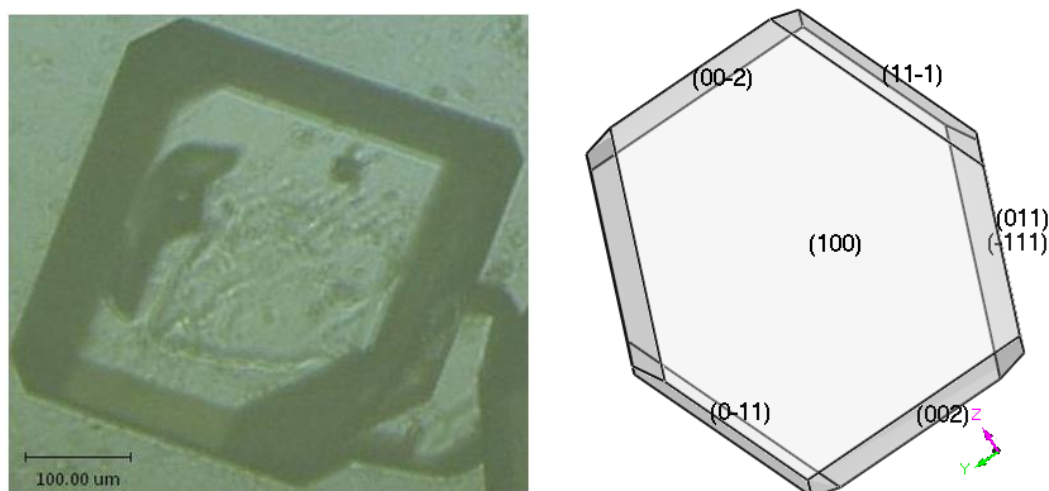


Figure 5.10: *Experimental (left) and simulated (right) habits of hydroquinone in the presence of acetone.*

As a result of the surface docking calculations for the hydroquinone crystals in the presence of acetone the frequently observed habit is produced (Figure 5.10). As a consequence of the computer simulations the $(10\bar{2})$ and (110) faces have lost their morphological importance in the presence of acetone. The attachment energy values in the presence and absence of acetone are given in Figure 5.11. Small differences in the attachment energy values indicate that morphological importance of a corresponding face decreases, hence, those faces lose their visibility. Figure 5.11 indicates that within the invisible faces of the simulated and the experimental habit the $(10\bar{2})$ and (110) faces show the highest deviations.

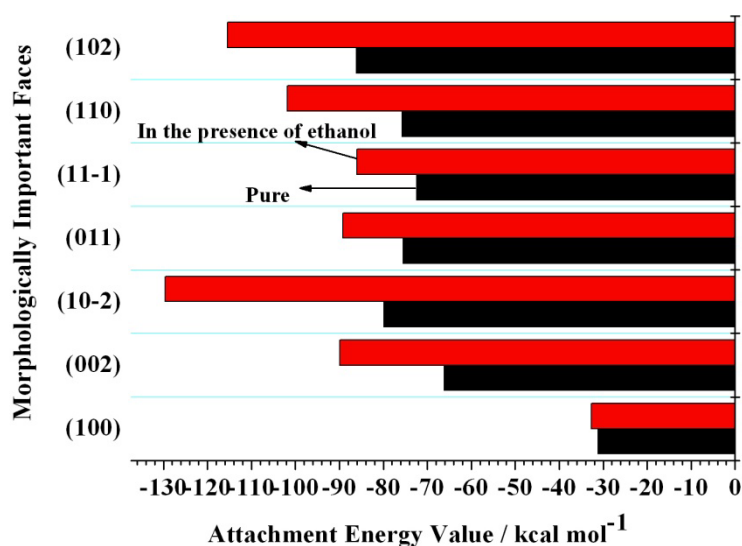


Figure 5.11: Attachment energy values of the morphologically important faces of hydroquinone. Pure hydroquinone attachment energy values are given in black and attachment energy values of hydroquinone in the presence of acetone are given in red.

5.3.3 Benzoic Acid

The mean size of benzoic acid crystals in ethanol water solution ranges from 69 to 218 μm while the aspect ratio varies from 1.3 to 10.2. The influence of process variables on the product size and shape were discussed in terms of supersaturation and of the solvent composition ([Hol99]).

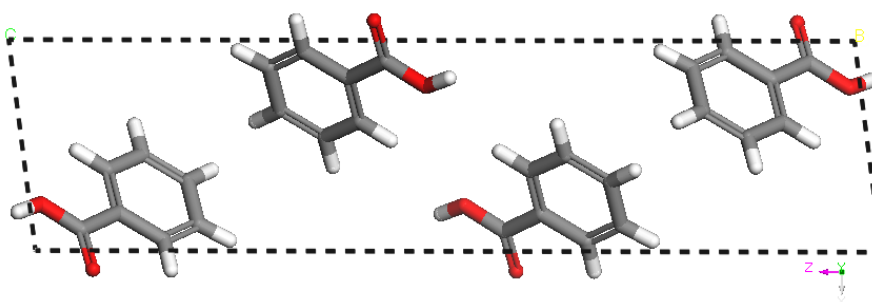


Figure 5.12: Lattice structure of the benzoic acid.

Benzoic acid has a stable habit in the presence of different kinds of additives. In order to reveal applied models accessibility experimental and computational results will be compared here.

As other sample substances, BFDH and attachment energy calculations are compared with an observed habit (Figure 5.13).

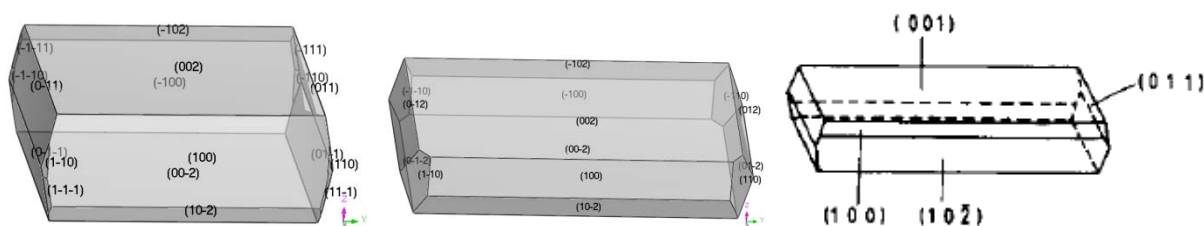


Figure 5.13: Habits of pure benzoic acid. Results of BFDH method (left), AE method (centre) and an observed crystal habit [Doc91].

Figure 5.13 indicates that the habit of pure benzoic acid can be simulated by both existed pure habit calculation methods, BFDH and AE giving similar results. Details of the attachment energy calculations are given in Table 5.5.

Table 5.5: Results of the Attachment Energy calculation of pure benzoic acid.

Surface	Attachment Energy / kcal · mol ⁻¹	Total Face Area / 10 ³ · Å ²
(002)	-13.4	14.8
(100)	-33.96	3.55
(10 $\bar{2}$)	-32.74	2.67
(011)	-63.59	0.00
(102)	-38.78	0.00
(012)	-59.72	3.04
(013)	-63.77	0.00
(110)	-63.77	0.950

Benzoic acid habit in the presence of ethanol

In order to observe the effect of the ethanol molecules on the habit of benzoic acid, the surface docking methodology is used. An ethanol molecule is docked on the suitable interaction site of every morphologically important face which was defined from the results of attachment energy calculations of pure crystals (Table 5.5).

In order to find the modified crystal habits of the benzoic acid crystals the experiments are performed in the presence of ethanol. A comparison between simulated and experimental habits of the benzoic acid crystals are given in Figure 5.14.

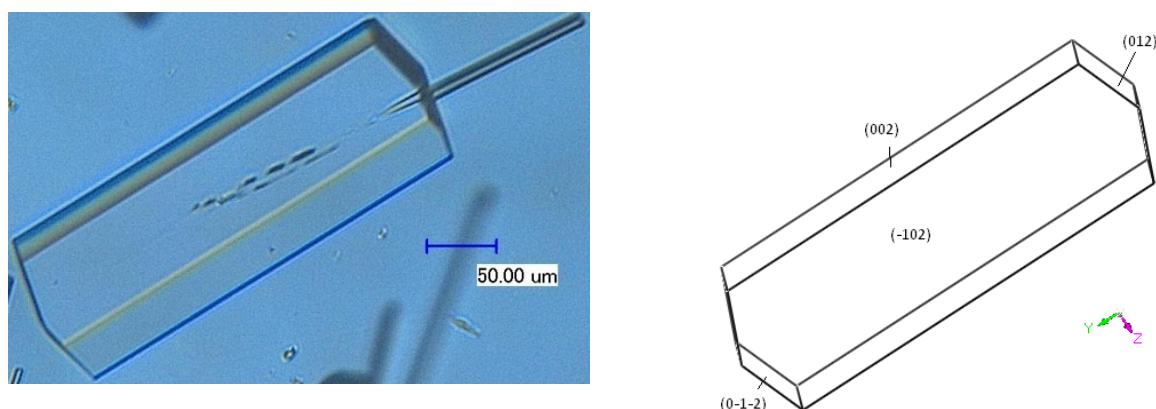


Figure 5.14: *Experimental (left) and simulated (right) habits of benzoic acid crystals in the presence of ethanol are shown.*

Experiments were carried out in the growth cell in which the saturated solution is gradually cooled from 25 °C to 17.5 °C until growth takes place. The simulated habit of benzoic acid crystals in the presence of ethanol matches the experimental habit with great accuracy.

The positive value of the attachment energy is proportional to the relative growth rate of the growing faces ($R_G \sim |E_{att}|$). Therefore, an increase of the attachment energy value leads to an increasing relative growth rate, hence, losing their morphological importance. A variation in the attachment energy values of the morphologically important faces of benzoic acid with and without ethanol is given in Figure 5.15.

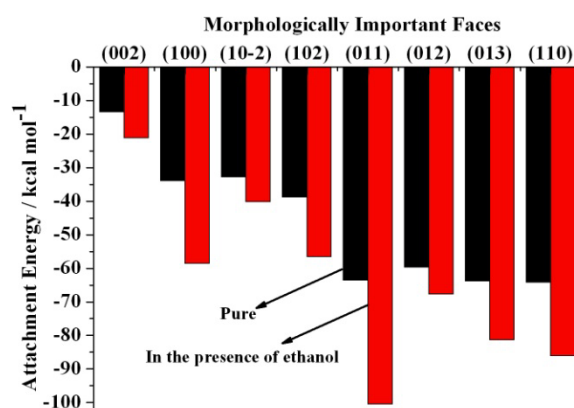


Figure 5.15: *Attachment energy values of the morphologically important faces of benzoic acid. Pure benzoic attachment energy values are given in black and attachment energy values of benzoic acid in the presence of ethanol are given in red.*

The highest variations at the attachment energy values are observed at the (100) and (011) faces. Therefore, these faces lose their morphological importance in the presence of ethanol. These faces are not significantly visible at the final morphology (Figure 5.14).

Benzoic acid habit in the presence of acetone

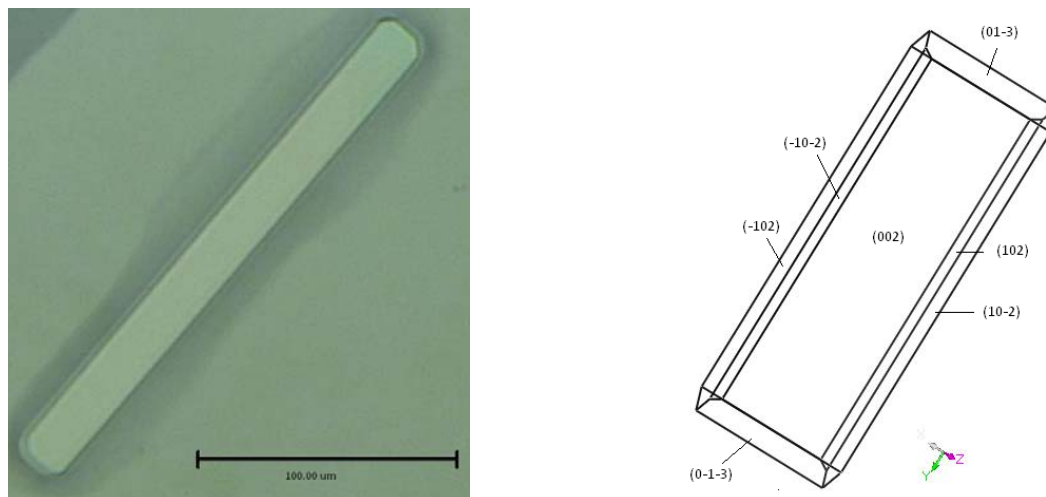


Figure 5.15: *Experimental (left) and simulated (right) habit of the benzoic acid crystal in the presence of acetone.*

The fast evaporation rate of the acetone leads to a spontaneously growth of rod shaped crystals. In order to avoid this, experiments were run in the Petri glass growth cell at room temperature. With the Petri glass cell the fast evaporation rate of the acetone was minimized and the acetone evaporated slowly. In these experiments the predicted habit of the benzoic acid crystals could be found one hour after the injection of benzoic acid-acetone mixture into the growth cell when almost the whole acetone was evaporated. The result is shown in Figure 5.15. Around the crystal the residue of the impure solution can be seen. The crystal itself is grown in a clear shape which could not be reached in the tempered growth cell.

A comparison of the attachment energy values in the absence and presence of acetone are given in Figure 5.16. The presence of acetone creates a massive deviation at the (012) and (110) faces. Acetone has no significant effect on other morphological important faces.

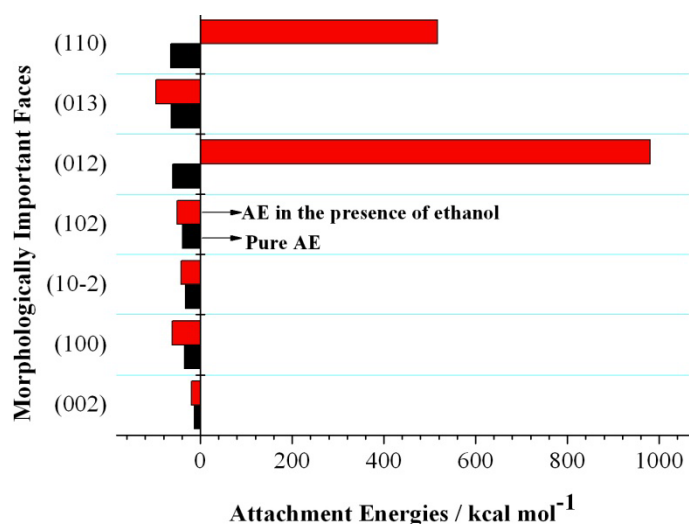


Figure 5.16: Attachment energy values of the morphologically important faces of benzoic acid. Pure benzoic attachment energy values are given in black and attachment energy values of benzoic acid in the presence of acetone are given in red.

5.4 Diffusion coefficient calculations (Figure 4.2, 3)

In the previous section some examples of useful methods and their useful results were shown. By using different main methodologies which were given in section 3.3 similar results can be produced. However, a routine methodology is still not postulated. Understanding the transport properties of the crystal liquid systems is the main priority this work. In order to simulate the transport properties of the specific materials, diffusivities of the amorphous cell simulations are simulated for the pure solute, solute-solvent and solid-liquid systems. In order to find the correct simulation conditions, different simulation conditions are tested for the simulations of the pure system.

The molecule assembly used in the simulation was set up using the amorphous cell module within the MaterialsStudio package. With this module a box of arbitrary size is filled with molecules according to user-defined criteria. The molecules are randomly placed within the box and the criterion used here to determine the size of the simulation box was the known density of benzophenone and hydroquinone at the temperature at which the simulation was carried out. The system thus created is optimised with respect to its total energy and then equilibrated at the temperature of the production run which lies above the melting point of benzophenone and hydroquinone. First, only hydroquinone or benzophenone molecules were inserted to the simulation box and system parameters were changed. Diffusion coefficient values in this part indicate the pure organic molecule diffusion in the absence of additives and

solvents. Results are given and discussed in the section “Diffusion coefficient simulations for pure solute”. Effects of the additive molecules on the physical properties of organic systems were investigated by the addition of solvent molecules into the simulation box. Findings in this section are given in the section “Diffusion coefficient calculations for solute-solvent systems”. In the final stages of the amorphous cell simulations, crystal surfaces were added to the system. The aim in this section is to simulate the growth rate of a single face by considering the transport mechanism of a solid-liquid system. The results are presented in the section “Diffusion coefficient calculations for solid-liquid systems”.

5.4.1 Diffusion coefficient simulations for the pure solute system (Figure 4.2, 3AA)

Diffusion coefficients were calculated using the linear part of the plot of the mean square displacement (MSD) against time, as obtained from MD simulations. In the initial stages of the simulations which were performed with benzophenone, the MSD displays a non-linear behaviour and as a result the diffusion coefficient decreases with increasing simulation time (Figure 5.17) and appears to approach a limiting value after a reasonably short simulation time (> 40 ps).

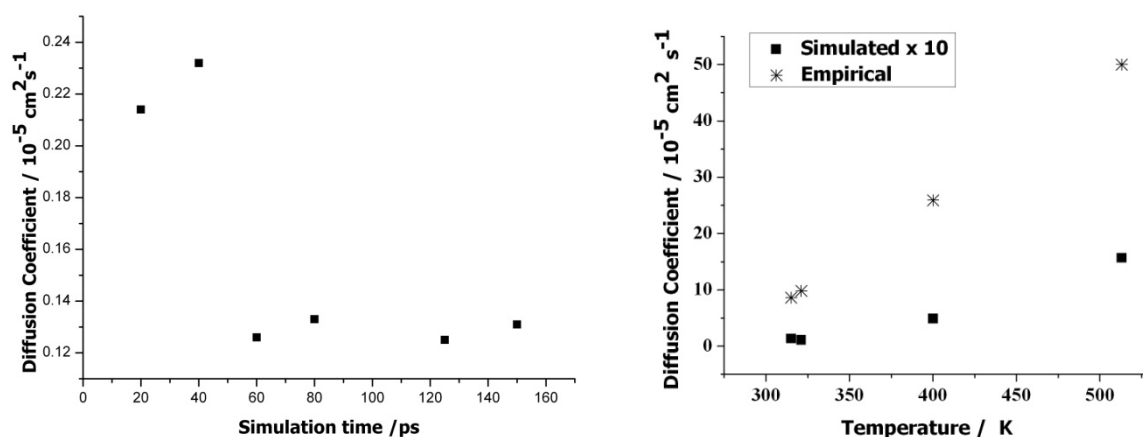


Figure 5.17: Dependence of the MSD-derived diffusion coefficient upon the MD simulation time for benzophenone (left) and temperature dependence of the diffusion coefficient (right, ■ - from MD calculations (multiplied by a factor 10), * - from Wilke-Chang empirical equation (eq. 2.23)).

In the case of benzophenone the value of the diffusion coefficients calculated using the Wilke-Chang equation (eq. 2.23) are an order of magnitude greater than the values obtained from the simulations (Figure 5.17). When accounting for the order of magnitude difference in scale, however, the tendency to change in D with T is similar for both data sets.

Table 5.18: *Influence of the force field on the diffusion coefficient on benzophenone.*

FORCE FIELD	Diffusion Coefficient /10⁻⁵ (cm²/s)	R²
COMPASS	0.214	0.99949
PCFF	0.228	0.99934
CVFF	0.091	0.99754
CFF91	0.120	0.99938

The influence of different force fields upon the simulation of benzophenone is shown in Table 5.18. The linear regression is successful for all force fields used ($R^2 > 0.99$). The diffusion coefficients do not differ significantly in response to the force field changes and stayed one order of magnitude lower than the empirical diffusion coefficient value. As in the case of varying simulation time, the diffusion coefficient appears to be underestimated, but it is important to remember that the data used for the comparison are estimated values based upon an empirical equation and not on real experimental data.

Since the morphology of benzophenone has no significant differences in the presence of additives (chapter 5.3.1) and the diffusion property is underestimated, benzophenone is not considered any further in this work.

Similar calculations were performed for hydroquinone for different system sizes, different simulation times and for the different force fields (Table 5.19). The diffusion coefficients for hydroquinone are an order of magnitude larger than for benzophenone and are in good agreement with the empirical values. For the simulations which are performed by using hydroquinone molecules, empirical values are also calculated with other empirical equations (Dullien equation, eq. 2.20). Simulated diffusion coefficient values for the hydroquinone molecule are in good agreement with empirical diffusion coefficient values which are calculated with the Dullien method. Some of the results for different conditions are given here.

Table 5.19: *Effect of the different temperature control methods on diffusion coefficient values of hydroquinone.*

Thermostats	Diffusion Coefficient / $10^{-5} \text{ cm}^2 \cdot \text{s}^{-1}$
Velocity Scale	2.041
Berendsen	1.223
Andersen	0.604
Nose	1.156
Velocity Scale (Eq) + Berendsen (Dyn)	1.42
Velocity Scale (Eq) + Andersen (Dyn)	0.58
Velocity Scale (Eq) + Nose (Dyn)	1.683

Table 5.19 indicates the effects of the different temperature control methods to the transport coefficients of the hydroquinone molecules. Simulated system contains 100 hydroquinone molecules. It was simulated at 450 K simulation temperature and 100 ps simulation time by 1fs simulation frame. For given conditions the empirical diffusion coefficient value is calculated to be $2.9 \cdot 10^{-5} \text{ cm}^2 \cdot \text{s}^{-1}$. For minor different conditions the empirical diffusion coefficient value varies in same order. For higher temperature values diffusion coefficient values are $3.1 \cdot 10^{-5} \text{ cm}^2 \cdot \text{s}^{-1}$ and $3.4 \cdot 10^{-5} \text{ cm}^2 \cdot \text{s}^{-1}$ for 310 K and 333 K, respectively. Even though, simulations which were performed with the velocity scale method give a closer diffusion coefficient value to the empirical value, for dynamics simulations the velocity scale method is not recommended since it is simplistic nature for dynamics simulation calculations. Simulations with Berendsen and Nosé thermostats give results relatively closer to the empirical values. In the presence of the right simulation conditions exact results can be obtained. The velocity scale method is a useful method for equilibration runs which prepares the working system (materials) for the dynamics calculations. The Berendsen and Nosé thermostats with velocity scale equilibrations produce the closest diffusion coefficient values compared to the empirical values (Table 5.19).

Other important simulation conditions are the starting geometry of the molecules within the amorphous cell and the applied force fields during the simulations. Since inter- and intra

molecular interactions are the main reason for the diffusion of the current system, effects of the starting geometry and calculation methods of inter- and intra molecular interactions (force fields) are given here.

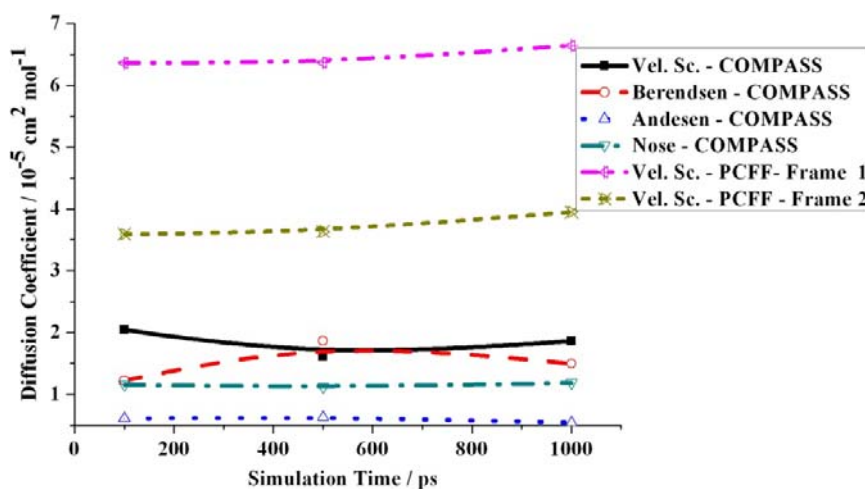


Figure 5.18: Effects of the starting geometry and used force field to the diffusion coefficient value for different simulation duration. Frame 1 and 2 represent different starting positions.

The importance of the force fields and the starting geometries can be seen in Figure 5.18. Diffusion is a physical process which needs a concentration difference to occur. In case of an amorphous system in this work molecules are well distributed within the amorphous cell. Interactions of the molecules create molecular movements. Considering molecular movements the Stokes-Einstein relation generalizes the diffusibility of the molecules within given conditions. Therefore, calculation methods of the interaction energies and the starting geometries have a significant effect on the final diffusion coefficient values.

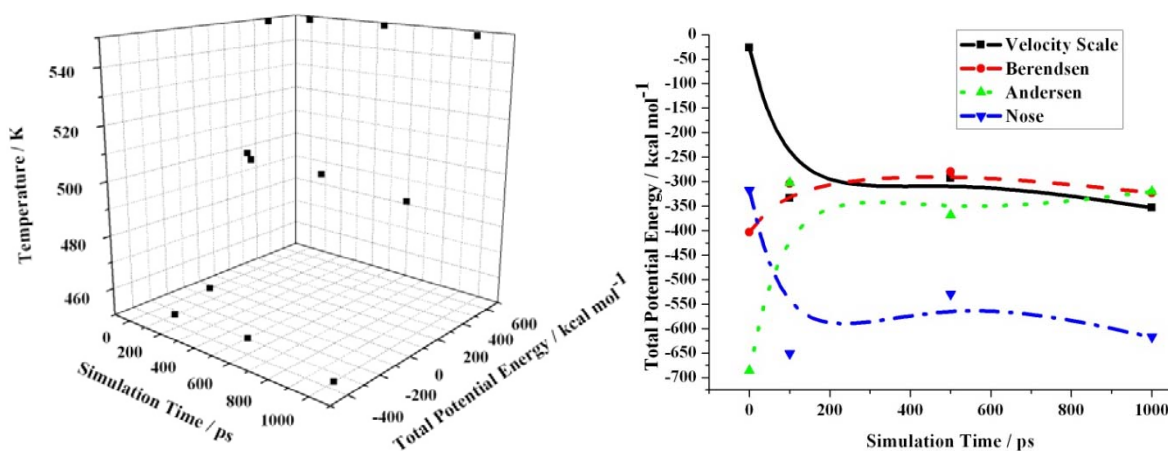


Figure 5.19: Total potential energy values of the simulations (left) performed with the velocity scale algorithm for different temperatures and simulation times, (right) for different temperature control algorithms.

A significant effect of the temperature control methods is given in Figure 5.19. On the first graph (left) the velocity scale method controls the temperature, hence, the majority of the total energy, in a similar manner. For different temperature values the total energy value is controlled by a similar tendency. On the second part of the Figure 5.19 effect of the methodology of the temperature control methods on total potential energy can be seen. Every single temperature control method - the thermostat in computer simulation language – has a separate method to control the temperature. The velocity scale-Nose thermostats and the Berendsen-Andersen thermostat familiarities can easily be distinguished.

5.4.2 Diffusion coefficient simulations for the solute solvent system (Figure 4.2, 3AB)

Simulations for the pure organic system (section 5.4.1) are not completely informative for a crystal growth mechanism. However, in order to be able to evaluate the effects of the solvents to the diffusion mechanism solely and obtaining the correct simulation conditions for the more relevant simulations, pure organic system simulations show a critical importance. Simulation experiences which were acquisitioned from pure organic system simulations will be used for the rest of this work.

In the second part of the results, the simulated diffusion coefficients in the presence of solvent molecules were compared with experimental diffusion coefficient values which are available in the literature.

The size and number of molecules present in the simulation box is determined by physical properties such as solubility and density of the system. Experimental solubility and density values at different temperatures [Li06, Tak96] were used to calculate the required numbers of the respective chemical species (Table 5.20). A suitable choice of the ratio of ethanol and hydroquinone molecules in the simulation box allows the diffusion coefficient to be determined as a function of (super)saturation (Table 5.20).

Table 5.20: *Hydroquinone /ethanol ratio at the saturation point and 100 kPa.*

Temperature /K	Density /g·cm ⁻³	Mole Fraction Solubility	Ethanol-Hydroquinone ratio
293	0.789	0.182	4.47
298	0.787	0.191	4.27
310	0.776	0.212	3.71
313	0.772	0.226	3.74
323	0.763	0.239	3.18
333	0.754	0.246	3.06
340	0.747	0.28	2.57

Molecular dynamics simulations for the amorphous cells were performed for different degrees of supersaturation. Solute-solvent mixtures are placed into the simulation box in two different initial arrangements. In the first arrangement, separate slabs of solute and solvent molecules are placed within the simulation box. In the second case, a completely random distribution of the solute and solvent molecules is generated. Both starting geometries of the simulation boxes are illustrated in Figure 5.20.

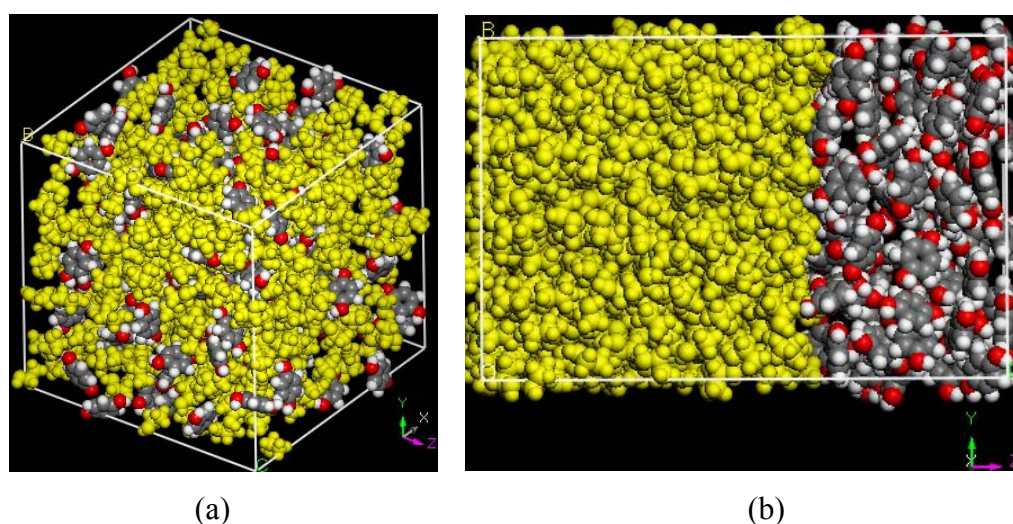


Figure 5.20: *Different initial arrangements of solute and solvent molecules: 100 hydroquinone (grey (carbon), white (hydrogen) and red (oxygen)) and 427 ethanol (yellow) molecules a) randomly located, b) separated located.*

Simulated diffusion coefficients were determined with respect to the different force fields, temperature values, location and arrangements of the molecules within the simulation box (Figure 5.21).

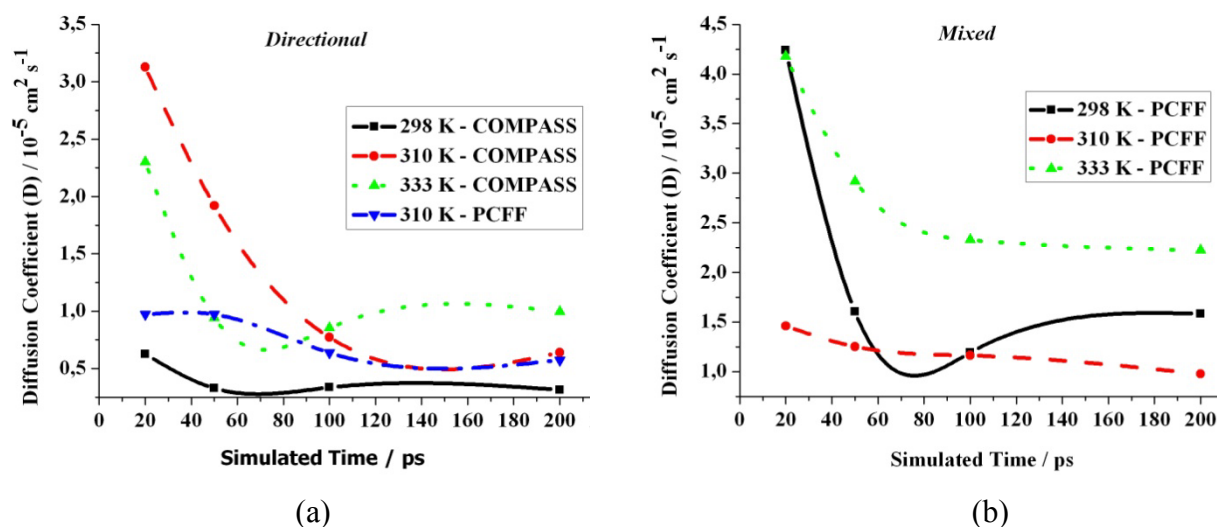


Figure 5.21: Dependence of the MSD-derived diffusion coefficient upon the MD simulated time for the hydroquinone-ethanol system at low saturated value and different system conditions such as temperature, force field and starting geometry. Molecules placed a) completely separated hydroquinone and ethanol molecules as starting geometry, b) randomly mixed hydroquinone and ethanol molecules as starting geometry.

Simulations were performed with hydroquinone and ethanol as solvent. Here, the diffusion behaviour is observed at very small supersaturation values (the relative supersaturation, (C/C_0) , is 1.007). According to the current simulations at small saturation values the diffusion coefficient value of hydroquinone at simulation times (around 70 ps) reaches a minimum value for the separated solute – solvent initial configuration (Figure 5.21a). Between 70 ps-100 ps simulation time the diffusion coefficient reaches a constant value and towards the end of this time interval the diffusion coefficient starts to increase marginally. The observed increases and decreases in Figure 5.21a are caused by the structure/arrangement of the molecules in the simulation box observed over time (Figure 5.21) with the system approaching a homogeneous mixture of the two components for the simulations performed with the COMPASS force field at 333K. As a result the dynamics simulation times given are not sufficient to extract the bulk diffusion coefficients if two species are initially separated. However, amorphous cell simulations were performed in order to be able to explain the movements of the molecules under the given conditions.

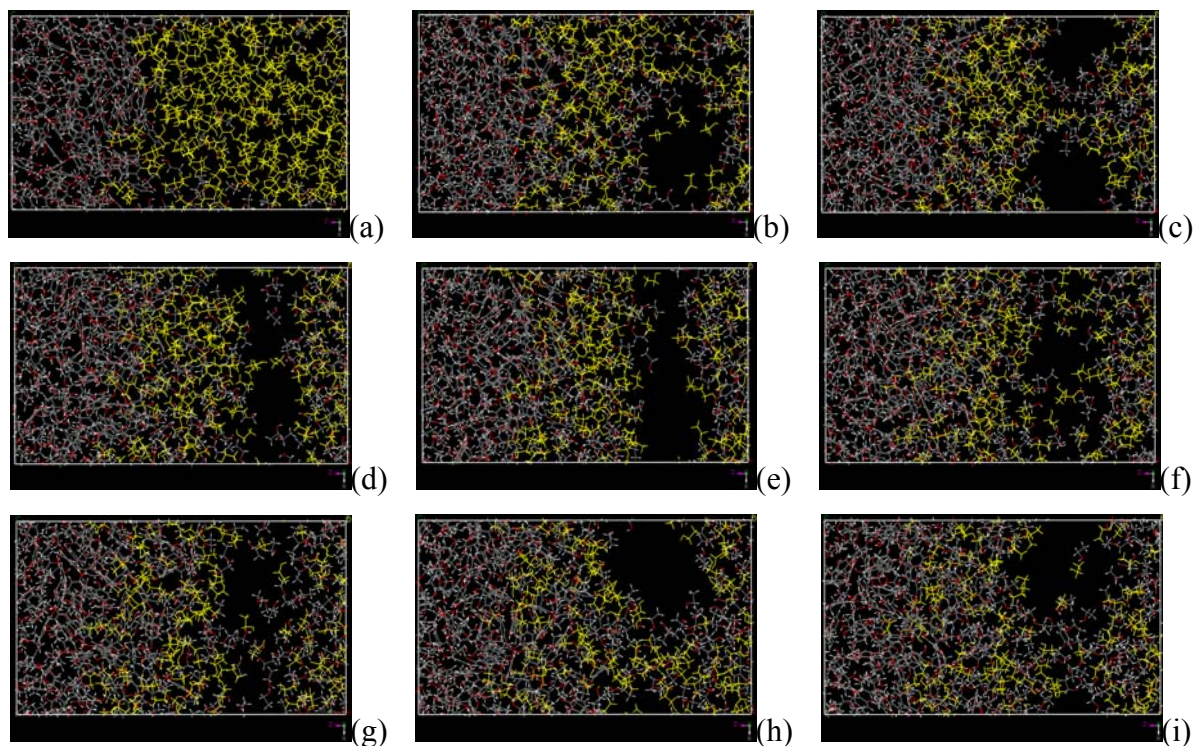


Figure 5.22: Snapshots of different frames of the simulation which were performed with 100 hydroquinone and 307 ethanol molecules at 333 K. Frame numbers: a) 1 ps, b) 60 ps, c) 70 ps, d) 80 ps, e) 100 ps, f) 130 ps, g) 150 ps, h) 175 ps and i) 200ps.

The positions of the hydroquinone and ethanol molecules for different frames are given in Figure 5.22. Changes of the curves in Figure 5.21a can easily be explained using the snapshots. During the simulation the first 60 ps small movements between hydroquinone and ethanol molecules are observed (Figure 5.22a and b) due to mixing. In order to assign hydrogen bonding during the calculation O and C as donors are selected. In that selection the maximum length of the hydrogen bond geometry is 2.5 Å and the angle of the donor-hydrogen-acceptor bonding is within the range of 90° to 180°. Carbon is selected as donor, Oxygen is selected as acceptor. When the entire system is considered diffusion of ethanol molecules into the hydroquinone molecules and diffusion of a number of hydroquinone molecules into the ethanol molecules leads to a measurable diffusion difference at 60 ps. Hydroquinone molecules are located at positions where they change their positions slightly because of the interaction distances, at this simulation time and the positions lead to less movement of these molecules. Therefore, the diffusion coefficient value decreases. A clear molecular level structuring can be observed between the simulation times of 60 ps and 100 ps (Figures 5.22 c, d, and e). At 100 ps two different molecular level structurings can be observed easily (Figure 5.21 e). The reason for the separation may be the scale of the simulation. This apparent separation is an overinterpretation of the data as in the bigger

picture it merely represents a momentary fluctuation that is to be expected. The distance between the two groups of molecules is higher than the maximum distance allowed for hydrogen bonding to be effective. However, the concentration difference between these two groups of molecules leads only to little diffusion. Hence, a small increase in the diffusion coefficient values is observed again (Figure 5.21a and Figures 5.22 f, g, h and i). At 200 ps, back diffusion can be observed and is likely to be the reason for the evident concentration differences (Figure 5.22 i).

Effects of the higher supersaturation values are going to be discussed later. However, in order to assess the results for the further stages of this section the current results are examined. It is important to understand the possible reason for the structuring in Figure 5.22 for the later stages of this work. Therefore, some detailed results for this simulation are given here.

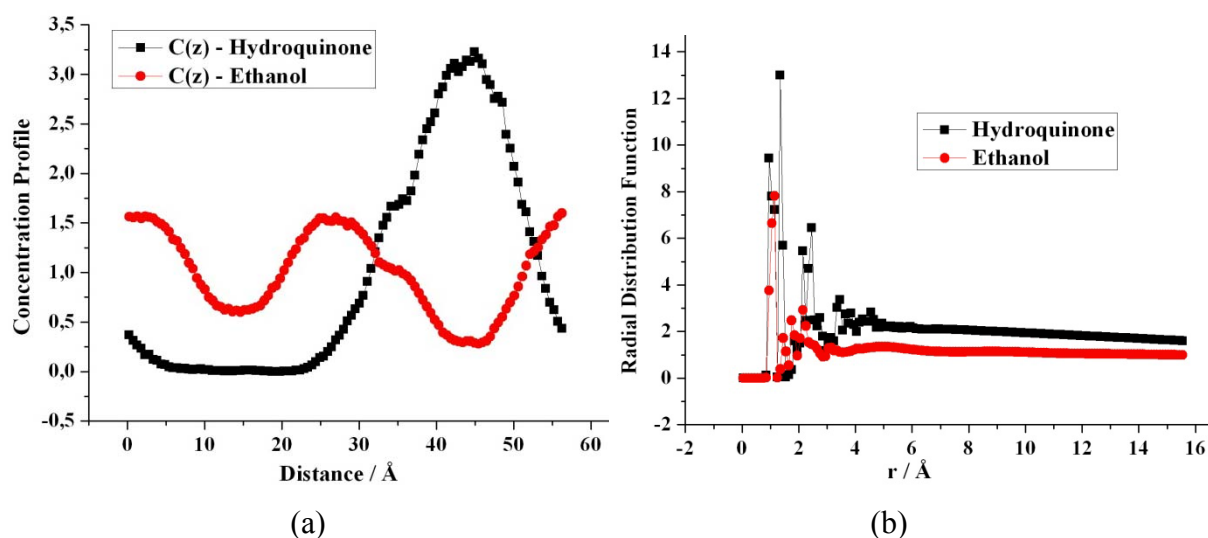


Figure 5.23: Concentration profiles of hydroquinone and ethanol in z direction (a) and total radial distribution function (b).

The concentration profiles of hydroquinone and ethanol molecules are significantly different in z direction compare to the x and y directions. At the first 30 Å the ethanol molecule concentration profile changes while the hydroquinone concentration profile remains constant (Figures 5.22 and 5.23a). This indicates that ethanol molecules move within this distance and prepare the system for the next movement. The length of the amorphous cell is 56.5 Å and the concentration profile deviations appear around 45 Å for both molecules. While the hydroquinone molecule concentration profile increases, the ethanol molecule concentration profile decreases at same distance. For the higher distances hydroquinone and ethanol concentration profiles show the contrary tendencies.

The radial distribution function (RDF) describes the probability of finding a particle in the distance r from another particle. In other words, RDF, $g(r)$, is an effective way of describing the average structure of a discovered molecular system such as a liquid. Also in systems like liquids where there is continual movement of the atoms and a single snapshot of the system shows only the instantaneous disorder, it is extremely useful to be able to deal with the average structure. Detailed information on the RDF can be found in literature [Han86]. In Figure 5.23b, the total radial distribution functions of hydroquinone and ethanol molecules are given. At short distances (less than atomic diameter) $g(r)$ is zero. This is due to the repulsive forces. The first (and large) peak for both molecules occurs at $r \approx 1.5 \text{ \AA}$ with $g(r)$ having values 13 (for hydroquinone) and 8 (for ethanol). This means that it is 13 (8) times more likely that two hydroquinone (ethanol) molecules would be found at this separation. The radial distribution function then falls and passes through a minimum value around $r \approx 2 \text{ \AA}$. The chances of finding two atoms with this separation are less. At long distances, $g(r)$ approaches one which indicates there is no long range order.

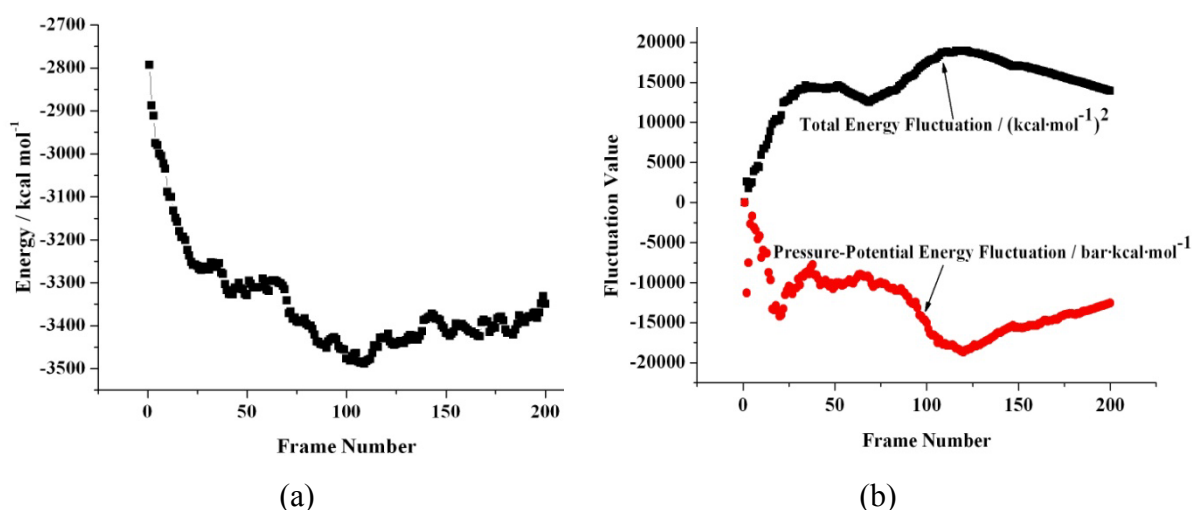


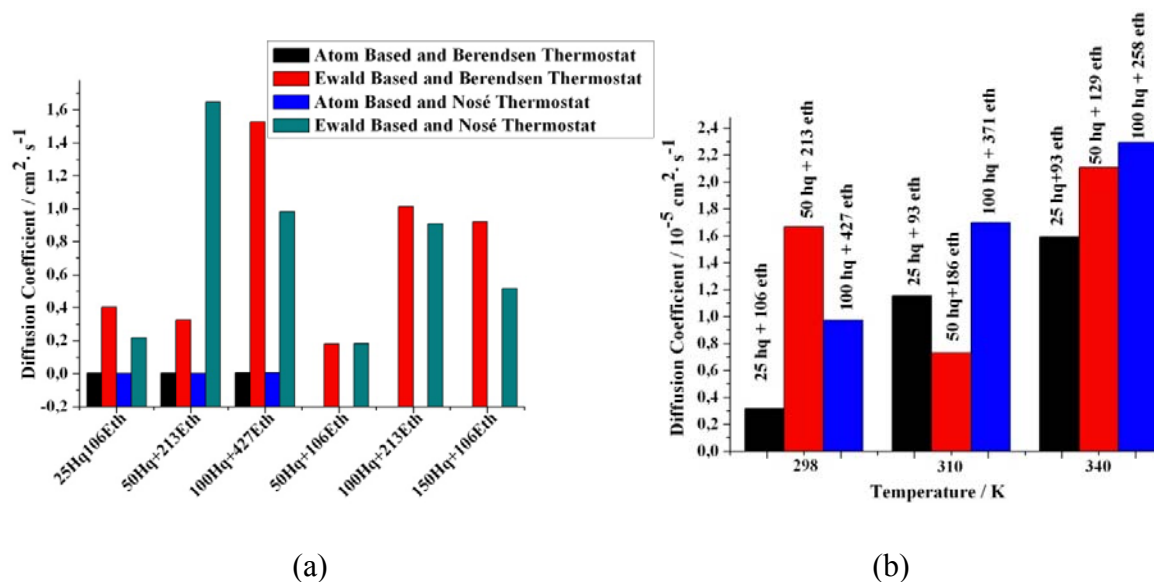
Figure 5.24: Total energy variation during the dynamic simulation (a) for the same system in Figure 5.21 and 22. Energy fluctuations during the entire final dynamics simulation (b).

The total energy variation during the 200 ps dynamics simulation duration is given at Figure 5.24a. The energy variation during the entire simulation may give a clearer explanation for the structuring in Figure 5.22. Potential energy fluctuation is the major part of the total energy fluctuations (Figure 5.24b and Table 5.21). Numerical energy values of all molecules within the amorphous cell considering the start and the end simulation frames are given in Table 5.21.

Table 5.21: Summary of dynamics simulations for 100 hydroquinone and 307 ethanol molecules at 333K.

Quantity	Initial	Final	Average	Std.Dev.
Tot. Energy / kcal·mol ⁻¹	-2606.87	-3349.53	-3348.90	123.670
Pot. Energy / kcal·mol ⁻¹	-5460.93	-6199.48	-6205.95	122.380
Kin. Energy / kcal·mol ⁻¹	2854.05	2849.95	2857.05	32.79
Temperature /K	333.0	332.52	333.35	3.83
Pressure /GPa	-0.239	-0.037	-0,062	0.02

After detailed examinations of the dynamics simulations which were performed in the case of the completely separated solute-solvent system, results of the completely random mixed solute-solvent system simulations for different simulation conditions such as high supersaturation value are given here.

**Figure 5.25:** Diffusion coefficient values of the hydroquinone-ethanol solute solvent system for different molecular interaction calculation methods, thermostats and supersaturation values.

In Figure 5.25 effects of the different simulation conditions on the diffusion coefficient value of hydroquinone in the presence of ethanol are given. In Figure 5.25a simulations were performed with the Compass force field, different temperature scaling algorithms

(thermostats) and different interaction energy calculation algorithms at 298 K for different supersaturation values. Atom based interaction energy calculations lead to high deviations in the diffusion coefficient compared to the experimental values. As it was expected simulations which are performed with the Ewald summation method supply relatively closer diffusion coefficient values to the experimental values. In Figure 5.25b similar simulations were performed with the PCFF force field, different supersaturation values and different temperatures. Even though, increasing supersaturation values lead the increase of the diffusion coefficient values, it could not create a hierarchical effect on the lower temperature values. However, at higher temperature values (Figure 5.25b) diffusion coefficient values increase with increasing supersaturation values, as it was expected. In the presence of ethanol simulations can be evaluated by experimental values. The experimental diffusion coefficient value of hydroquinone in the ethanol solution at 298K temperature is $0.595 \cdot 10^{-5} \text{ cm}^2 \cdot \text{s}^{-1}$. Diffusion coefficient values of the pure hydroquinone molecule vary between ~ 2 to $5 \times 10^{-5} \text{ cm}^2 \cdot \text{s}^{-1}$. Relevant computer simulation results for diffusion coefficient values are matching these values. In the presence of ethanol molecules in simulations, diffusion coefficient values also decrease as in the experimental diffusion coefficient values. Hence, simulated diffusion coefficient values match with relevant empirical and experimental values for different simulation conditions (Figure 5.25).

5.4.3 Diffusion coefficient simulations for the solid-liquid system (Figure 4.2, 3AC)

Crystal growth takes place by mass deposition of the growth units on the crystal surface under relevant interaction mechanisms. Similar simulations are performed in the presence of the solid surface. Morphological important faces (MIF) are selected to be examined because of the high probability to grow. MIF interact strongly with the growth units compared to the other faces. Prywer [Pry02] confirmed the fact, which had been concluded by the BFDH method, that the larger the interplanar distance is the more morphologically importance the corresponding crystal face has. Therefore, a crystal growing under realistic conditions possesses a limited number of faces which are the ones growing most slowly. Hence, only the faces that are morphologically important and do not disappear fast such as (100), (002), (10 $\bar{2}$), (011) and (11 $\bar{1}$) will be considered. Morphological important faces are defined by the results of the attachment energy calculations (section 5.3). Basic cleaved crystal surfaces are given in Figure 5.26.

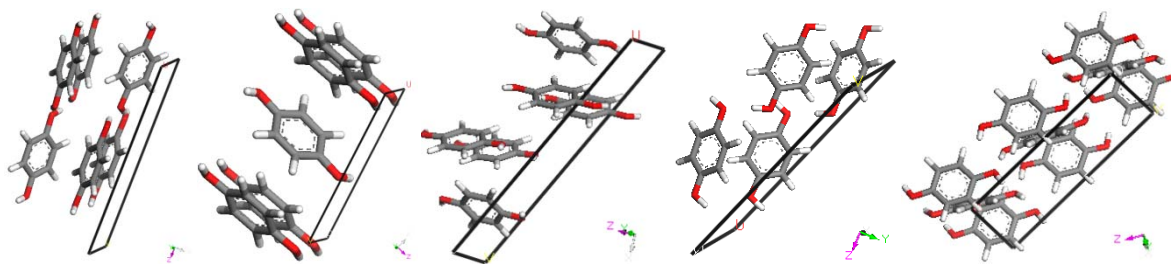


Figure 5.26: Basic moieties of the morphological important faces (100) , (002) , $(10\bar{2})$, (011) and $(11\bar{1})$, respectively.

When hydroxyl groups are oriented perpendicular to the surface, this face is considered a polar face [Hen09]. The growth rate of polar faces can be affected by the presence of polar substances in the surroundings. Therefore, the $(10\bar{2})$ and the (011) faces can be classified as polar and (100) , (002) and $(11\bar{1})$ faces are semi-polar. Theoretically polar and semi-polar faces are able to have strong molecular interaction with the hydroxyl parts of the hydroquinone and ethanol molecules. Non-polar surfaces generally have no intensive interest to the additives and hydroquinone molecules.

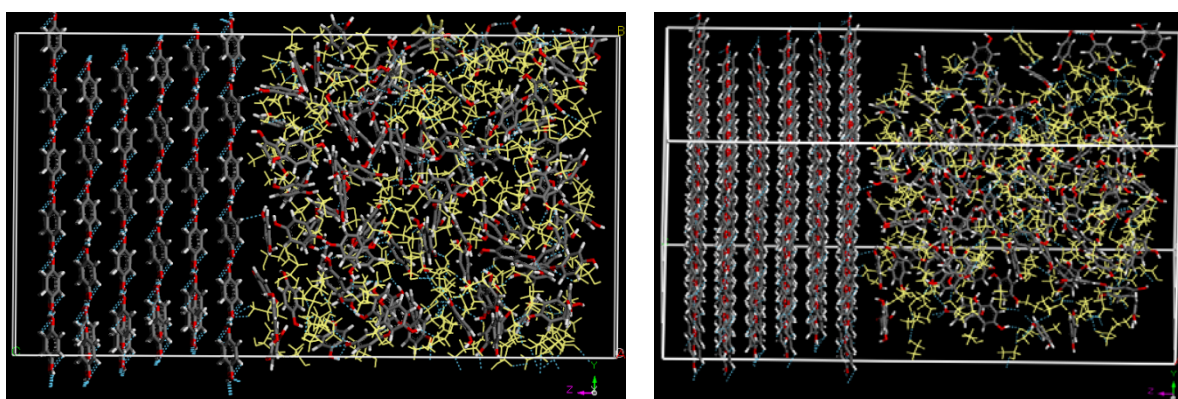


Figure 5.27: An example for solid liquid amorphous cell structure is given. Results of the simulation of the amorphous cell which contains 100 hydroquinone and 213 ethanol molecule combined with (100) surface of the hydroquinone crystal here. In order to obtain a similar cell size with the amorphous cell the (100) face structure is modified to a supercell by increasing the size 7×7 times the unit cell dimensions and fixing them.

Results from the simulation of the hydroquinone and ethanol amorphous cell (section 5.4.2) are expanded to the presence of a solid surface. The solid surface and the hydroquinone-ethanol solution are combined depending upon the hydrogen bonding interactions. Supercells are generated in order to obtain a solid surface depending upon the amorphous cell dimensions. The positions of the hydroquinone molecules in the solid part (crystal surface) of

the solid-liquid cell are fixed (Figure 5.27). Therefore, during the dynamics simulations positions of the hydroquinone molecules in the solid part are not affected by the system conditions. An example of solid-liquid amorphous cell structure is given in Figure 5.27:

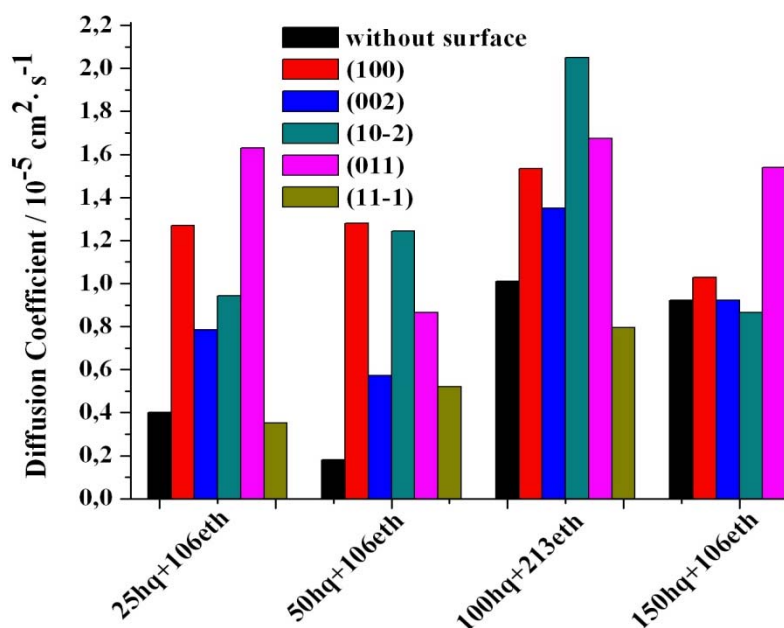


Figure 5.28: Diffusion coefficient values of hydroquinone in the amorphous cell part of the solid-liquid system. Different supersaturation degrees combined with different morphological important faces.

Simulations are performed for the different degrees of supersaturation. Figure 5.28 indicates that diffusion coefficient values increase in the presence of solid surfaces. However, diffusion coefficient values in this case represent only parallel diffusion to the crystal surface since the presence of the solid surface breaks the symmetry. The Einstein relation is valid only for total symmetrical systems [Liu04]. Parallel diffusion coefficient values may give useful hints for the surface growth mechanism. In Figure 5.28 the highest increase in diffusion coefficient values are observed for the (10 $\bar{2}$) face and 100 hydroquinone/213 ethanol solution simulation. Solid - liquid amorphous cell dynamic simulation snapshots help to understand the increase.

It is difficult to evaluate the high diffusion coefficient value in the presence of solid surfaces. The high mass increase may result an increase on the growth rate of the surface and may cause to lose the morphological importance of this face. On the other hand diffusion of growth units is required for the face in order to keep its importance. In order to find a clearer explanation the growth mechanism has to be known at given conditions. However, understanding the behaviour of molecules at different system conditions remains the first priority here.

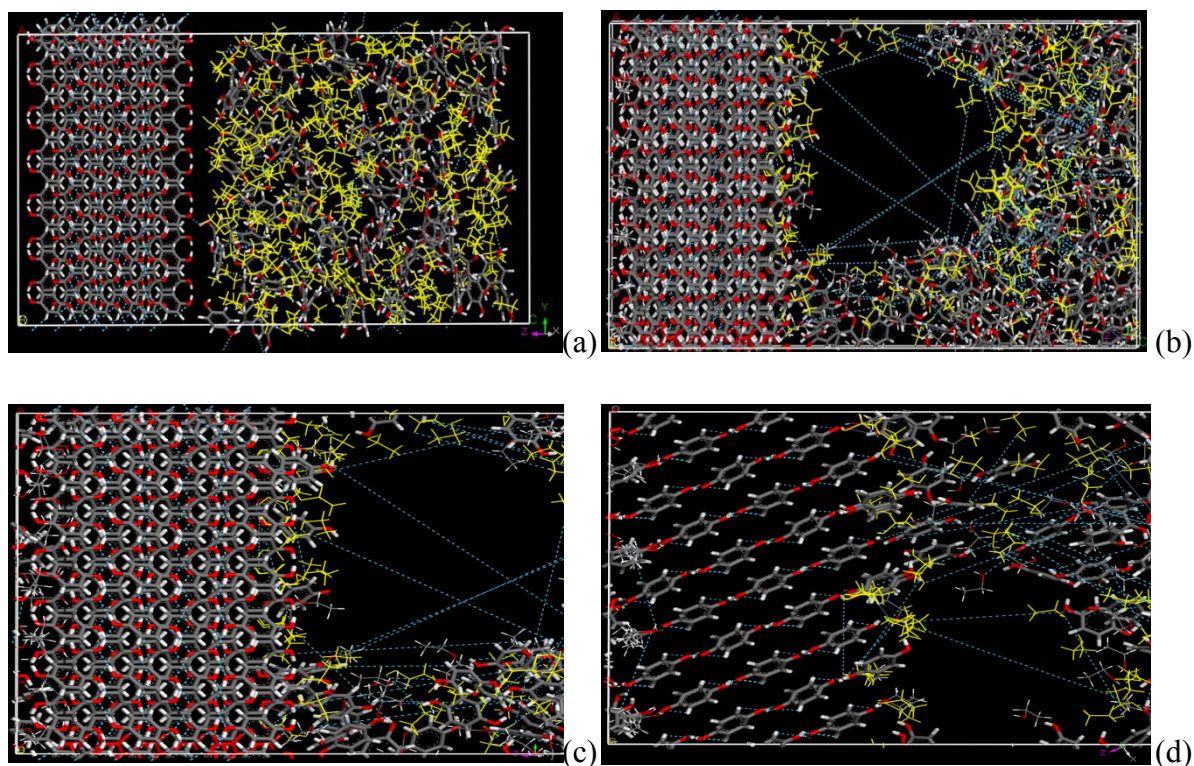


Figure 5.29: *Dynamic simulation snapshots for the $(10\bar{2})$ surface and 100 hydroquinone / 213 ethanol solution. a) $t = 0$ ps, b) $t = 100$ ps, c) a close look to the situation at $t = 100$ ps, d) a close look to the situation from a different angle at $t = 100$ ps.*

Positions of the molecules in the solid - liquid system simulations are given in Figure 5.29. For a starting geometry a reasonable starting position depends upon the hydrogen bonding between the solid and the solution (Figure 5.29a). At the end position of the simulation ($t=100$ ps) a group of molecules are separated from the rest of the hydroquinone/ethanol solution and are located on the solid surface (see Figure 5.29b). Close looks to the final positions of the molecules (Figures 5.29 c and d) indicates that small groups of ethanol molecules are mainly docked on the crystal surface by an interaction of the hydroxyl group of ethanol with the polar parts of the $(10\bar{2})$ face. The reason of the increase at the diffusion values in the presence of solid surface can be explained as the contribution of the surface diffusion on the crystal surface. The presence of ethanol molecules on the $(10\bar{2})$ face leads some hydroquinone molecules from the solution part to hold on the crystal surface. Therefore, the presence of solute hydroquinone molecules together with the ethanol molecules on the crystal surface leads to surface diffusion. As a result of this an increase of the diffusion coefficient value is observed.

In order to see the molecular arrangement of the solute and solvent molecules another example which supports the mentioned assumption is given in Figure 5.30. In Figure 5.30 the same $(10\bar{2})$ face is combined with a lower number of molecules (25 hydroquinone and 106 ethanol molecules) in order to see the interactions more clearly. Small groups of ethanol molecules and their positions on the $(10\bar{2})$ face is noticeably seen. A single hydroquinone molecule is covered by sufficient ethanol molecules and takes position on the $(10\bar{2})$ face.

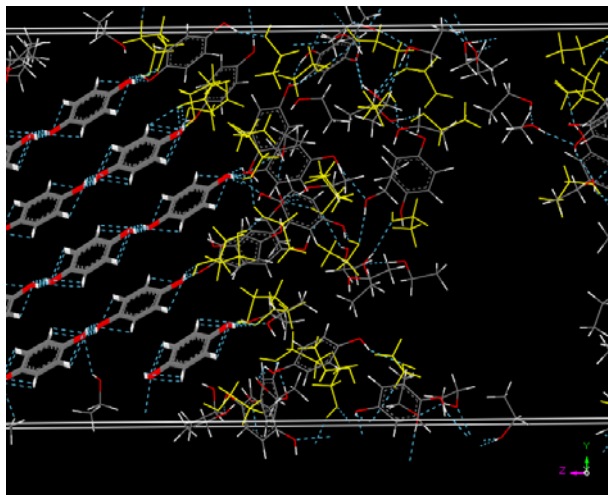


Figure 5.30: The $(10\bar{2})$ face and 25 hydroquinone and 106 ethanol molecules. Interactions between ethanol and hydroquinone molecules from the amorphous part and their contribution to the surface growth mechanism can easily be seen.

6. Discussions

The growth rate of a crystal face is an expression of the rate of mass deposition onto the crystal surface. In order to deposit mass onto the surface, it must be brought into the vicinity of the crystal and this is achieved by mass transport. The overall rate of the mass transport should account for all different kinds of processes such as solvent adhering, desolvation of solute, dissolution or displacement of adsorbent, etc. For the purpose of this discussion, these processes are not treated explicitly. One further factor that is ignored in the discussion of crystal growth rates is heat transfer and the coupling thereof to the mass transport. It is assumed that the heat transport is a negligible factor and that heat dissipation is achieved such that it must not be explicitly treated in the discussion of crystal growth.

6.1 A general overview at the “discussions” chapter

In the previous chapter the results of molecular modelling studies of different model systems at different simulation conditions were presented. Computer simulation data are compared with experimental or empirical data which are available in the literature. Simulations were performed by using organic model systems such as benzophenone, hydroquinone and benzoic acid. In order to investigate the transport properties of the organic systems by a computationally simulation methodology they are brought in a logical order. First organic sample molecules are optimized in order to obtain the right molecular structure and to test the simulation tools such as force field, summation method, working temperature and etc (Figure 4.2, 1). Second main stage of the results chapter is to define the morphological important faces and find the morphology of the working systems without (Figure 4.2, 2C) and with impurity effects (Figure 4.2, 2D). In order to find the final morphology with and without additives the attachment energy and the surface docking method were used, respectively. After this section benzoic acid is not considered for the further stages of the results because the simulated habit of benzoic acid is a good agreement with experimental habit. One of the important evaluation and comparison parameters for the simulated and experimental habits is the habit aspect ratio. Depending upon the value of habit aspect ratio many physical and chemical properties can be defined such as unique electronic and optical properties [Liu07]. The next section after the morphology calculations are the simulations of transport properties (Figure 4.2, 3) of the working systems within an amorphous structure (Figure 4.2, 3A). This part has also different stages according to the simulation setup. In the first instance, simulations were carried out using a system representing a liquid phase for the pure organic system (Figure 4.2, 3AA). It means organic model systems are filled into an amorphous cell

in the absence of additives or solvents. Molecules are located randomly and they are able to move freely without any motional constraints within the amorphous cell. Results of this part are evaluated with the well known empirical equations [Wil55, Dul63]. The outcome of this part is used for the next stage which is the determination of the transport properties in the presence of solvent molecules for various supersaturation values (Figure 4.2, 3AB). Evaluated simulations for the transport properties of organic systems in the presence of solvent molecules are in a good agreement with experimental values. The final stages of the transport property simulations are the simulations of the transport properties of organic molecules in the presences of solvents and solid crystal surfaces (Figure 4.2, 3AC). Once more the outcomes of the previous stages are used in this section. The findings of the final amorphous cell simulations are used in the face growth rate calculations (Figure 4.2, 3B and 3C). Here details of every single section and findings are discussed intensively.

6.2 Molecule structure optimization (Figure 4.2, 1)

Geometry optimizations of single organic molecules are performed in order to obtain the correct molecular structure of the molecules. The reason for that single molecule geometry has an important effect on the results of the rest of the work (amorphous cell simulations). To evaluate the molecular geometry conformation deviations in several dimensions such as distance, angle and torsion angles are measured and results are compared with the literature data. Simulations were performed with different kinds of calculation algorithms such as molecular mechanics and semi-empirical ones.

In later stages of this chapter, it will be seen that physical properties of working samples are different. The results of the molecular dynamics simulations indicate that the benzophenone molecules experience an increase in the torsion angle. For benzophenone, molecular geometry optimizations indicate that only minor average deviations are obtained when molecular mechanics optimization methods are used (Table 5.1). Therefore, a slightly more “bent” structure is obtained. This results in larger deviation from planarity for benzophenone. Within the given methods, the molecular dynamics simulations which were performed with the Dreiding force field give the best condition for a comparison to literature values (Table 5.1). Simulations which are performed with the Compass force field have also a close approximation to the literature data. Here it should be kept in mind that the Compass force field has its own partial charges which are different than in the Dreiding force field. Regardless of the charge calculation method the Compass force field attains the charge values of a molecule according to the results of its own charge calculation method. Charging

algorithm is also an important effect for the molecular geometry. Hence, the molecular structure of benzophenone has a bent shape after the simulations (Figure 6.1).

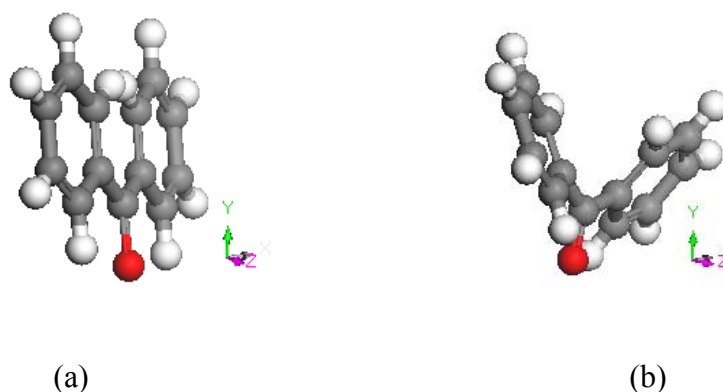


Figure 6.1: A single benzophenone molecule a) before optimization, b) after optimization.

In contrast, the geometry of the hydroquinone molecules is planar, as expected (Table 5.2). A change in torsion angle for the hydroxyl-hydrogen atoms was not observed for hydroquinone. For the hydroquinone the molecular geometry optimization simulations indicate that both molecular mechanical or semi-empirical methods supply close molecular geometries compared to the literature data (Table 5.2). Deviations from the literature data are quite similar for all calculation methods. High deviation on the geometrical values for the simulations which were performed with the Dreiding force field has its origin in the different charge calculations. The chemical structure of the hydroquinone molecule is, however, planar as expected. Torsion angle values for the hydroquinone molecule are obviously the same for all calculations (Table 5.2). Planar molecules are incapable of forming hydrogen bonds and diffuse reasonable fast [Ski75]. Hence, these molecules have a higher diffusion ability compared to non-planar molecules. Significant effects of this fact will be seen in the following chapter.

Considering the findings from the geometry optimization simulations for benzophenone and hydroquinone, mainly the Compass and the PCFF force fields will be used for the simulations which will be given on the rest of the thesis.

6.3. Morphologies of the substances (Figure 4.2, 2A, 2B and 2C)

The correct description of the morphology of the substance is the main aim of all experimental and theoretical investigations of crystallization. Even though, some experimental and theoretical models can characterize the right morphology, these models have special conditions in order to be applied. A routine methodology is still required in order

to provide a precise morphology for general conditions. As it was indicated before the aim of this work is to define the morphological important faces which are likely to appear on the final morphology and to test the reliability the methodology which was followed.

6.3.1. Benzophenone

Morphology calculations of benzophenone were already investigated [Lu04, Fie07]. Simulated morphologies of benzophenone for different additive molecules are matching with experimental habits successfully [Lu04]. Similar benzophenone habits were obtained in the presence of different kinds of additive molecules either experimental or in simulated approaches. Effects of different optimization methods, such as semi-empirical and density functional theories, to the binding energy values of benzophenone were also investigated [Fie07]. Here, the habit of benzophenone is investigated in the presence of ethanol and acetone as additives and the results are compared with experimental data which are available in the literature.

Morphology simulations and experiments of this work indicate also that even though very tiny differences between the final morphologies in the presence of the selected additives exist, benzophenone shows an identical habit (Figure 5.4). The modified morphology of benzophenone is defined from the modified attachment energy calculations. Therefore, modified attachment energies for selected faces are also in a similar range (Figure 5.5).

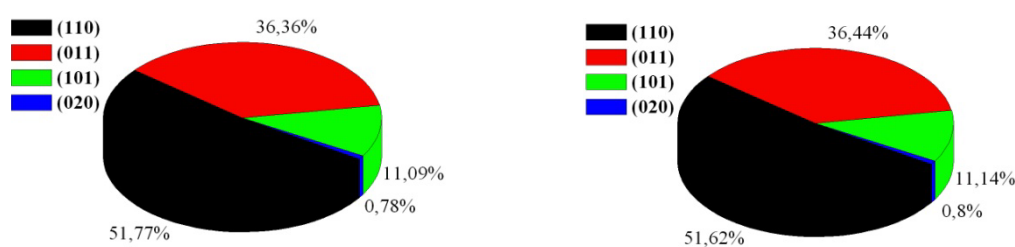


Figure 6.2: Total percentage of all symmetry related faces for pure benzophenone (left) and in the presence of ethanol (right).

The variation in the total percentage of the all symmetry related faces is given in Figure 6.2. As it can be seen, that between the pure habit and simulated habit in the presence of ethanol, the percentage of the morphological important faces is nearly the same. Habit aspect ratio values for all simulations are 1.51 as it is for the pure benzophenone morphology.

A comparison for the binding energy differences of this work and of Lu's work [Lu04] is given in Figure 6.3. Even though between the some binding energy values huge differences

are observed, the simulated morphologies are almost the same. The reason for that is the relative value of the faces are the same and, therefore, the resulting morphology is the same.

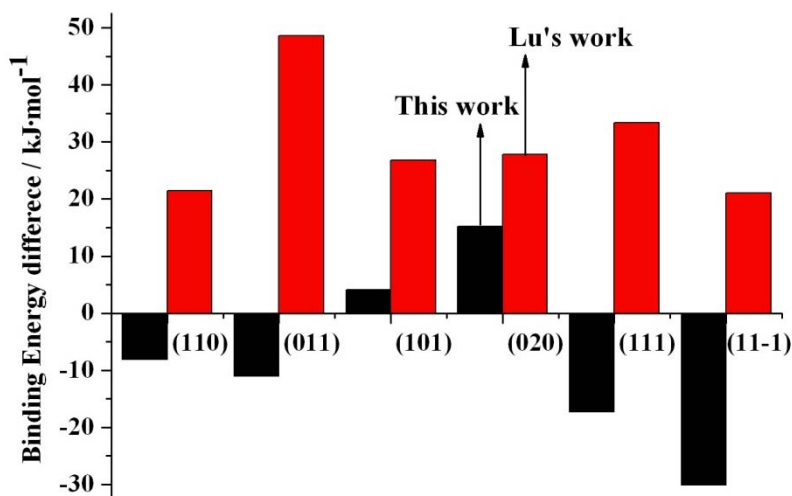


Figure 6.3: Determined binding energy differences of benzophenone in the presence of ethanol. Results of Lu [Lu04] are shown in red and results determined by this work are shown in black.

When the binding energy difference is negative, the additive has strong interactions with the applied face. A large numerical value of the binding energy difference indicates that the interaction is strong. In Lu's work, binding energy differences which indicate the interactions between additive and surface were found to be stronger than the results which were obtained by this work. However, as it was indicated before relative tendencies of the faces in the presence of ethanol are similar. Therefore, the obtained morphologies are almost the same.

Fiebig [Fie07] investigated the surface properties and the binding energy calculations for benzophenone for different optimization algorithms and force fields. Fiebig indicated that the minimum binding energies of benzophenone molecules vary strongly from batch to batch. Simulations of impurities exhibited a similar behaviour indicating a significant degree of uncertainty of the determined results [Fie07]. In this work, depending upon the above results for benzophenone the same conclusions is achieved. In the same work [Fie07], it is also indicated that the faces (011) and (101) are similar in the way of how the ketone group is oriented with respect to the surface plane. Therefore, additives involving substitutes of the ketone group and similar geometry of the phenyl rings were expected to interact in a similar way with the surface. Thus, no large binding energy differences were expected unless other properties of the impurity molecule interfered with the parallel orientation. A perpendicular orientation of ketone group is observed for the face (020). Impurities with ketone substitutes were assumed to have an alternating effect on the surface and therefore an affinity of impurity

species was expected to be very specific. The face (110) possessed a kind of dual character meaning that the ketone group of benzophenone was found to orient between close to parallel and an angle of approximately 45 degrees with respect to the surface plane. Similar results for benzophenone are obtained in the presence of the other additive molecules acetone and benzoic acid.

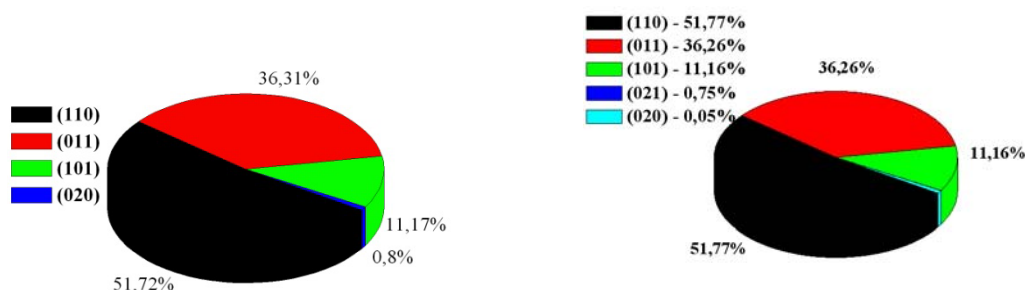


Figure 6.4: Total percentage of all symmetry related faces for the final morphology of benzophenone in the presence of acetone (left) and in the presence of benzoic acid (right).

In the presence of an acetone molecule the benzophenone morphology is also similar to the pure habit. However, the simulated habit of benzophenone is relatively similar to Lu's results. A comparison between the results of this work and Lu's work is given in Figure 6.5.

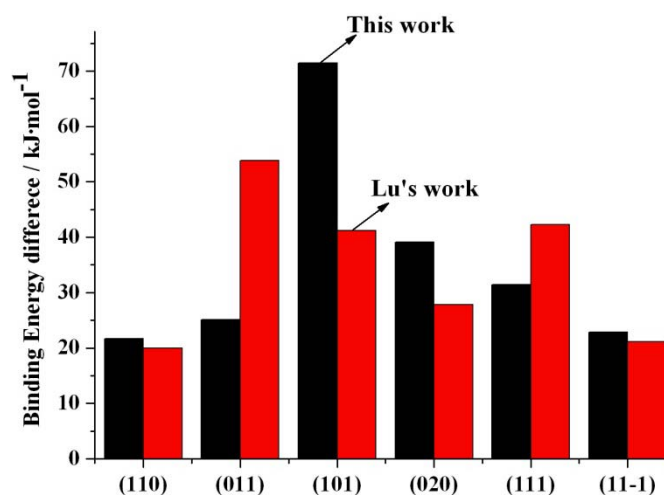


Figure 6.5: Determined binding energy differences of benzophenone in the presence of acetone. Results of Lu [Lu04] are shown in red and results determined by this work are shown in black.

The simulation of the habit of benzophenone in the presence of benzoic acid also produces a similar habit as the pure benzophenone crystal structure. However, a very tiny difference separates the resulting habit of benzophenone in the presence of benzoic acid. The presence of

benzoic acid leads to an appearance of the (021) face on the final habit (Figure 6.4). Longitudinal changes of the benzophenone habit in the presence of benzoic acid can also be differentiated from the pictures of the experimental habit (Figure 5.4).

An additive molecule which is structurally similar to the host molecule can even in small amounts create a large deviation in crystal growth, hence, the crystal habit [Nag98]. Such structurally similar additives are called “tailor-made” additives (chapter 3.3). From a structural resemblance point of view ethanol and acetone additive molecules are not structurally similar to the benzophenone molecule. This is one of the main reasons to observe almost the same final habit of benzophenone in the presence of ethanol and acetone as in the absence of ethanol and acetone. Benzoic acid additive has a structural similarity to benzophenone compare to the other additive molecules. The presence of a phenyl ring in the benzoic acid structure leads to a minor change in the final habit of benzophenone. Effects of ketone and phenyl rings were explained before by citing Fiebig’s works [Fie07, Fie07b].

6.3.2 Hydroquinone

The results of the γ – modification within the extracted polymorphs of hydroquinone crystal structures from the database [Csd07], are used for the further investigation in this work. The typical morphology of the hydroquinone has a longitudinal, rod-like, habit. The habits of hydroquinone at vapour conditions have different morphologies for all polymorphs (Figure 5.7). Habit aspect ratios of the vapour habits of the γ , α and β morphologies are 2.95, 4.71 and 2.03, respectively. Pure attachment energy calculations indicate that the γ -polymorph of hydroquinone produces a kind of rod-like habit (Figure 5.7). The morphological important faces of the γ -polymorph of hydroquinone are defined by the attachment energy calculations and given in Table 5.4. The (100) and (002) faces of the crystal are the dominant faces in final habits.

In order to find the effect of an additive molecule on the habit of hydroquinone, the surface docking method is applied in the presence of ethanol and acetone molecules. Depending upon the structural resemblance between the additive molecule and the host molecule, hydroquinone habit changes in the presence of these additive molecules. The total percentage of all symmetry related faces for the final morphologies are given in Figure 6.6.

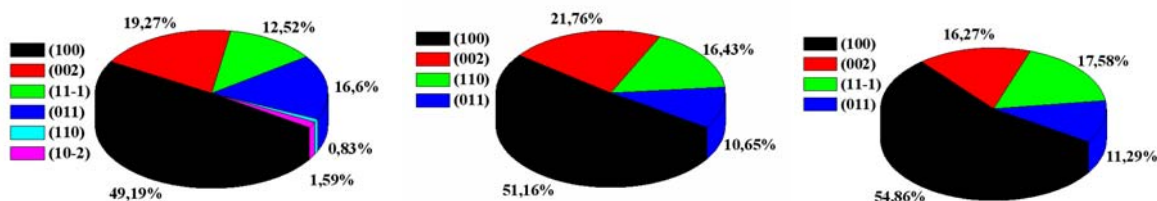


Figure 6.6: The total percentage of all symmetry related faces of the final morphology of hydroquinone in vapour (left), in the presence of ethanol (centre) and in the presence of acetone (right).

Simulated hydroquinone habits in the presence of ethanol differ significantly compare to the vapour habit. The $(11\bar{1})$ and $(10\bar{2})$ faces lose their morphological importance in the presence of ethanol (Figure 6.6). As a matter of fact to lose the morphological importance means not to be able to keep the relative size of the surface area of a face while other morphologically important faces increase their surface area. In other words, a face which loses its morphological importance cannot compete with other faces in terms of surface increment and stays relatively smaller. The largest attachment energy deviations are also observed for the $(11\bar{1})$ and $(10\bar{2})$ faces (Figure 5.9).

A hydroquinone molecule contains two hydroxyl groups in its chemical structure. These hydroxyl groups lead the resemblance with the ethanol molecule since ethanol has a hydroxyl group in its chemical structure. Therefore, ethanol can be classified as structurally similar to hydroquinone. The mentioned effect of resemblance is noticeable from the morphology change of hydroquinone in the presence of ethanol. The vapour habit of γ -hydroquinone has a kind of rounded shape. It has a 2.9 habit aspect ratio and a $1.1 \cdot 10^6 \text{ \AA}^3$ habit volume (Figure 5.7a). However, in the presence of an ethanol molecule the final morphology of hydroquinone has a 3.58 habit aspect ratio and a $1.84 \cdot 10^6 \text{ \AA}^3$ habit volume. These values represent the optimized habit of hydroquinone which has a rather elongated shape in the presence of ethanol molecule. The experimental habit of hydroquinone in ethanol matches also with simulated habit (Figure 5.8).

In the presence of an acetone molecule the (110) and the $(10\bar{2})$ faces lose their morphological importance (Figure 6.6). The largest deviations of the attachment energy values are observed on these faces (Figure 5.11). However, in the presence of acetone the final habit of hydroquinone is quite similar to the vapour habit. The final habit of hydroquinone in the presence of acetone has a 2.95 habit aspect ratio and a $1.1 \cdot 10^6 \text{ \AA}^3$ habit volume which are similar values to these of the vapour case. Simulated and experimental habits are matching

also with the vapour habit (Figures 5.10 and 5.7b). Even though, the morphological importance of the (110) and the $(10\bar{2})$ faces are lost and the general hydroquinone habit maintains its general habit. Experimental investigations also confirm this interesting fact. Acetone easily evaporates under normal experimental conditions. For that reason an experiment with acetone has to be performed in a special setup. Experimental morphologies of hydroquinone in the presence of acetone are performed in a well sealed petri-dish growth cell. The saturated solution was injected into the special growth cell and the acetone was evaporated controlled at room temperature. However, interactions between acetone and the hydroquinone crystal were difficult to be obtained. Hence, the experimental habit of hydroquinone in the presence of acetone molecules is quite similar to the vapour habit. This remarkable fact indicates that the attachment energy method might provide the right morphology whenever an additive has not a strong effect on the morphology.

6.3.3 Benzoic acid

Similar calculations were performed for benzoic acid crystals in the presence of ethanol and acetone. Benzoic acid contains carboxylic, ketone, phenyl, and hydroxyl functional groups in its chemical structure. These functional groups play important roles in the chemical resemblance of the host and additive molecules, hence, the habit. The simulated habit aspect ratio of benzoic acid in the vapour phase is obtained to 3.42 which lies in the reported value range [Hol99] and the volume of the simulated habit in the vapour phase is $8.1 \cdot 10^6 \text{ \AA}^3$. Ethanol and acetone are used also as additives. Simulation results of the surface docking approach are given in Figure 6.7.

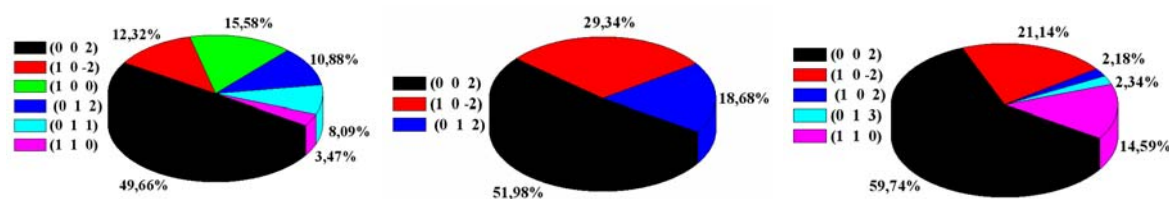


Figure 6.7: The total percentage of all symmetry related faces for the final morphology of benzoic acid in vapour phase (left), in the presence of ethanol (centre) and in the presence of acetone (right).

The simulated habit of benzoic acid in vapour phase is compared with the one presented in literature (Figure 5.13). The simulated habit of benzoic acid in the presence of ethanol differs from the vapour habit. The (100), (011) and (110) faces are lost their morphological importance in the presence of ethanol (Figure 6.7). Ethanol has a strong effect on the final

habit of benzoic acid. The simulated and the experimental habits also confirm this strong effect (Figure 5.14). The hydroxyl group of benzoic acid has a strong interaction with the ethanol molecules. Hence, habit of benzoic acid gains a longitudinal final form. The habit aspect ratio of the final benzoic acid habit is 4.1 and the volume is $5.06 \cdot 10^6 \text{ \AA}^3$. The habit volume value decreases in the presence of ethanol. However, the habit aspect ratio value is increased compare to the vapour phase habit. The final habit is changed in a more longitudinal direction (Figure 5.14).

Acetone has a different effect on the benzoic acid morphology as it is for other substances. In the presence of acetone the (100), (012) and (011) faces lose their morphological importance. However, the (013) and (102) faces gain in morphological importance in the presence of acetone, even though, they did not have morphological importance in vapour phase case. The (002), $(10\bar{2})$ and (110) faces increase their morphological importance in the presence of acetone. Structural similarity plays an important role as it is in the case of ethanol. The ketone group in benzoic acid is the part of the cause for this similarity. Benzoic acids final habit has in the presence of acetone a similar morphological tendency to change as in the case of ethanol. While the habit aspect ratio increases the habit volume decreases in the presence of acetone. The simulated habit aspect ratio is 6.13 and the habit volume is $6.5 \cdot 10^6 \text{ \AA}^3$. An expansion in the longitudinal direction of benzoic acid in the presence of acetone is more determined than in the case of ethanol. Therefore, the final habit has a needle like shape (see Figure 5.15).

6.4. Diffusion coefficient calculations (Figure 4.2, 3)

Morphologies of the working samples in the presence and absence of the additive molecules are given in the previous section. So far known methodologies are used. The results of the previous sections are confirmations of the existing theories and an extension towards the new working systems. The current section is the major and the key part of this thesis.

The overall rate of mass transport should account for crystal growth processes. For the purpose of this discussion, processes such as desolvation of a solute, dissolution or displacement of an adsorbed solvent are not treated explicitly here. One further factor that is generally ignored in the discussion of crystal growth is heat transfer and the coupling thereof to the mass transport. It is generally assumed that in crystallization from solutions heat transport is a negligible factor and that heat dissipation is achieved in such a way that it must not be explicitly be treated in a discussion of crystal growth.

The major difficulty in relating growth of a crystal face to transport properties is the lack of experimental information. Although bulk diffusion coefficients can be measured, the processes at the interface are not easily accessible for experimental methods. Here, molecular dynamics simulations are used to gain insights into the transport steps that govern crystal growth and into the rate determining steps. Depending upon the conditions certain growth processes are diffusion controlled, whereas others are controlled by the rate of growth-unit integration into the surface of a crystal. With the aid of molecular dynamics simulations the individual processes are directly observable and can be quantified. In addition, MD simulations allow the system studied to be tailored to match commonly encountered experimental conditions of temperature and solution composition. This provides access to information that is otherwise difficult to obtain. The limiting factors in the simulations are the quality of the force field employed to model the interactions between the molecules involved and the computation time required in order to achieve a reasonable representation of a solid liquid system.

Simulations are employed particularly to study diffusion coefficients for the organic systems. Computer experiments are performed of systems representing the melt or the solution (amorphous cell) and characteristic changes of transport parameters depending upon changes in the external parameters were determined. The data obtained from these simulations are used to calculate the transport properties of the molecules and growth rates of morphological important faces under given conditions and are compared to results of empirical equations which are available in literature.

6.4.1. Diffusion coefficient simulations for the pure solute system (Figure 4.2, 3AA)

In the first instance simulations were carried out using a system representing a liquid phase in the presence of only a solute system in order to assess the available force field and the influence of the choice of the system parameters upon the outcome, in particular the diffusion coefficient. This part of the work was carried out using the first model systems, benzophenone and hydroquinone.

The molecule assembly used in the simulation was set up using the amorphous cell module within the MaterialsStudio package. With this module a box of arbitrary size is filled with molecules according to user-defined criteria. The molecules are randomly placed within the box and the criterion used here to determine the size of the simulation box was the known density of working samples at the temperature at which the simulation has to be carried out. The system thus created is optimised with respect to its total energy and then equilibrated at

the temperature of the production run. Temperature values lie above the melting point of working systems. The equilibration simulation is carried out under NVE conditions (constant particle number, volume and energy) with a time step of 1 fs. Production runs follow and are carried out under NVT conditions (constant particle number, volume and temperature) using the same time step of 1 fs.

The self-diffusion coefficient can be calculated from the knowledge of the motion of a given molecule. For homogeneous fluids, a method, which relates the diffusion coefficient to the mean square displacement of the molecule, can be applied using the Einstein equation. The means square displacement is easily obtained from the molecular dynamics trajectories of the molecules considered in the simulation.

For the benzophenone molecule, effects of simulation conditions on the diffusion coefficient values are assessed in Figure 5.17. Effects of simulation duration on the diffusion coefficient are already known from other techniques [Fre96]. Therefore, a systematically increase in simulation durations for the production runs from 20 ps to 150 ps for a system containing 100 molecules (2400 atoms) at 325 K are carried out.

The diffusion coefficient is found to decrease with increasing simulation time (Figure 5.17). With the exception of the outlier at 100 ps, D appears to a limiting value after reasonable short simulation times, so that it is reasonable to assume that even higher simulation times will not significantly change the results obtained in the benzophenone case. The value of the diffusion coefficient calculated using the Wilke-Chang equation ($D_{WC} = 7.81 \cdot 10^{-5} \text{ cm}^2 / \text{s}$) is more than an order of magnitude greater than the values obtained from the simulations.

The influence of different force fields upon the simulation was also investigated depending upon the available force fields in the software index. As can be expected different force fields yield different diffusion coefficients (Table 5.18), however, all force fields allow a good linear regression of the derived MSD against time and the diffusion coefficients do not differ significantly. One of the important reasons for this similarity is the family of force fields. All force fields (COMPASS, PCFF, CVFF and CFF) have the same basic family and each of them is parameterised for specific aims. For example, the PCFF force field is developed based on the protein CFF91 force field [Map88] and augmented with a dozen functional groups that are typical constituents of the most common organic and inorganic polymers [Sun94]. COMPASS force field (Condensed Phase Optimized Molecular Potentials for Atomic Simulation Studies) was optimized PCFF force field for condensed phase applications by changing the nonbond parameters. Optimization of a force field for a specific aim is not aim

of this work since it needs long time and a separate investigation. Here, selection of the right force field by testing simulation is performed.

The results of the molecular dynamics simulations indicate that in case of benzophenone molecules the torsion angle increases and benzophenone molecules geometry becomes less planar after molecular optimization runs (Table 5.1). The torsion angle values of benzophenone increase in relation to the optimization simulations. Hence, the molecular structure of benzophenone gets a bent like shape after the simulations. It is reported [Ski75] that the molecule geometry has a significant effect on the physical properties of complete system especially on diffusion. In terms of diffusion the simulations with hydroquinone molecules give closer results to the empirical diffusion coefficient values.

Diffusion coefficient values change depending upon the thermostat which is used in the simulations (Table 5.19). The thermostat term in molecular modelling represents the way to control the temperature during simulations. More literally: A modification of the Newtonian MD scheme with the purpose of generating a thermodynamical ensemble at constant temperature is called a thermostat algorithm [Hün05]. Production runs of the molecular dynamics simulations are performed with NVT statistical ensemble. The selection of the right temperature control method is rather important concerning the result of the simulations. Another important simulation parameter is the choice of the right force field in order to obtain the desired properties in right order. A comparison of the diffusion coefficient value of hydroquinone for the force fields, thermostats and different starting geometries are given in Figure 5.18. As it was indicated in the results section, force fields, temperature control methods and starting geometries are affecting the interaction of the molecules. Every single condition can be significantly effective on the results. The effect of the starting geometries on diffusion coefficients can be seen in Figure 5.18. The diffusion coefficient value of the simulation which is performed with the Frame 1 starting geometry produces relatively close to the empirical diffusion coefficient value. Frame 1 is the ideal equilibrium starting geometry for molecules in the amorphous cell. Frame 2 is a less favourable starting geometry than Frame 1. As it was indicated in the results section that in order for diffusion to occur a concentration difference which result of molecular interaction is necessary. Molecular modelling calculates the diffusion property of working system from the movements which are the results of molecular interactions. New positions of molecules create concentration differences, hence, diffusion. In the following sections, this finding will be seen more clearly. Energy distributions during the simulations which are performed with the Velocity Scale thermostat for different temperature values are given in Figure 6.8.

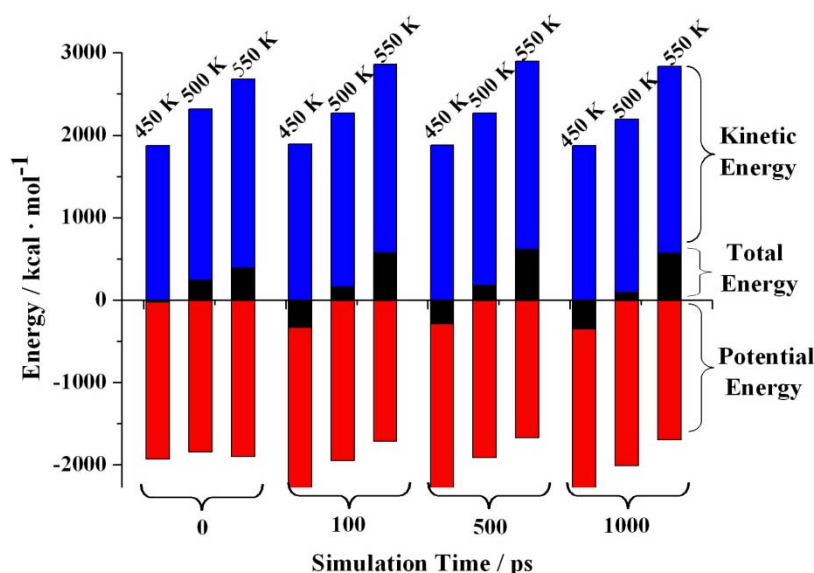


Figure 6.8: Energy configuration of the simulations for different simulation durations and temperatures. For all simulations the velocity scale thermostat and the compass force field are used.

Energy contributions during the simulations indicate that an increase in simulation duration has no significant effect on energy values for the short simulation durations (100ps). However, at longer simulation times (500ps and 1000ps = 1ns), temperature increase significantly effects to the energy distribution. For 0.5 and 1ns simulations times the temperature increase is concluded to increase the kinetic energy and potential energy (see Figure 6.8).

From these starting configurations the importance of minimization and equilibration procedures can be seen. In all simulations the Berendsen thermostat gives the closest results to the empirical diffusion coefficient values. The Berendsen method involves the exchange of thermal energy between the system and a heat bath. The Berendsen method is smooth and deterministic but time irreversible. The Andersen thermostat method on the contrary is non-deterministic and time irreversible. Moreover, it has the disadvantage of being non-smooth, i.e., generating a discontinuous velocity trajectory where the randomly-occurring collisions may interfere with the natural dynamics of the system [Hün05]. The Nosé equation of motion (the Nosé thermostat) is smooth, deterministic and time reversible. However, it has different mathematical calculation methods in order to calculate some important parameters. This method allows that heat may flow in and out of the system in an oscillatory fashion [Nos93], leading to almost periodic fluctuations. However, the dynamics of the temperature evaluation should not be oscillatory, but rather result from a combination of stochastic fluctuations and

exponential relaxation [Hün05]. The Berendsen thermostat will be the first thermostat preference on the simulations after this point.

The large differences between the diffusion properties of hydroquinone and benzophenone have their origin in the different molecular geometries of the molecules. The molecular geometry is known to have an influence on diffusion behaviour [Ski75] and the change in torsion angle observed in these simulations may contribute to discrepancies observed between the diffusion coefficients derived from MD simulations and those derived from the Wilke-Chang equation.

Torsion angle values of benzophenone increase in relation to the optimization simulations. Hence, the molecular structure of benzophenone becomes a bent like shape after simulations. The chemical structure of the hydroquinone molecules are, however, planar, as expected (see Table 5.2). It has been reported, that planar molecules that are incapable of forming hydrogen bonds diffuse reasonably fast [Ski75] and that these molecules have higher diffusion ability compared to non-planar molecules. The molecular weight is, of course, also another important factor which has a big influence on the diffusion coefficient.

6.4.2 Diffusion coefficient simulation for the solute-solvent system (Figure 4.2, 3AB)

In order for crystallization to take place a solution must be supersaturated. Therefore, the simulations of amorphous cells should embody supersaturated solutions and dynamic calculations are performed in order to investigate the transport properties of a system for the crystal growth process. In this context, the amorphous cell simulations are expanded with the addition of solvent molecules.

The supersaturation is formed depending upon the solubility values of solute in solvent systems. Solubility values of hydroquinone in ethanol for different temperature values are obtained from literature [Li06] and the hydroquinone/ethanol ratio is calculated depending on density value of hydroquinone for different temperatures (Table 5.20).

Results of the previous section and single molecule geometry optimization section indicated that geometry of the single molecule and positions of the molecules in simulated systems have significant importance on transport properties. In this sense, solute and solvent molecules are placed into the simulation box in two different arrangements (Figure 5.20). Similar dynamic simulations were performed with respect to the changes of the force fields, temperatures and positions of the molecules (Figure 5.21).

Simulations were performed for different degrees of supersaturation. One important reason is to observe the changes on the transport properties of organic solute system at different supersaturation values. Simulations at small supersaturation values are also important to hinder the possibility of the parasitic (undesired) nucleation to occur. At high supersaturation value the possibility of surface deposition also increases. In order to control the growth mechanism this distinction has to be done carefully.

At small supersaturation values simulations were performed for different force fields, temperature and positions of the solute and solvent molecules. After a definite simulation time diffusion coefficient values are observed to be continuously decreasing and at further simulation times to be continuously increasing (Figure 5.21). For separated solute – solvent arrangement the simulations of this diffusion coefficient decrease is also observed from the simulation snapshots for different simulation times (Figure 5.22). The diffusion coefficient decrease for the separated solute – solvent simulations at first 70 ps is the reason for the driving force for the solute molecules to find an optimum position in terms of molecular interactions. Hydroquinone molecules are in the equilibrium position at the beginning of the simulations. The presence of ethanol molecules blocks the possible movement sites of the hydroquinone molecule in the amorphous cell. Therefore, the diffusibility of the hydroquinone molecules decreases methodically. On the other hand the presence of ethanol molecules causes a structuring in the amorphous cell depending upon the molecular interactions between ethanol - ethanol, ethanol - hydroquinone molecules. During the simulations the maximum length of the hydrogen bonding is attained as 2.5 Å. When the distance between two molecules exceeds 2.5 Å molecules have no bond interactions anymore and separated from each other. This structuring can be seen in Figure 5.22. An increase of the diffusion coefficient value is observed at higher simulation times (>100ps). A short time after the structuring an increase of the diffusion coefficient values is observed. This may be the reason for back diffusion because of the concentration difference between two groups of molecules.

Similar diffusion coefficient behaviour according to the simulation time is observed for the randomly located solute–solvent amorphous cell simulations (Figure 5.21b). However, a definite structuring due to the simulations cannot be observed from the simulation snapshots. Even though, a very slight molecular level structuring appears at longer simulation times, this slight structuring for the simulated times is not enough to create a concentration difference for a diffusion process. Hence, a significant diffusion coefficient increase cannot be observed in this case. In order to observe a significant diffusion in the case of concentration differences

for mixed systems, simulations should be performed with longer simulation times (e.g. > 1 ns).

In order to demonstrate the significant difference between the locations of the molecules, same simulation conditions except the starting arrangement were applied to two systems. Two different simulations at 310 K and PCFF force field are performed for separated and random solute/solvent molecules (Figure 5.21). For the separated simulations diffusion coefficient values are in the range of $0.75 \cdot 10^{-5} \text{ cm}^2 \cdot \text{s}^{-1}$. On the other hand simulated diffusion coefficient values for randomly located molecules are in the range of $1.3 \cdot 10^{-5} \text{ cm}^2 \cdot \text{s}^{-1}$. Randomly located solute and solvent molecules have higher diffusion coefficient values for the same simulation conditions. Hydroquinone molecules in randomly located group are more mobile than in the other case. The reasons for this difference are the positions of the ethanol molecules and their positive or negative contributions on the molecular interactions. Energy profiles during these two simulations will be more informative for this diffusion coefficient differences. Average total and potential energy values for different simulation times are given in Figure 6.9.

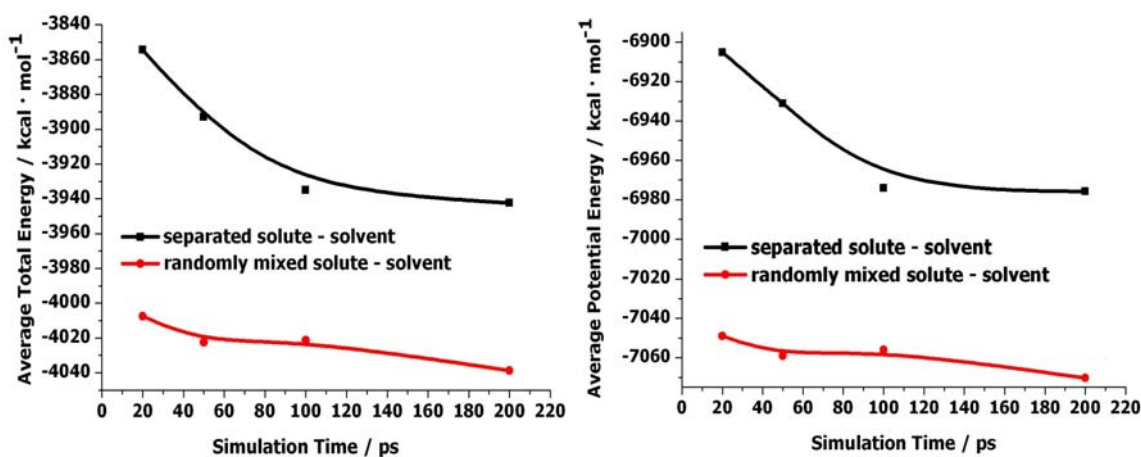


Figure 6.9: Average total and potential energy values of the simulations for different simulation times. Simulations were performed with 100 hydroquinone molecules and the pcff force fields at 310 K.

Figure 6.9 indicates that the total energy is dominated by the potential energy. Both the total and the potential energy for the “separated” initial configuration is much higher than for the random initial configuration, while both decrease with simulation time for both systems, the decrease is stronger for the “separated” initial configuration due to lowering of energy of the mixing components. Since simulations were performed at the same temperature (310 K) the average kinetic energy values are quite similar for both simulations and the kinetic energy values do not significantly change during the entire simulation. Figure 6.9 also indicates that diffusion coefficient differences between the random and the separated slab initial

configurations take their origin in the molecular interaction (potential) energy differences. Here, this causes the diffusion coefficient value difference between the two cases (Figure 5.21a and b).

As it was indicated in the force field descriptions (chapter 3.2) interaction energies are calculated by the deviations of the atoms from their equilibrium positions. Whenever an atom in a molecule changes its location depending on the intra- and intermolecular interactions, interaction energy gains a more negative value. In Figure 6.9 more negative potential energies can be seen for short simulation durations. It means that atoms in the molecules are changing their equilibrium positions until they find better position in terms of interactions. However, in higher simulation times potential energy values stay constant for two different cases (Figure 6.9). This constant energy regime indicates that molecules find equilibrium positions or their interactions cutoff due to some reason: It should be noticed that simulation times ranges (70ps – 100ps) where average energies change their trend from decreasing to constant values are the same values where diffusion coefficients change their tendency (Figures 5.21 and 5.22).

The reasons of the observed structuring in the amorphous cell are explained with the possible reasons: In order to define the reasons more clearly and picture the phenomena some other physical properties for this simulation are given in the chapter “results”. From the concentration profile of the relevant simulations (Figure 5.23a), it was figured out that ethanol molecules are mainly located in two different positions in the amorphous cell (15 Å and 45 Å). The hydroquinone molecules are mainly located 45 Å (in z direction) where most of the hydroquinone and ethanol molecules exchange their location. A clear structuring can also be seen with the concentration profiles. The parallel to the concentration profile results observed radial distribution function results indicate the probability that hydroquinone molecules within an 1.5 Å distance are $13/8 = 1.625$ times higher than in the ethanol case. That means the hydroquinone group contains higher numbers of molecules than the ethanol group.

As it was several times stated in this thesis that supersaturation has an important role on the crystal growth mechanism. After clear identifications of the role of the molecule interaction temperature and other simulation parameters on physical properties such as the effect of supersaturation on diffusion mechanism is carefully investigated. The effect of the supersaturation on the diffusion is investigated together with different temperature scaling and interaction energy algorithms. The diffusion coefficient value of hydroquinone has a more regular response to the increase of the supersaturation at higher temperatures (Figure 5.25b).

The empirical diffusion coefficient value of pure hydroquinone varies between ~ 2 to $5 \cdot 10^{-5} \text{ cm}^2 \cdot \text{s}^{-1}$ at different temperatures. In the presence of ethanol molecule this value decreases to ~ 0.5 to $0.8 \cdot 10^{-5} \text{ cm}^2 \cdot \text{s}^{-1}$. The experimental diffusion coefficient value of hydroquinone in the presence of ethanol was reported to be $0.595 \cdot 10^{-5} \text{ cm}^2 \cdot \text{s}^{-1}$ at 298K [Cha98]. The result for the value of the diffusion coefficient from the simulations with pure hydroquinone are between ~ 1 to $6.5 \cdot 10^{-5} \text{ cm}^2 \cdot \text{s}^{-1}$ at 298 K (Figure 5.18) which are in the range of empirical values. However, simulated diffusion coefficient values decrease to $\sim 0.5 \cdot 10^{-5} \text{ cm}^2 \cdot \text{s}^{-1}$ which is same diffusion coefficient decrease on the empirical values. Diffusion coefficient values are outlined in Table 6.1.

Table 6.1: *Diffusion coefficient values of hydroquinone at different conditions.*

Case	Diffusion coefficient of hydroquinone/ $10^{-5} \text{ cm}^2 \cdot \text{s}^{-1}$
Empirical (pure) at 298,310 and 333K	$\sim 2 - 5$
Empirical (with ethanol) at 298,310 and 333K	$\sim 0.5 - 0.8$
Experimental (with ethanol) at 298K	0.595
Simulated (pure) at 298 K	$\sim 1 - 6.5$
Simulated (with ethanol) at 298 K	~ 0.5

6.4.3 Diffusion coefficient simulation for the solid-liquid system (Figure 4.2, 3AC, 3ACA)

Some computer simulations for diffusion coefficient calculations may take for a single value longer than a day in time. Therefore, it is important to have correct definitions of the simulation conditions in order to use the full advantage of computer methods. This is the reason why, careful investigations were performed in order to obtain the conditions depending upon the simulated substances. Simulation experiences which were obtained from the previous sections are used in order to reach the main target of this work.

Solid-liquid simulations were performed by considering the morphological importance of the investigated faces because of their high tendency to incorporate the growth units. An important point for the solid-liquid simulations is the direction of the diffusion coefficient. The Einstein relationship (eq. 4.2), which correlates mean square displacements of the molecules in a given time with the diffusion coefficient is for a fully symmetrical unbounded

infinite system. However, in the presence of the solid surface the symmetry of the entire system is broken and the diffusion coefficient has to be calculated taking this boundary into account. The Einstein relationship is not a valid approach for the solid-liquid case. Diffusion coefficient calculations should be different for the perpendicular and the parallel direction to the solid surface. Calculation of the directional diffusion needs intensive mathematical investigations. A detailed mathematical analysis which presents the calculation methods of the perpendicular and parallel diffusion coefficients with selective ways can be found in literature [Liu04].

For the determination of the diffusion coefficients perpendicular to the interface a dual simulation method was proposed [Liu04]. The dual simulation method requires two separate simulations to be performed: a molecular dynamics simulation and a sequence of Langevin dynamics simulations.

Here, for the determination of the diffusion coefficient parallel to the interface an approximation method is used. The method used is producing the suitable results for the aim of this work. However, the method should be implemented by considering the additional considerations for further investigations. The Einstein relationship was generalised by the addition of the survival probability of the solute molecules in a definite zone. The survival probability was defined as the probability to find the solute molecules in the simulated region. The simulations in this work are all performed with periodic boundary conditions. All solute molecules in the liquid part were considered in the calculation. Therefore, all solute molecules are used during the entire calculations. The survival probability is therefore considered to be 1 in this case. Thus, the generalised Einstein relationship is the same as in the usual relationship for the parallel diffusion coefficient calculations. Therefore, the Einstein relationship is used here. Periodic boundary conditions and diffusion coefficients are represented in Figure 6.10.

Periodic boundary conditions ensure that the simulated system has a continuous structure. The sense of using the Einstein relationship for the parallel diffusion coefficient can be seen from the Figure 6.10. On the parallel direction to the solid surface the symmetry of the fluid is partially protected. Therefore, the usual Einstein relationship is a close approximation for the parallel diffusion coefficients.

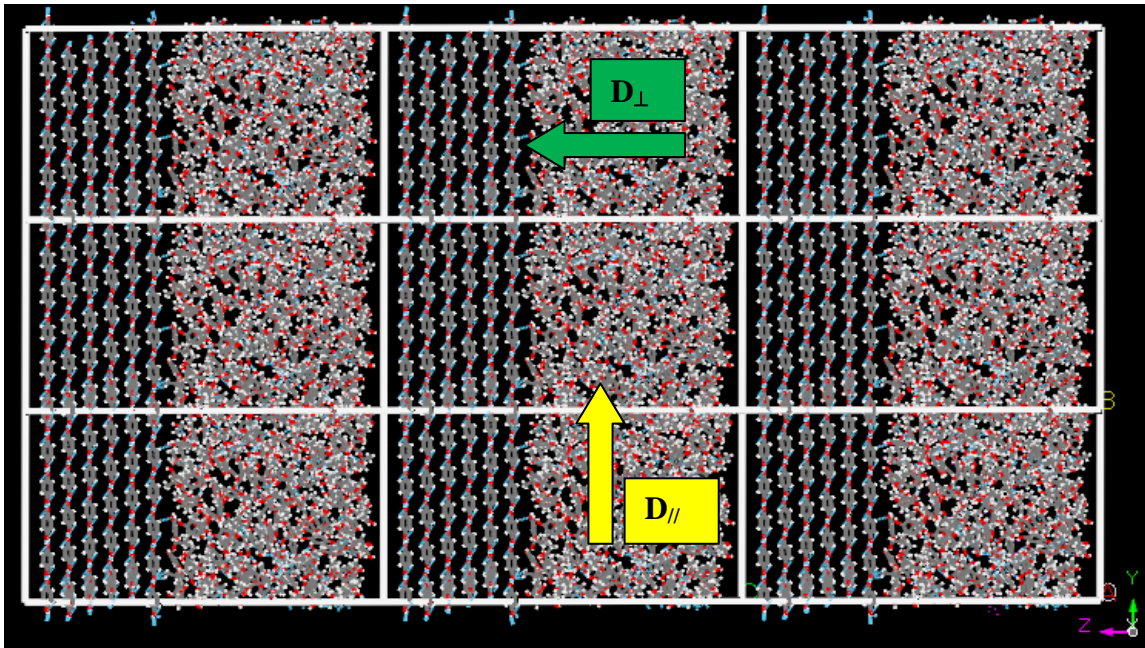


Figure 6.10: *A typical representation of the periodic boundary conditions and directional diffusion coefficients depending upon the solid surface.*

Considering the assumptions above computer simulations were performed in order to calculate the diffusion coefficient. The directions of the diffusion coefficient were considered carefully. Diffusion coefficients parallel to the solid surface will be calculated here. Since the morphologically important faces have a high probability to grow, solid-liquid simulations were examined by only their consideration. Morphological importance of the faces was already calculated by attachment energies. Positions of the molecules on the solid surfaces give grounds to classify the faces with regard to their polar structure. In accordance with the definition [Hen09], the $(10\bar{2})$ and the (011) faces can be classified as polar and the (100) , (002) and $(11\bar{1})$ faces are semi-polar.

The diffusion coefficient values parallel to the surfaces were calculated for different supersaturation values (Figure 5.28). However, a tendency for the increase of the diffusion coefficient was not observed in the simple diffusion coefficient calculations. In order to have a clearer picture of the changes in the system details in the simulation were observed by the simulation snapshots (Figure 5.29). As it was observed for the solute-solvent simulations a structuring during the simulations was observed here, too. However, within the time scale of the simulation the solute molecules remain on the surface. In this case a different growth mechanism has to be considered for further stages. The initial and final positions of the simulated system were given in Figure 6.11.

Final dynamics simulations were performed with the NVT statistical ensemble. That means during the simulations molecule numbers, volume of the simulated amorphous cell and temperature during the simulations are maintained. The liquid side in Figure 6.11 is supersaturated at the start and is therefore in disequilibrium. Simulation conditions enable to give a coherent explanation for the in the first view “empty” zone in Figure 6.11. The simulation snapshots designate the positions of the molecules which were attained (molecules which were filled into the simulation box) before and after the simulations. During a simulation the system protects given conditions such as molecule numbers. Whenever a molecule leaves the simulation box the simulation software attains new molecules. Therefore, by the help of the periodic boundary conditions and fixed molecule number considerations, the software attains new molecules to substitute the leaving molecules in the calculations during the simulations. However, *the software used does not illustrate* the replaced molecules in computer graphical interface. This illustration drawback leaves an impression that an “empty” zone exists as a result of the simulation. The software illustrates only the motion of the given molecules at the beginning of simulation.

An average velocity of the selected solute molecules can be calculated by computer simulations. In order to calculate the average velocities of the selected solute molecules initial and final positions of the solute molecules in a definite time interval are used. Three selected molecule positions will be given here. Interactions of the molecules with the solid surface have the major importance within the selection criteria of the molecules.

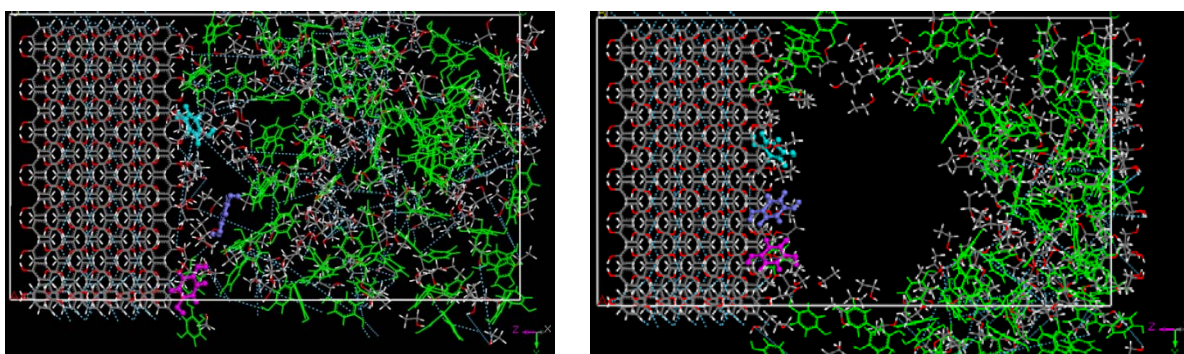


Figure 6.11: *Initial (left) and final (right) positions of the selected hydroquinone molecules during the 100ps dynamic run. Selected molecules were given in different colour than the rest of the hydroquinone molecules. The simulation cell contains 100 hydroquinone and 213 ethanol molecules.*

The investigated molecules have different colours in order to distinguish them from the rest. One of the molecules (purple colour) shows an important difference compare to the two other molecules. At the beginning of simulation the purple molecules are in the bulk part of the system and later they are docked on the solid surface. Blue, purple and pink molecules displacements in different directions were given in Figure 6.12.

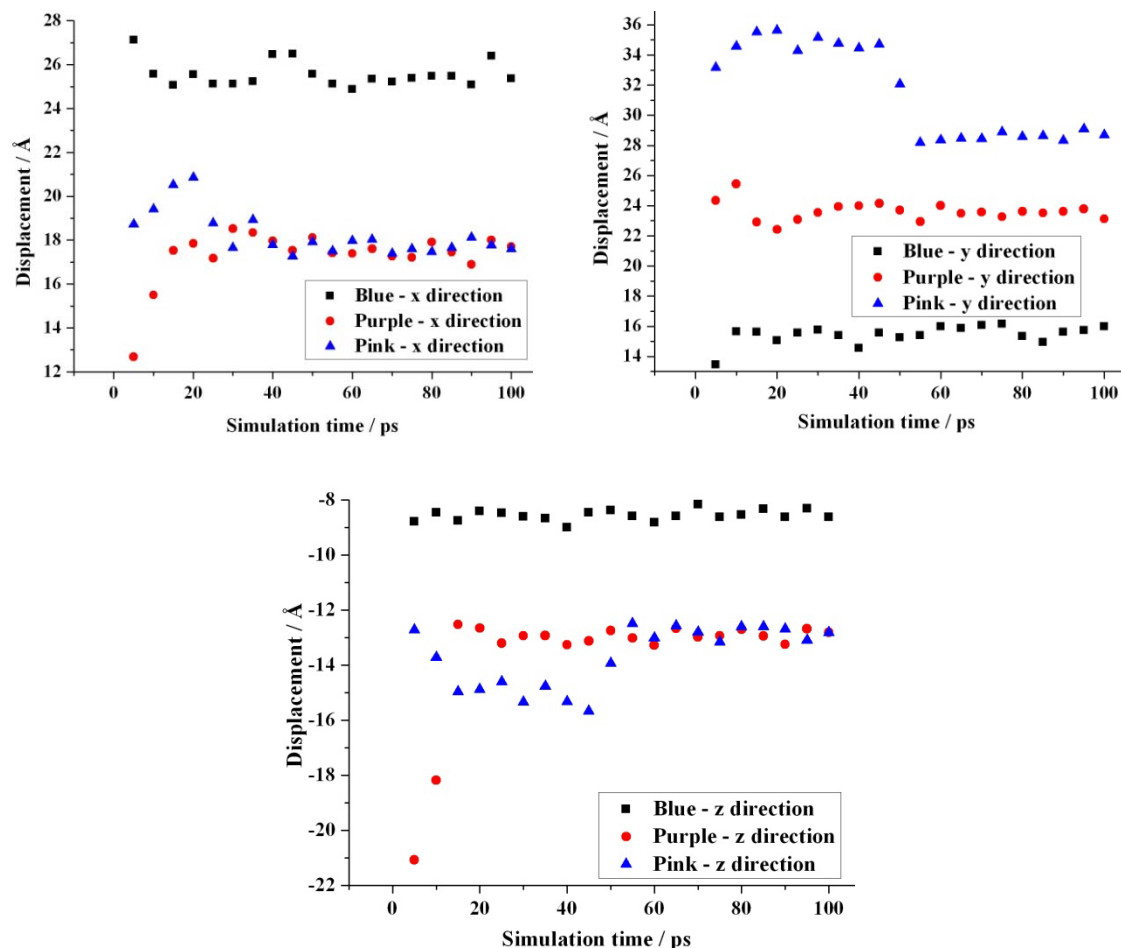


Figure 6.12: Displacement values of the selected molecules on the x (left), y (right) and z (bottom) directions during the dynamic simulation.

It is possible to define the exact arrival time of the purple molecule from the bulk solution on the solid surface by the position values. As it can be seen from the Figure 6.12 the position of the purple molecules has not changed much in the parallel directions x and y. However, the purple molecules arrived on the solid surface in z direction changed much in their position in the first 15 ps simulation time. Right after the purple molecule arrived to the surface the purple molecules have small changes on their position in the parallel directions to the solid surface. This is assumed to be the effect of the purple molecules in taking part in the surface integration step right after arriving from the bulk of the solution on the solid surface. Average

velocity values of the selected molecules give a detailed idea about the effect of the solid surface on the movabilities of the molecules.

As it was indicated before, the average velocity of the purple molecule in the first 15 ps is extremely high compared to the rest of the simulation time and in the same range of the other velocity values. The presence of the solid surface shows its effect on the mobility of the molecules when the molecule arrives to the surface.

Table 6.2: *Average velocity of the selected hydroquinone molecules for different time intervals for the (10 $\bar{2}$) face and 100 hydroquinone and 213 ethanol molecule solution.*

	5 – 15 ps			20 – 100 ps			5 – 100 ps		
	V_x / $\text{\AA}\cdot\text{ps}^{-1}$	V_y / $\text{\AA}\cdot\text{ps}^{-1}$	V_z / $\text{\AA}\cdot\text{ps}^{-1}$	V_x / $\text{\AA}\cdot\text{ps}^{-1}$	V_y / $\text{\AA}\cdot\text{ps}^{-1}$	V_z / $\text{\AA}\cdot\text{ps}^{-1}$	V_x / $\text{\AA}\cdot\text{ps}^{-1}$	V_y / $\text{\AA}\cdot\text{ps}^{-1}$	V_z / $\text{\AA}\cdot\text{ps}^{-1}$
Blue	-0.205	0.217	0.003	-0.002	0.011	-0.002	-0.018	0.026	0.0017
Purple	0.485	-0.142	0.855	-0.001	0.0087	-0.002	0.053	-0.013	0.087
Pink	0.179	0.235	-0.225	-0.041	-0.087	0.026	-0.012	-0.047	-0.021

Here, in order to calculate the parallel to the surface components of the growth rates an average molecule velocity can be used since the diffusion coefficient calculations are performed only with parallel components. Hence, growth rate calculations are performed only for the molecules which are on the solid surface. This needs to define the movements of the molecules during the simulation.

The average velocity of the selected hydroquinone molecules in the parallel direction to the solid surface is calculated by:

$$\vec{V}_{\parallel} = (V_x^2 + V_y^2)^{1/2} \quad (6.1)$$

Average parallel velocities are calculated when a hydroquinone molecule moves on the $(10\bar{2})$ face. Therefore, the parallel velocity of the purple molecule is calculated between the times of 20ps and 100 ps. According to the eq. 6.1:

$$\overrightarrow{V_{\parallel}^{blue}} = 0.3235 \text{ \AA} \cdot ps^{-1} \quad (6.2)$$

$$\overrightarrow{V_{\parallel}^{purple}} = 0.0089 \text{ \AA} \cdot ps^{-1} \quad (6.3)$$

$$\overrightarrow{V_{\parallel}^{pink}} = 0.04836 \text{ \AA} \cdot ps^{-1} \quad (6.4)$$

The average parallel velocity of the hydroquinone molecule which has a purple colour has the smallest value within the selected molecules. However, the smallest average velocity has not the meaning that this face has the slowest growth rate, hence the largest morphological importance. A molecule's average velocity is one of the parameters which contribute to the definition of the growth rate. However, the average velocity is not used to define the growth rate here. It gives an idea about the mobility of the molecules. The average velocity gains importance when the bulk diffusion mechanism dominantly affects the growth mechanism.

Considering all above mentioned the calculated growth rate of the $(10\bar{2})$ face is given by an empirical equation derived from the consideration of simple engineering approximations [Oha73]. This method considers only molecular diffusion and it proposes complicated geometrical models to describe the movement of solute molecules from the bulk to the crystal surface. In order to approximate the overall growth rates of the growth mechanism for the specific face has to be clarified. The calculations are not used to compute the growth morphology here. Current findings allow the growth rate of a single face to be calculated. However, the methodology is limited depending on the growth mechanism (surface diffusion or bulk diffusion) which dominates the growth.

First the K_G value of every faces was calculated according to the molecule numbers which is transferred from bulk to the solid surface using eq. 2.11. The calculations were performed for the results of the simulations which were given in Figure 5.28. Even though some diffusion coefficient values are high compare to the others in the simulations which were performed in the presence of some other faces, a significant mass increase is not observed. It can be concluded that the mass increase does not only depend on the diffusion coefficient value of solute, but also on the structure of the surface. These faces which have no mass increase were

not included in the growth rate calculations. According to the values of K_G the growth mechanism was defined by using the ratio of the relative resistance of bulk diffusion to surface integration (ξ) and amorphous cell size (L) values.

For all faces for which an increases in mass was observed the $\xi \cdot L$ values are lower than 1. Therefore, all investigated face growth rates are controlled by the surface integration mechanism. Calculated $\xi \cdot L$ values are given in Table 6.3 together with the calculated growth rates.

Table 6.3: *Calculated ξL values for the investigated faces. For some faces a significant increase in mass was not observed.*

ξL values	For (100) $/ g \cdot cm^{-3} \cdot 10^{-6}$	For (002) $/ g \cdot cm^{-3} \cdot 10^{-6}$	For (10 $\bar{2}$) $/ g \cdot cm^{-3} \cdot 10^{-6}$	For (011) $/ g \cdot cm^{-3} \cdot 10^{-6}$	For (11 $\bar{1}$) $/ g \cdot cm^{-3} \cdot 10^{-6}$
25Hq+106Eth	-	-	0.059	-	-
50Hq+106Eth	0.044	0.483	0.128	0.137	-
100Hq+213Eth	0.144	0.733	0.214	0.242	-
150Hq+106Eth	0.112	0.895	0.772	0.387	-

According to the $\xi \cdot L$ values in all cases surface integration dominates the growth kinetics. To calculate the growth rates, equation 2.20 has to be modified in order to consider the surface integration mechanism and this is done by neglecting the $\xi \cdot L$ term in equation. Hence, growth rate can be calculated by:

$$R_G = K_G \Delta C \quad (6.5)$$

Here ΔC is the supersaturation.

According to the values which were obtained above, growth rate values of faces are given in Table 6.4.

Table 6.4: *Calculated growth rates of the examined faces depending on supersaturation values.*

R_G	For (100) / $10^{-6} \text{ \AA}\cdot\text{ps}^{-1}$	For (002) / $10^{-6} \text{ \AA}\cdot\text{ps}^{-1}$	For (10 $\bar{2}$) / $10^{-6} \text{ \AA}\cdot\text{ps}^{-1}$	For (011) / $10^{-6} \text{ \AA}\cdot\text{ps}^{-1}$	For (11 $\bar{1}$) / $10^{-6} \text{ \AA}\cdot\text{ps}^{-1}$
25Hq+106Eth	-	-	0.051	-	-
50Hq+106Eth	0.47	0.137	0.101	0.097	-
100Hq+213Eth	0.130	0.481	0.31	0.35	-
150Hq+106Eth	0.064	0.322	0.427	0.467	-

All data and procedures to calculate growth rates for surface integrated controlled growth rates of faces are given here. However, if the growth rate was dominantly affected by the bulk diffusion mechanism, calculations would not be the same because the diffusion coefficient value must be different. In the case of a bulk diffusion controlled growth mechanism the diffusion coefficient should not only be calculated in parallel direction to the surface, but also in the perpendicular directions, since bulk diffusion takes place in parallel and in perpendicular direction. A way to the calculation perpendicular diffusion coefficient is not given here. Calculation of perpendicular diffusion coefficients and application on the growth rate calculations are left to the further works. The way to calculate growth rates for the surface integration case of growth based on an example was successful here. It shows the way how to proceed in future but it is only half of the way! The problem of bulk diffusion controlled growth has been not solved yet.

By giving the right conditions, the mechanism of crystal growth can be controlled. The result of the solid-liquid simulations indicates that surface integration controls the growth rate mechanism for all simulations for the example given here. This result was reached by the multiplication of the relative resistance of bulk diffusion to the surface integration (ζ) and amorphous cell length (L). Since value of ζ is defined by the simulation time, the surface size and the supersaturation value, these values should be rearranged in order to reach the surface

integration limited growth rate zone. Simulations should be performed for longer simulation times, larger surface areas and higher supersaturation values.

6.5. Conclusions

Conventional crystal habit modelling only considers the solid side. However, consideration of the liquid side is an essential part of understanding solution growth and should be considered in crystal growth investigations. For crystal growth to take place a solution must be supersaturated. In this paper, the effect of different simulation conditions on the basic diffusion properties was investigated with a view to characterising crystal growth. The results part of this work has a deductive structure. It means, all results of this work are related to each other and are in a sequence to proceed. In other words, the results of the last part of a chapter are the results of initial part of a coming chapter.

Initially molecule structure optimization investigations were performed (1, underlined numbers are corresponding to the numbers in Figure 4.2 and lead through the simulation). The aim was here to obtain the most proper molecule geometry as a result of the optimization algorithms. As it was indicated before, the correct molecule structure has high importance of all results throughout this thesis. Furthermore, a type of molecule geometries within a group of molecules may affect the entire systems of physical properties such as the diffusion coefficient. Simulations were performed in order to obtain the most similar structure for benzophenone and hydroquinone to the experimental chemical structures. Simulations indicate that some of the force fields, such as Dreiding and Compass produce a chemical structure closer to the literature values than other force fields. Differences are due to the optimization algorithms in the force fields. While the Dreiding force field has no special charging algorithms, the Compass force field has a special charging algorithm. No matter how the bond, angle and torsion values vary the charge values of the molecules are the same in the simulation which were performed with the Compass force field. On the other hand, the Dreiding force field's bond, angle and torsion angle calculation algorithms make a difference within the force field index. Compatibility of these two force fields for selected molecules was also confirmed in other works [Fie07]. Benzophenone molecule optimization caused benzophenone molecules to become a knee like (bent) structure. Hence, benzophenone molecules lose their planarity after optimization. This creates some changes in the physical properties of the benzophenone molecule. However, for the hydroquinone molecule the torsion angle has not changed with the optimization procedure. This is related to the hydroquinone molecules chemical structure which has benzene and two hydroxyls groups.

Right after the molecule structure optimization crystal morphologies of the working substances were investigated (2). For a few reasons this investigation has an importance. Morphologies of experimental and simulated molecules were obtained and matched. Hence, the accuracy of the simulation was tested. Morphological important faces were identified (2A and 2B). The definition of the morphological important faces is required in order to perform solid-liquid simulations which are the last simulation steps in the procedure of the entire thesis. Also the responses of the morphological important faces to the presence of additive molecules were investigated. Simulation indicated that experimental habits of benzophenone, hydroquinone and benzoic acid in the presence of ethanol and acetone molecules were successfully generated by computer simulations (2D). Solid-liquid simulations were performed by considering the findings of this stage. A perfect match for benzoic acid gave cause not to go on with the investigation because of the high success of the existed models in terms of the model simulations.

Pure simulations of diffusion coefficients were performed only with benzophenone and hydroquinone molecules by a creation of an amorphous cell (3AA). At first the diffusion coefficient simulation were performed in the presence only of organic molecules (without any solvent or additive). These simulations were performed in order to find suitable simulation conditions and contributions of the organic molecule itself in its diffusivity. Results were evaluated by an empirical method since the difficulties in finding experimental results for the cases. As a result of this part a close fitting diffusion coefficient value for the case of benzophenone could not be obtained. The reason for this can be found in the molecular structure optimization section (1). Benzophenone molecules high torsion angle (bend) affects its diffusivity. On the other hand, in the case of hydroquinone diffusion coefficient values for the pure system were simulated successfully. In some cases the simulated and empirical diffusion coefficient values are matching with only minor differences. Hydroquinone molecules with non-bent like structure play an important role here. Right along with bent structure, benzophenone molecules the molecular weight differences play another important role in diffusion coefficient differences.

Another step in calculations of the diffusion coefficients is the adding of solvent molecules to the diffusion coefficient calculations (3AB). In this case solvent molecules were selected depending upon the results of the morphology calculation sections of this work (2D). In this respect the ethanol molecule was selected as a solvent in order to proceed. As a result of ambiguities in the simulations which were performed with the benzophenone molecule, the simulations with benzophenone molecule were not carried out here. Ethanol molecules were

inserted to the amorphous cell depending upon different supersaturation values of hydroquinone. Empirical diffusion coefficient values decreased significantly when solvent molecules are included in the calculations. Experimental diffusion coefficient values are also in the same range with empirical values in the presence of solvent molecules. Simulated diffusion coefficient values which were produced by this work are also matching with both empirical and experimental values. Under proper simulation conditions groupings between the molecules within an amorphous cell were demonstrated depending upon intermolecular interactions. This grouping has a great importance for the crystal growth investigations. The effect of intermolecular interactions was examined and its importance was clearly demonstrated together with starting geometries of the simulations and the related energy diagrams.

The most important stage of the entire work is the solid-liquid simulations (3AC). These were performed as the last simulation stage of this work. The faces investigated were cleaved in order to combine them with solute-solvent systems. The cleaved faces were combined with the amorphous (solution) cells at different supersaturation values and molecular dynamics calculations were performed with a similar dynamics algorithm. An increase in the supersaturation value resulted in an increase in the diffusion coefficient values, as expected. Polar and semi-polar structures of the cleaved faces played a significant role with respect to the diffusion coefficient value as a result of the different intermolecular interactions between bulk liquid and crystal surface. However, used software's impracticableness for the cleaving of the surface and sometimes the failure in cleaving the surfaces in the right way caused some unexpected results.

The clear clustering of molecules on the solid surface as a result of solid-liquid simulation gives a possibility to examine the growth mechanism (3B). Depending upon the amount of solute on the crystal surface after the simulations the growth mechanism was determined in a definite time interval. However, the availability of the methodology of this part allows only the calculation of the parallel diffusion coefficient value of hydroquinone relative to the crystal surface examined (3ACA). This means that if bulk diffusion dominates the diffusion coefficient calculation method can theoretically not be used. Clear mass increases on some of the faces were observed and related calculations were performed in order to define the growth mechanism. As a result of the theoretical calculations it is concluded that for all possible faces in this case the surface integration mechanism dominantly defines the growth process. This result was reached by the multiplication of the relative resistance of bulk diffusion to the surface integration (ζ) and amorphous cell length (L). By defining the correct conditions the

mechanism of crystal growth can be modelled. The value of ζ is defined by the simulation time, the surface size and the supersaturation value. It needs to be ascertained that the simulation results are in the surface integration limited growth rate zone (3C). Calculated face growth rate values are given in Table 6.4. Future optimization can be achieved if simulations are performed for larger surface areas and higher supersaturation values.

6.6. Outlook

Since 19th century many unknown phenomena related to crystallization were answered with great success. However, some problems are still not answered in such a way to have routine methodologies. The usage of computer simulations has already brought along not only many advantages but has also raised many questions which have to be answered. Efforts to find logical answers to the problems of computer simulations are currently under investigation by many researches. Some weak points related to this work were addressed in the chapter aim of this work. This work aims to perform required investigation in order to fill gaps between the useful applicable theories.

The diffusion mechanism is one of the fundamental phenomena of the crystal growth mechanism. Diffusion under different system condition has to be clearly differentiated and described. When this is achieved the most missing points in the crystallization theory and its applications are going to be answered. For this purpose the diffusion mechanisms of organic molecules were investigated from the simplest case to the most complicated case.

Findings of this work can be used in order to successfully simulate well known theories in computer environments. This work would become more of an issue if the following points could be added or optimized:

- The used method should be optimized by taking more experimental data instead of approximations. This would bring more quantitative structure to the thesis.
- The diffusion coefficient value which is obtained by the Einstein relationship represents a homogeneous diffusion coefficient. Homogeneous diffusion coefficients are applicable for homogeneous systems. Directional diffusion coefficients for parallel and perpendicular components have to be calculated. Even though, the homogeneous diffusion coefficient is a good approximation for parallel components of the diffusion (because of periodic boundary conditions) a clear methodology needs to be given.
- Calculation methods of the bulk diffusion and surface integration were envisaged by this work. Depending upon the directional diffusion coefficient, growth rate

calculations should be performed when the bulk diffusion limits the growth rate. In this work surface integration dominantly limits the growth rate and in this case using the diffusion coefficient values is a good approximation. A diffusion coefficient value of this work represents the parallel diffusion coefficient in the presence of a crystal surface.

- When parallel and perpendicular diffusion coefficient values are modeled successfully, hence bulk diffusion and surface integration, simulation conditions should be carefully analyzed and desired growth rate should be envisaged by supplying the correct conditions.
- Corresponding to the growth rate calculations final morphology of the working systems should be calculate and compared with the existing results which can be obtained using existing morphology calculation methods.
- Errors which were caused by the software should be considered carefully. The commercial software makes errors during the cleaving of the morphological important faces. Alternative methods have to be considered in order to not to have the errors or usage of similar computer simulation software should be considered.
- Simulations were performed in the absence of water molecules. Since many of the industrial crystallization processes take place in the presence of water molecules, simulations should be performed in the presence of water. However, water molecules need a special treatment in computer simulation environments because of their high polarity. Existing water models should be implemented carefully by considering water's possible cluster structure. Hence, water molecules have to be added to the simulation studies of this work.

7. Summary

Crystallization is employed as a purification and separation operation for a large number of products in a number of industry sectors, in particular in the pharmaceutical and speciality chemical sectors, for food and feed products and agrochemicals. In many of processes crystals grow in solution, which means that a subsequent solid-liquid separation is required. Crystal shape has a significant impact on this and other downstream processes such as formulation (i.e. tableting for pharmaceutical products) and packaging. In solid-liquid separation the shape of the crystals plays a critical role in the efficiency of separation. Tabular crystals tend to inhibit filtration due to significant pressure drop, needle-shaped crystals tend to retain a large amount of mother liquor, resulting in an elevated level of impurities. In terms of other operations, extreme geometries can effect compressibility or lead to excessive dust formation as a result of breakage, thus increasing the risk posed by the materials. These problems are reduced greatly when handling compact crystals. It is therefore desirable to be able to control the shape of the product crystals during processing, in order to manufacture a product with suitable properties with a high degree of reproducibility.

Controlling crystal shape necessitates controlling those process parameters that influence the growth of the crystals. These factors include the supersaturation, solvent composition, and the concentration of heteromolecules present. The latter is often a result of previous process steps such as chemical reactions which naturally produce by-products and is therefore not trivial to control. The former, the level of supersaturation or undercooling are process parameters that are entirely under the control of the operator. It is at this point that growth can be controlled with least effort, providing the influence of the driving force upon crystal growth is known. However, returning to impurities it is conceivable and has indeed been demonstrated, that impurities can have a significant influence on individual crystal face growth rates. The presence of impurities cannot be excluded entirely and they are either the result of preceding chemical reactions (by-products) or introduced by virtue of their presence in the solvent or the reactants employed. However, the effect of impurities also opens a path to manipulating growth rates by deliberately adding growth-modifying materials (tailor-made additives) to the crystallization broth.

Research on crystal growth has been conducted for well over 100 years and for at least the past 50 years theories have been available that allow the calculation of crystal habit *based upon the properties of the solid*. Since the importance of the growth environment for the resulting crystal habit was recognised very early, theoretical approaches generally took this factor into consideration. With the advent of computers, automated calculations of crystal

habit have been possible and computer programs exist, that enable the routine computation of crystal habit based upon energetic considerations of crystal faces. To this day, however, there exists *no routine* prescription for including the effect of the growth environment upon the resulting crystal habit.

Based on the simple geometrical properties of a crystal, morphology of investigated crystal can be modelled by well known Bravais – Friedel – Donnay – Harker (BFDH) method [Win98] and further investigation on Hartman – Perdok (HP) method [Har55a, b, c]. Further theories were aimed to consider the role of external environments by modifying the above theories. However, every improved theory could deal with the crystallization theory for a special case. A general theory which simulates the right habit is required. Objective of this work is to find a response which assists to find the right methodology by considering the transport properties of solid-liquid system. However, in order to model the role of transport mechanism on solid-liquid system growth rates, computer experiments have to be started from the simplest case (single molecule geometry optimization) and go on until the growth rate of a single face calculation. Benzophenone and hydroquinone organic molecules were selected as model substances in this work.

In particular, within this work some important findings were confirmed and by combination of the related findings in the right order allow to simulate the growth rate of a single face. For example, the importance of the correct single molecule geometry is given by molecular structure optimization calculations. These calculations indicate that planar structure of the investigated molecule has an important effect on the physical properties of the same molecule. As it was indicate before simulations should be followed by one step further depending upon the results. Habits of the selected organic systems in the presence of various additive molecules were investigated by experiments and existed simulation methods. Both experimental and simulated results were compared with each other and literature. Correct results were used in order to perform additional calculations and, meantime, they indicated that used simulation conditions are adequate for further calculations.

Transport coefficient calculations were performed with the amorphous cell and investigation on the changes of physical and system parameters of the amorphous cell. The effect of system parameters such as temperatures, simulation times, temperature control algorithms, used molecular interaction force fields, simulation start conformations as well as supersaturation values on transport properties were investigated for pure materials and solution systems. Results were evaluated either empirical or experimental values when they are available in literature.

Successful transport coefficient calculations were allowed to perform similar calculations in the presence of the solid surface. The transport coefficient calculation methods have to be investigated according to the system conditions because in the presence of solid surfaces the system has loses some properties such as the symmetry. Hence, a significant modification on the methodology has to be considered. Depending upon the direction of the transport coefficient with respect to the solid surface mass increase on the investigated face was calculated. The definite mass increase allows to calculate the growth rate of the investigated face in the consideration of the effects of crystallizing environment.

The obtained results indicate that the growth rate of a crystal face can be calculated starting from a single molecule consideration to the solid (crystal surface) – liquid (bulk liquid) amorphous system simulations. A simulation itself takes a long preparation and calculation time. However, in order to perform efficient simulations and decrease the time cost, a significant simulation experience should be gained. This work spotlights the methodology (Figure4.2) which can be followed. Even though, the growth rate of a face is calculated morphology calculations were not performed. Morphology calculations can be performed right after enough simulation practice is obtained.

8. Zusammenfassung

Die Kristallisation wird in einer Vielzahl technischer Prozesse zur Aufreinigung und Trennung von Produkten eingesetzt. Anwendung findet dieses Verfahren insbesondere in der pharmazeutischen Industrie, wie auch in Herstellungsverfahren für Agro- und Spezialchemikalien, ebenso in der Lebensmittel- und Grundstoffindustrie. Diese Prozesse basieren vorwiegend auf der Lösungskristallisation, und erfordern dementsprechend eine fest-flüssig Trennung. Die Kristallform hat einen maßgeblichen Einfluss auf den Trennungsvorgang, sowie auf anschließende Prozessschritte, wie die Weiterverarbeitung (z.B. die Tablettierung pharmazeutischer Stoffe) und Verpackung. In fest-flüssig Trennprozessen wirkt sich die Kristallform entscheidend auf die Effizienz der Trennung aus. Beispielsweise können flache Kristalle in Filtrationsprozessen einen starken Druckabfall verursachen und den Betrieb behindern. Nadelförmige Kristalle können zur Rückhaltung von Mutterlösung führen, und damit eine Reduzierung des Produktreinheitsgrades hervorrufen. Kristalle mit extremer Geometrie können die Kompressibilität beeinflussen, und in Folge von Kristallbruch zu starker Staubbildung führen. Diese Probleme können durch die Herstellung und Verwendung kompakter Kristalle umgangen werden. Daher ist es wünschenswert, die Form der produzierten Kristalle während der Herstellungsprozesses steuern zu können, um in der Lage zu sein, unter der Voraussetzung der Reproduzierbarkeit, ein Produkt von hoher Reinheit und mit den gewünschten Eigenschaften herzustellen.

Die Kontrolle der Kristallform erfordert eine Steuerung der Prozessparameter, die das Kristallwachstum beeinflussen. Diese Faktoren beinhalten die Übersättigung, die Zusammensetzung des Lösungsmittels und die Konzentration der beteiligten Heteromoleküle. Letzteres resultiert meist aus vorangegangenen Prozessstufen, wie beispielsweise chemische Reaktionen, bei denen Nebenprodukte entstehen und die nur schwer zu kontrollieren sind. Ersteres, der Grad der Übersättigung bzw. Unterkühlung, sind Prozessparameter, die im Betrieb vollständig regulierbar sind. Durch Steuerung der Triebkraft kann hier die Kontrolle der Wachstumsrate des Kristalls mit dem geringsten Aufwand erfolgen.

Nachgewiesen ist der maßgebliche Einfluss den Verunreinigungen auf die Wachstumsraten spezieller Kristallflächen haben. Die Anwesenheit einer Verunreinigung kann nicht vollständig ausgeschlossen werden, denn er kann entweder das Ergebnis einer chemischen Reaktion sein, oder wurde durch das Lösungsmittel bzw. die Reaktanden in den Prozess eingetragen.

Dennoch eröffnet die Wirkung der Verunreinigungen auch die Möglichkeit zur Beeinflussung der Wachstumsraten einzelner Kristallflächen durch gezielte Zugabe von modifizierenden Additiven (tailor-made Additive) in die Lösung.

Das Kristallwachstum wird seit über 100 Jahren erforscht, innerhalb der vergangenen 50 Jahre wurden Theorien entwickelt, mit deren Hilfe es möglich ist, die Berechnung des theoretischen Kristallhabitus durchzuführen, allein *auf Feststoffeigenschaften basierend*. Die Bedeutung der Wachstumsumgebung wurde bereits früh erkannt. So binden theoretische Betrachtungsweisen diesen Faktor ein. Durch den Fortschritt in der Computerentwicklung wurden automatisierte Berechnungen von Kristallmorphologien möglich. Gegenwärtig existiert eine Anzahl von kommerziell erhältlichen Computerprogrammen, mit deren Unterstützung, basierend auf energetischen Betrachtungsweisen der Kristallflächen, eine routinierte Berechnung der Kristallhabiti durchgeführt werden kann. Dennoch existiert bis heute *keine Routinerezeptur*, die die Auswirkung des Wachstumsumfeldes auf die resultierende Kristallform beschreibt.

Anhand der geometrischen Eigenschaften eines Kristalls, ermöglichen es die Anwendung Methode nach Bravais, Friedel, Donnay und Harker (BFDH) [Win98] und die weiteren Erkenntnisse nach Hartman – Perdok (HP) [Har55a, b, c] die Morphologie des unter Betrachtung stehenden Kristalls zu modellieren. Weitere Theorien sollen die Rolle der äußeren Wachstumsumgebung durch Anpassung der vorgenannten Modelle einbeziehen. Dennoch konnte jede verbesserte Methode nur die Kristallisationstheorie eines speziellen Falles widerspiegeln. Eine allgemeingültige Theorie zur Vorhersage der korrekten Kristallform wird benötigt. Das Ziel der vorliegenden Arbeit ist es, durch das Einbeziehen der Transportvorgänge im fest-flüssig System, zur Entwicklung einer zuverlässigen Methode zur Morphologievorhersage beizutragen. Um die Rolle des Transportmechanismus in fest-flüssig Systemen abzubilden, setzten die Computerexperimente bereits mit dem einfachsten Fall, der Geometrieoptimierung eines Moleküls, ein und reichen weiter bis hin zur Berechnung der Wachstumsrate einer Kristallfläche. Als Modellsubstanzen wurden im Rahmen dieser Arbeit die organischen Stoffe Benzophenon und Hydrochinon untersucht.

Im Rahmen dieser Arbeit konnten wichtige Erkenntnisse bestätigt werden, durch ihre gezielte Kombination mit anderen Methoden und Anwendung in der richtigen Reihenfolge, ist es möglich die Wachstumsraten einzelner Kristallflächen zu bestimmen. Beispielsweise wurde die Geometrie einzelner Moleküle durch vorangestellte molekulare Optimierung berechnet. Diese Berechnungen zeigen, dass die planare Struktur der betrachteten Moleküle einen bedeutsamen Einfluss auf die physikalischen Eigenschaften dieses Moleküls haben. Wie

bereits angedeutet, sollten die folgenden Simulationen stufenweise und basiert auf den vorangegangenen Ergebnissen durchgeführt werden. Die Kristallformen der ausgewählten organischen Substanzen unter Einfluss verschiedener Additive wurden experimentell und in Computersimulationen mit Hilfe bereits bestehender Modelle bestimmt. Die experimentellen und computergestützten Ergebnisse wurden untereinander und mit Literaturangaben verglichen. Korrekte Ergebnisse wurden für weitere Berechnungen verwendet, gleichzeitig konnte gezeigt werden, dass die angewendeten Simulationsbedingungen auch für weitere Berechnungen geeignet sind.

Die Berechnungen des Transportkoeffizienten, sowie die Untersuchungen zur Änderung physikalischer und der Systemparameter wurden in einer amorphen Zelle durchgeführt. Untersucht wurde der Einfluss von Systemparametern, wie Temperatur, Simulationszeit, Algorithmen zur Temperaturkontrolle, verwendete Kraftfelder für die molekularen Wechselwirkungen, Zusammensetzung zu Beginn der Simulation, wie auch der Grad der Übersättigung, auf die Transporteigenschaften der Reinstoff- sowie der Lösungssysteme. Die empirischen und experimentellen Ergebnisse wurden ausgewertet, soweit Literaturangaben verfügbar waren.

Die erfolgreiche Berechnung des Transportkoeffizienten erlaubten in folgenden Schritten die Durchführung ähnlicher Berechnungen für die Anwesenheit einer festen Oberfläche. Die Berechnungsmethoden für den Transportkoeffizienten müssen je nach Systembedingungen angepasst werden, denn in Gegenwart einer festen Oberfläche verliert das System einige seiner Eigenschaften, wie beispielsweise die Symmetrie. Folglich muss eine maßgebliche Änderung der Methode vorgenommen werden. In Abhängigkeit der Richtung des Transportkoeffizienten, unter Berücksichtigung der Oberfläche, wurde das Massenwachstum einer Fläche berechnet. Der genaue Massenzuwachs erlaubt so die Berechnung der Wachstumsrate der Fläche unter Berücksichtigung der Wachstumsumgebung.

Die abgeleiteten Ergebnisse zeigen, dass die Berechnung der Wachstumsrate einer Kristallfläche möglich ist, durch die Betrachtung eines einzelnen Moleküls in einer amorphen Zelle beim Phasenübergang fest (Kristallfläche)-flüssig (Lösung). Eine Computersimulation allein bedarf einer langen Vorbereitungs- und Rechenzeit. Daher sollten um effiziente Berechnungen durchzuführen und die Rechenzeit zu reduzieren im Voraus Erfahrungen und Informationen im Umgang mit Computersimulationen gesammelt werden. Diese Arbeit beleuchtet in diesem Zusammenhang eine Methodik der gefolgt werden kann (siehe Abb. 4.2). Trotz dass die Flächenwachstumsraten berechnet wurden, sind keine

Morphologievorhersagen getroffen wurden. Nachdem aber eine hinreichende Anzahl dieser Berechnungen durchgeführt wurde, können auch Morphologieberechnungen erfolgen.

Latin Letters:

ΔG	<i>joule</i>	<i>Gibbs Free Energy</i>
f	$\text{g}\cdot\text{m}^{-1}\cdot\text{s}^{-2}$	<i>Driving force per unit area</i>
V	m^3	<i>Volume per molecule</i>
k	$\text{J}\cdot\text{K}^{-1}$	<i>Boltzmann constant</i>
T	K	<i>Absolute temperature</i>
P	Pa	<i>Partial pressure</i>
C	$\text{mol}\cdot\text{L}^{-1}$	<i>Solution concentration</i>
f_k	-	<i>Crystallographic factor</i>
$A(n_i)$	m^2	<i>Face area in the orientation n_i</i>
l_i	m	<i>Length of a vector</i>
L	m	<i>Characteristic crystal dimension</i>
D	$\text{cm}^2\cdot\text{s}^{-1}$	<i>Diffusion coefficient</i>
D_{WC}	$\text{cm}^2\cdot\text{s}^{-1}$	<i>Empirical Diffusion Coefficient</i>
m_C	g	<i>Mass</i>
C	$\text{mol}\cdot\text{L}^{-1}$	<i>Solute concentration at bulk</i>
C_i	$\text{mol}\cdot\text{L}^{-1}$	<i>Solute concentration at interface</i>
k_i	$\text{cm}^2\cdot\text{s}^{-1}$	<i>Rate constant</i>
k_d	$\text{cm}^2\cdot\text{s}^{-1}$	<i>Diffusion rate constant</i>
Sh	-	<i>Sherwood number</i>
Re	-	<i>Reynolds number</i>
Sc	-	<i>Schmidt number</i>
u_s	$\text{m}\cdot\text{s}^{-1}$	<i>Particle slip velocity</i>
K_G	$\text{m}\cdot\text{s}^{-1}$	<i>Rate constant</i>
ΔC	$\text{mol}\cdot\text{L}^{-1}$	<i>Concentration (supersaturation)</i>
g	$\text{m}\cdot\text{s}^{-1}$	<i>Parameter represents a size independent growth rate when surface integration is dominating</i>
R_g	$\text{m}\cdot\text{s}^{-1}$	<i>Face growth rate</i>
C	$\text{mol}\cdot\text{L}^{-1}$	<i>Solution concentration</i>

C_0	$\text{mol}\cdot\text{L}^{-1}$	Saturation concentration
M	g	Molecular mass
V_c	cm^3	Critical volume of the solute
R	$\text{J}\cdot\text{K}^{-1}$	Gas constant
T	K	Temperature
t	s	Time
N	mol	Number of particles
k_i	-	Force constant
l_i	m	Bond length
$l_{i,0}$	m	Bond length reference value
V_n	m	Barrier for rotation, (n periodicity)
$q_{i,j}$	coulomb	Charge value
r_{ij}	m	Bond length
K_{inv}	-	Force constant for inversion terms
m_i	g	Mass
x_i	m	Displacement
F_i	N	Force
E_{att}^{hkl}	$\text{kcal}\cdot\text{mol}^{-1}$	Attachment energy of (hkl) face
E_{cr}	$\text{kcal}\cdot\text{mol}^{-1}$	Crystallization energy
E_{sl}^{hkl}	$\text{kcal}\cdot\text{mol}^{-1}$	Slice energy of (hkl) face
d_{hkl}	m	Slice thickness
T_m	$^{\circ}\text{C}$	Melting point
T_b	$^{\circ}\text{C}$	Boiling point
ΔH_{form}	$\text{kJ}\cdot\text{mol}^{-1}$	Formation enthalpy
ΔH_{fus}	$\text{kJ}\cdot\text{mol}^{-1}$	Fusion enthalpy
ΔH_{sub}	$\text{kcal}\cdot\text{mol}^{-1}$	Latent heat of sublimation
ΔH_{vap}	$\text{kcal}\cdot\text{mol}^{-1}$	Latent heat of evaporation
$V_{x,y,z}$	$\text{\AA}\cdot\text{ps}^{-1}$	Average molecule velocity

Greek Letters:

σ	-	Supersaturation
ρ_a	$\text{g}\cdot\text{m}^{-3}$	Adatom density
α	-	Surface roughness factor
$\gamma(n_i)$	$\text{N}\cdot\text{m}^{-1}$	Surface energy
δ	m	Boundary layer thickness
ρ	$\text{g}\cdot\text{m}^{-3}$	Solution density
μ	$\text{mPa}\cdot\text{s}$	Solution viscosity
ε_0	$\text{C}^2\cdot\text{N}^{-1}\cdot\text{m}^{-2}$	Permittivity of free space
ζ	$\text{g}\cdot\text{m}^{-4}$	Relative resistance of bulk diffusion to surface integration
ρ	$\text{g}\cdot\text{cm}^{-3}$	Density
φ	-	Molecular association factor
η	cP	Viscosity of solvent
μ	$\text{mPa}\cdot\text{s}$	Liquid viscosity
ω	degree	Torsion angle
γ	degree	Dihedral angle
ε_{ij}	m	Well depth of the potential energy curve
σ_{ij}	m	Collision diameter
θ_i	degree	Angle
$\theta_{i,0}$	degree	Angle reference value
Ψ	degree	Angle between bond and plane

- [Acc06] Accelrys Software Inc. (2006) Materials Studio®, Software.
- [Ako00] Akopyan, M. E.; Kleimenov, V. I.; Feofilov, A. G., *Stepwise ionization of hydroquinone vapor by monochromatic radiation*, High Energy Chemistry, 34, (2000), 107-111.
- [Ald57] Alder, B. J.; Wainwright, T.E., *Phase transition for a hard sphere system*, J. Chem. Phys., 27, (1957), 1208-1209.
- [All87] Allen, M. P.; Tildesley D. J., *Computer simulations of liquids*, Clarendon Press, Oxford Science Publications (1987).
- [And26] Andrews, H. C.; Lynn, G.; Johnston, J., *The heat capacities and heat of crystallization of some isomeric aromatic compounds*, J. Am. Chem. Soc., 48, (1926), 1274-1287.
- [Ben69] Bennema, P., *The importance of surface diffusion for crystal growth from solution*, J. Cryst. Growth, 5, (1969), 29-43.
- [Ben73] Bennema, P.; Gilmer G.H., *Kinetics of crystal growth*, In Crystal Growth; Ed: Hartmann P., North-Holland; Amsterdam, (1973), 263-327.
- [Ben93] Bennema, P., *Growth and morphology of crystals: integration theories of roughening and hartman-perdok theory in growth mechanisms*. In Handbook of Crystal Growth 1a: Thermodynamics and Kinetics, Ed: Hurler D.T.J., North Holland, Amsterdam, (1993), 477-581.
- [Ber85] Berkovitch-Yellin, Z.; Van Mil, J.; Addadi, L.; Idelson, M.; Lahav, M.; Leiserowitz, L., *Crystal morphology engineering by "tailor-made" inhibitors; a new probe to fine intermolecular interactions*, Journal of the American Chemical Society 107, (1985), 3111-3122.
- [Bon35] Bonner, W.D.; Kinney, C.R., *The direct carboxylation of carbon compounds. III. The free energy of benzoic acid at 522°K*, J. Am. Chem. Soc., 57, (1935) 2402-2403.
- [Bos05] Bosse, D., *Diffusion, viscosity, and thermodynamics in liquid systems*, PhD thesis, Technischen Universität Kaiserslautern, Kaiserslautern, (2005).

- [Bro85] Brooks, C. L. III; Montgomery P. B.; Karplus, M., *Structural and energetic effects of truncating long range interactions in ionic and polar fluids*, *J. Chem. Phys.*, 83, (1985), 5897-5908.
- [Bur51] Burton, W. K.; Cabrera, N.; Frank, F. C., *The growth of crystals and the equilibrium structure of their surfaces*, *Philosophical Transactions of the Royal Society of London*, A 243, (1951), 299-358.
- [Cha98] Chan, T. C.; Chen, N.; Lu, J.G., *Diffusion of Disubstituted Aromatic Compounds in Ethanol*, *J. Phys. Chem. A*, 102, (1998), 9087-9090.
- [Che61] Chernov, A.A. *The spiral growth of crystals*, *Soviet Physics Uspekhi*, 4, (1961), 116-148.
- [Che84] Chernov, A.A., *Modern crystallography. III. Crystal Growth* New York, Springer-Verlag (1984).
- [Che05] Chen, W.; Yin, Q.; Wang, J.; Li, X., *Computer modeling of the solvent effect on hydroquinone crystal habit*, 16th International Symposium on Industrial Crystallization, Ed:J. Ulrich, VDI-Berichte 1901.1, Düsseldorf, (2005), 441-446.
- [Chi02] Chirico, R. D.; Knipmeyer, S. E.; Steele, W. V., *Heat capacities, enthalpy increments, and derived thermodynamic functions for benzophenone between the temperatures 5 K and 440 K*, *The Journal of Chemical Thermodynamics*, 34, (2002), 1885-1895.
- [Chi03] Chianese, A.; Luozzo, M. D.; Kubota, N., *Effect of Pyrogallol additive on the growth rate and the habit of hydroquinone crystals*, *Crystal Growth & Design*, 3, (2002), 425-430.
- [Cly94a] Clydesdale, G.; Roberts, K.J.; Lewtas, K.; Docherty, R., *Modelling the morphology of molecular crystals in the presence of blocking tailor-made additives*, *J. Crystal Growth* 141, (1994a), 443-450.
- [Cly94b] Clydesdale, G.; Roberts, K.J.; Docherty, R., *Modelling the morphology of molecular crystals in the presence of disruptive tailor-made additives*, *J. Crystal Growth* 135, (1994b), 331-340.

- [Csd07] Cambridge Structural Database, Cambridge Crystallographic Data Centre, 12 Union Road, Cambridge, (2004-2007), CB2 1EZ, UK.
- [Doc91] Docherty, R.; Clydesdale, G.; Roberts, K. J.; Bennema, P., *Application of bravais-friedel-donnay-harker, attachment energy and ising modles to predicting and understanding the morphology of molecular crystals*, J. Phys. D: Appl. Phys. 24, (1991), 89-99.
- [Dul63] Dullien, F. A. V., *New Relation between Viscosity and the Diffusion Coefficients based on Lamm's Theory of Diffusion*, Transactions of the Faraday Society, 59, (1963), 856-868.
- [Ewa21] Ewald, P. P., *Die Berechnung optischer und elektrostatischer Gitterpotentiale*, Annalen der Physik, 64, (1921), 253-287.
- [Ert73] Ertl, H.; Dullien, F. A. V., *Self-diffusion and Viscosity of some liquids as a function of temperature*, AIChE Journal, 19, (1973), 1215-1223.
- [Fic55] Fick, A., *On liquid diffusion*, Phil. Mag.10, (1855),31-39.
- [Fie07] Fiebig, A., *Prediction of crystal morphology for a limited range of impurity concentrations*, PhD thesis, Martin-Luther-Universität Halle-Wittenberg, Shaker Verlag, Aachen, (2007).
- [Fie07b] Fiebig, A.; Jones, M.J.; Ulrich, J., *Predicting the effect of impurity adsorption on crystal morphology*, Crystal Growth Des., 7, (2007), 1623-1627.
- [For06] Foresman, J. B.; Frisch, Æ., *Exploring chemistry with electronic structure methods*, 2nd edition, Gaussian, Inc. USA, (2006).
- [Fre96] Frenkel, D.; Smit, B., *Understanding molecular simulation: from algorithms to applications*, Academic Press, San Diego, (1996).
- [Fro38] Frossling, N., *Über die Verdunstung fallender Tropfen*. Gerlands Beitrage zur Geophysik. 52, (1938), 170-216.
- [Gal01] Gallagher, D. A., *Guide to conformational searching with CAChe*, Fujitsu, (2001).

- [Gas80] Gasteiger, J.; Marsili, M., *Iterative partial equilization of orbital electronegativity – A rapid access to atomic charges*, Tetrahedron, 36, (1980), 3219-3228.
- [Gil71] Gilmer, G.A., Ghez, R., Cabrera, N., *An analysis of combined surface and volume diffusion processes in crystal growth*, J. Crystal Growth, 8, (1971), 79-93.
- [Gre87] Greengard, L.; Rokhlin, V. I., *A fast algorithm for particle simulations*, J. Comput. Phys., 73, (1987), 325-348.
- [Han86] Hansen, J. P.; McDonald, I.R., *Theory of simple liquids*, 2nd edition, Academic press, London, (1986).
- [Har55a] Hartman, P.; Perdok, W.G., *On the relation between structure and morphology of crystals I*, Acta Cryst. 8, (1955a), 49-52.
- [Har55b] Hartman, P.; Perdok, W.G., *On the relation between structure and morphology of crystals II*, Acta Cryst. 8, (1955b), 521-524.
- [Har55c] Hartman, P.; Perdok, W.G., *On the relation between structure and morphology of crystals III*, Acta Cryst. 8, (1955c), 525-529.
- [Har99] HARMM, Molecular Dynamics Simulations Tutorial, 1999, http://www.ch.embnet.org/MD_tutorial/pages/index2.html
- [Hen09] Hengstermann, A.; Kadam, S.; Jansens, P. J., *Influence of supercooling and water content on crystal morphology of acidic acid*, Crystal Growth & Design, 9, (2009), 2000-2007.
- [Hir34] Hirsbrunner, H., *Über das gleichgewicht der thermischen dissoziation der salicylsäure*, Helv. Chim Acta, 17, (1934), 477-504.
- [Hol99] Holmbäck, X.; Rasmuson, Å. C., *Size and morphology of benzoic acid crystals produced by drowning-out crystallization*, J. Cryst. Growth, 199, (1999), 780-788.
- [Hün05] Hünenberger, P. H. *Thermostat algorithms for molecular dynamics simulations*, Adv. Polym. Sci., 173, (2005), 105-149.

- [Igl07] Iglesias, O.S.; Medina, I.; Pizarro, C.; Bueno, J.L., *On Predicting self-diffusion coefficients from viscosity in gases and liquids*, Chemical Engineering Science, 62, (2007), 6499-6515.
- [Jac58] Jackson, J.A., *Mechanism of growth*. In Liquid Metals and Solidification. American Society for Metals: Cleveland, (1958), 174-186.
- [Job87] Joback, K. G.; Reid, R. C., *Estimation of Pure-Components Properties from Group Contributions*, Chem. Eng. Comm., 57, (1987), 233-243.
- [Kar02] Karpinski, P.H.; Wey, J.S., (2002) *Precipitation processes*, in Handbook of industrial crystallization. Ed: Myerson A. S., 2nd edition, Butterworth-Heinemann, Boston, (2002), 141-160.
- [Kae64] Kaeding, W.W., *Oxidation of aromatic acids. IV. Decarboxylation of salicylic acids*, J. Org. Chem., 29, (1964), 2556-2559.
- [Kin91] King, G. S., *Hydrogen bonds in crystals*, in *Intermolecular forces: an introduction to modern methods and results*, Ed. P. L. Huyskens, Springer Verlag Berlin, Heidelberg, (1991).
- [Kla09] Klaus, N., *Free energy of surfaces, wulff's theorem and wulff's plot*, PhD thesis, Centre for Surface- and Nanoanalytics (ZONA) Johannes Kepler University Linz, (2009).
- [Koo02] Kooijman, H. A., *A Modification of the stokes-einstein for diffusivities in dilute binary mixtures*. Ind.Eng. Chem. Res. 41, (2002), 3326-3328.
- [Kop55] Kopp, H. *Untersuchungen über das spezifische gewischt, die Ausdehnung durch Wärme und Siedepunkt einiger Flüssigkeiten*, Justus Liebigs Annalen der Chemie, 94, (1855), 257-320.
- [Kos34] Kossel, W., *Zur energetik von oberflächenvorgängen*, Annalen der Physik, 21, (1934), 457-480.
- [Kru83] de Kruif, C. G.; van Miltenburg, J.C.; Blok, J. G. *Molar heat capacities and vapour pressures of solid and liquid benzophenone*, The Journal of Chemical Thermodynamics, 15, (1983), 129-136.

- [Kun09] Kundin, J.; Yürüdü, C.; Ulrich, J.; Emmerich, H., *A Phase-field/monte-carlo model describing organic crystal growth from solution*, Eur. Phys. J. B, 70(3), (2009), 403-412.
- [Lan06] Lan, C. W.; Yu, W. C.; Hsu, W.C., *Bulk single crystals, growth of*, In Encyclopedia of Surface and Colloid Science Vol.2, 2nd Edition, Ed. P. Somasundaran, CRC Press, Taylor&Francis, New York, (2006).
- [Lan80] Landau, L.D.; Lifshitz, E. M., *Statistical physics, course of theoretical physics*, Volume 5, Butterworth-Heinemann, Oxford, (1980).
- [Lea01] Leach, A. R., *Molecular modelling: principles and applications*, Pearson Education EMA, Harlow - Essex, England, (2001).
- [Lev97] Levi, A.C.; Kotrla, M., *Theory and simulation of crystal growth*, J. Phys.: Condens. Matter, 9, (1997), 299-344, *and references therein*.
- [Li01] Li, J.; Liu, H.; Hu, Y., *A mutual-diffusion-coefficient model based on local composition*, Fluid Phase Equilibria, 193, (2001), 187-188.
- [Li06] Li, X.; Yin, Q.; Chen, W.; Wang, J., *Solubility of Hydroquinone in Different Solvents from 276.65 K to 345.10 K*, J. Chem. Eng. Data, 51, (2006), 127-129.
- [Lin81] Lindeman, S. V.; Shklover, V. E.; Struchkov, Y. T., *The β -Modification of hydroquinone*, Cryst. Struct. Com., 10, (1981), 1173-1179.
- [Liu71] Liu, C. Y.; Tsuei, H. S.; Youngquist, G. R., *Crystal growth from solution*, Chem. Eng. Progr. Symp. Ser., 67 (110), (1971), 43-52.
- [Liu95] Liu, X.Y.; Boek, E.S.; Briels, W.J.; Bennema, P., *Analysis of morphology of crystals based on identification of interfacial structure*, J. Chem. Phys. 103, (1995), 3747-3754.
- [Liu96] Liu, X.Y.; Bennema, P., *Prediction of the growth morphology of crystals*, J. Crystal Growth 166, (1996), 117-123.
- [Liu04] Liu, P.; Harder, E.; Berne, B. J., *On the calculation of diffusion coefficients in confined fluids and interfaces with an application to the liquid-vapor interface of water*, J. Phys. Chem. B, 108, (2004), 6595-6602.

- [Liu07] Liu, C. P.; Wang, R. C.; Kuo, C. L.; Liang, Y. H.; Chen, W. Y., *Recent patents on fabrication of nanowires*, *Recent Patents on Nanotechnology*, 1, (2007), 11-20.
- [Lob69] Lobanova, G. M., *Molecular and crystal structure of benzophenone*, *Soviet Physics – Crystallography*, 13, (1969), 856-858.
- [Lu04] Lu, J.J., *Predicting crystal morphology in the presence of additives by molecular modelling*, PhD. Thesis, Martin-Luther-Universität Halle-Wittenberg, Shaker Verlag, Aachen, (2004).
- [Maa66] Maartmann-Moe, K., *The crystal structure of γ -hydroquinone*, *Acta Cryst.*, 21, (1966), 979-982.
- [Map88] Maple, J. R.; Dinur, U.; Hagler, A. T., *Derivation of force field for molecular mechanics and dynamics from ab initio energy surfaces*, *Proc. Natl. Acad. Sci.* 85, (1988), 5350-5354.
- [Mat99] Mattos, M., *Zur übertragung der einbau-annäherung auf die kristallhabitusänderung durch adsorption*, PhD thesis, Universität Bremen, Bremen, (1999).
- [May90] Mayo, S.L.; Olafson, B.D. and Goddard, W.A., *DREIDING: A generic force field for molecular simulations*, *J. Phys. Chem.* 94, (1990), 8897-8909.
- [Max52] Maxwell, J.C., *The scientific papers of James Clerk Maxwell*. Ed.: W.D. Niven, Dover Publications New York, (1952).
- [Mer06] The Merck Index, *An encyclopedia of chemicals, drugs, and biologicals*, Whitehouse Station, O'Neil, M.J. (Ed.). NJ, Merck and Co. Inc., 833, (2006).
- [Miy01] Miyabe, K.; Guiochon, G., *Correlation between surface diffusion and molecular diffusion in reversed-phase liquid chromatography*, *J. Phys. Chem. B*, 105, (2001), 9202-9209.
- [Mor72] Morawetz, E., *Enthalpies of vaporization for a number of aromatic compounds*, *J. Chem. Thermodynamics*, 4, (1972), 455-460.
- [Mul01] Mullin, J.W., *Crystallization*, Butterworth-Heinemann, Oxford, (2001).

- [Mye02] Myerson, A. S.; Ginde, R., *Crystals, crystal growth and nucleation*, in Handbook of industrial crystallization. Ed: Myerson A. S., 2nd edition, Butterworth-Heinemann, Boston, (2002), 33-63.
- [Mye99] Myerson, A. S., *Crystallization basics*. In Molecular Modeling Applications in Crystallization. Ed. A. S. Myerson, Cambridge University Press, New York, (1999), 55-106.
- [Nag98] Nagashima, N., *Effects of additives (other amino acids) on crystal morphology and polymorphisim of amino acids*, in International symposium on industrial crystallization, Tokyo, Japan, 243-255, (1998).
- [Nie97] Niehörster, S., *Der Kristallhabitus unter additiveinfluß: eine modellierungsmethode*, PhD thesis, Universität Bremen, Bremen, (1997).
- [Nos93] Nosé, S., *Dynamical behaviour of a thermostated isotropic harmonic oscillator*, Phys. Rev. E, 47, (1993) 164-177.
- [Nyv85] Nyvlt, J.; Sohnel, O.; Matuchova, M.; Broul, M., *The kinetics of industrial crystallization*. Amsterdam, Elsevier, (1985).
- [Oha73] Ohara, M., Reid, R. C., *Modeling crystal growth rates from solution*, Prentice-Hall, Englewood-Cliffs, (1973).
- [Ola64] Olah, G. A., Friedel-Crafts Ketone Synthesis, United States Patent Office Assignor to The Dow Chemical Company, Midland, (1964).
- [Pal48] Palin, D.E.; Powell, H.M., *The structure of molecular compound. Part VI. The β -type clathrate compounds of quinol*, J. Chem. Soc., (1948), 815-821.
- [Par50] Parks, G.S.; Mosley, J. R.; Peterson, P. V. J., *Heats of combustion and formation of some organic compounds containing oxygen*, The Journal of Chemical Physics, 18, (1950), 152-153.
- [Pry02] Prywer, J., *Correlation between growth of high-index faces, relative growth rates and crystallographic structure of crystal*, Eur. Phys. J. B, 25, (2002), 61-68.

- [Pue97] Puel, F.; Marchal, P.; Klein, J., *Habit transient analysis in industrial crystallization using two dimensional crystal sizing technique*, Chemical Engineering research and design, 75, (1997), 193-205.
- [Pue03] Puel, F.; Fevotte, G.; Klein, J. P., *Simulation and analysis of industrial crystallization process through multidimensional population balance equations. Part I: a resolution algorithm based on the method of classes*, Chem. Eng. Sci. 58, (2003), 3715-3727.
- [Rap91] Rappe, A.K.; Goddard, W.A. III, *Charge equilibration for molecular dynamics simulations*, J. Phys. Chem., 95, (1991) 8, 3358-3363.
- [Rut92] Rutten, P. W. M. *Diffusion in Liquids*, PhD thesis, Technical University of Delft, Delft university press: Delft, Netherlands, (1992).
- [Rya90] Ryan, J.C.; Lawandy, N.M, *Model of linear- and nonlinear-optical properties of β -quinol clathrates*, Phys. Rev. B, 41, (1990), 2369-2374.
- [Sch60] Schmitt, R. G.; Hirt, R. C., *Investigation of the protective ultraviolet absorbers in a space environment. I. Rate of evaporation and vapor pressure studies*, Journal of Applied Polymer Science, XLV, (1960), 35-47.
- [Sch91] Schmidt, K. E.; Lee, M. A., *Implementing the fast multipole method in three dimensions*, J. Stat. Phys., 63, (1991), 1223-1235.
- [Sch04] Schmiech, P., *Zur Vorhersage des Kristallhabitus unter fremdstoffeinfluß mittels PBC-Vektoren*, PhD thesis, Martin-Luther-Universität Hale-Wittenberg, Shaker Verlag, Aachen, (2004).
- [Sci08] SciFinder Scholar Database, *calculated using advanced chemistry development (ACD/Labs) software V8.14 for Solaris* (© 1994-2008 ACD/Labs), (2008).
- [Ski75] Skipp, C.J.; Tyrrell, H.J.V., *Diffusion in Viscous Solvents. Part 2- planar and spherical molecules in Propane-1,2-diol at 15,25 and 35°C*, J. Chem. Soc., Faraday Trans. 1, 71, (1975) 1744-1753.
- [Sti74] Stillinger, F. H.; Rahman, A., *Improved simulation of liquid water by molecular dynamics*, J. Chem. Phys., 60, (1974), 1545-1558.

- [Str28] Stranski, I. N., *Zur Theorie des Kristallwachstums*, Z. Phys. Chem., 136, (1928), 259-278.
- [Sun94] Sun, H.; Mumby S. J.; Maple J. R.; Hagler A. T., *An ab initio Cff93 all-atom force fields for polycarbonates*, J. Amer. Chem. Soc., 116, (1994), 2978-2987.
- [Sun98] Sun, H., *Compass: An ab initio force field optimised for condensed phase applications-overview with details on alkane and benzene compounds*, J. Phys. Chem. B 102, (1998), 7338-7364.
- [Tak96] Takiguchi, Y.; Uematsu, M., *Densities for Liquid Ethanol in the Temperature Range from 310 to 363K at pressures up to 200MPa*, J. Chem. Thermodynamics, 28, (1996), 7-16.
- [Ulr90] Ulrich, J., *Kristallwachstumsgeschwindigkeiten bei der Kornkristallisation. Einflußgrößen und Meßtechniken*, Habilitationsschrift, Reihe Verfahrenstechnik, Verlag Shaker, Aachen, (1990).
- [Ver08] Verevkin, S. P.; Kozlova, S.A., *Di-hydroxybenzenes: Catechol, resorcinol, and hydroquinone Enthalpies of phase transitions revisited*, Thermochemica Acta, 471, (2008), 33-42, and references therein.
- [Wal80] Wallwork, S. C.; Powell, H. M., *The crystal structure of α form of quinol*, J. Chem. Soc. Perkin Trans.2, 188, (1980), 641-646.
- [Wan01] Wangnick, K.; Ulrich, J., *Experimentelle untersuchung zum einfluss von additives auf den habitus von benzophenon*, Chemische Technik, 52, (2001), 210-216.
- [Wil55] Wilke, C.R.; Chang, P., *Correlation of diffusion coefficients in dilute solutions*, AIChE Journal, 1, (1955), 264-270.
- [Win98] Winn, D.; Doherty, M.F., *A new technique for predicting the shape of solution-grown organic crystals*, AIChE Journal 44, (1998), 2501-2514.
- [Win00] Winn, D.; Doherty, M.F., *Modeling crystal shapes of organic materials grown from solution*, AIChE Journal, 46(7), (2000), 1348-1367.

- [Yür08] Yürüdü C; Jones, M. J.; Ulrich, J. (2008) *Determination of the effect of external environment on growth kinetics using molecular modelling – calculating diffusion coefficients*, proceedings, 17th International Symposium on Industrial Crystallization (ISIC), Eds: J.P. Jansens, J. Ulrich, Netherlands, 2008, Volume 1, 431-438.
- [Yür09] Yürüdü, C.; Jones, M. J.; Ulrich, J. (2010) *Modelling of diffusion for crystal growth*, in press, Soft Materials.

Selbständigkeitserklärung

Ich versichere hiermit ehrenwörtlich, dass ich die vorliegende Arbeit selbstständig und nur unter Benutzung der angegebenen Literatur und angefertigt habe. Die aus fremden Quellen direkt oder indirekt übernommenen Stellen sind als solche kenntlich gemacht und werden in der Arbeit aufgeführt.

Die Arbeit hat in gleicher oder ähnlicher Form noch keiner Prüfungsbehörde vorgelegen.

Halle (Saale), 01.06.2010

Caner Yürüdü

Lebenslauf

Persönliche Daten

Name: Caner Yürüdü
Geburtsdatum: 07.09.1979
Geburtsort: Karaman/Türkei
Nationalität: Türkisch
Familienstand: ledig
E-Mail: caneryurudu@gmail.com

Beruflicher Werdegang

März 2006 - Februar 2010
Martin-Luther-Universität Halle-Wittenberg,
Zentrum für Ingenieurwissenschaften,
Thermische Verfahrenstechnik /TVT
Wissenschaftlicher Mitarbeiter/Doktorand

Hochschulausbildung

März 2006 – Juli 2010
Martin-Luther-Universität Halle-Wittenberg
Zentrum für Ingenieurwissenschaften,
Thermische Verfahrenstechnik/TVT
PhD (Doctor of Philosophy)
Angenommen als Kandidat zum: Dr.-Ing.

September 2002 – Juni 2005
Istanbul Technical University, Istanbul, Türkei
Institute of Science and Technology of Istanbul
Technical University, Physical Engineering
MSc (Master of Science)

September 1997 – Juni 2002
Kocaeli University, Kocaeli, Türkei
Faculty of Science and Letters, Physics
BSc (Bachelor of Science)

Veröffentlichungen

- Yürüdü C., İsci S., Atici O., Ece Ö.I., Güngör N. “*Synthesis and Characterization of HDA/NaMMT Organoclay*” Bull. Mater. Sci., 28 (2005), 623-628.
- Yürüdü C., İsci S., Ünlü C., Atici O., Ece Ö. I., Güngör N. “*Preparation and Characterization of PVA/OMMT Composites*” J. Appl. Polym. Sci. 102 (2006), 2315–2323.
- Yürüdü C., Jones M. J., Ulrich J. “*Determination of the Effect of External Environment on Growth Kinetics Using Molecular Modelling–Calculating Diffusion Coefficients*” Proceedings (double refereed), 17th International Symposium on Industrial Crystallization (ISIC), Ed: J.P. Jansens–J. Ulrich, 14-17 September 2008, Maastricht, Niederlande.
- Kundin J., Yürüdü C., Ulrich J., Emmerich H., “*A Phase-Field/Monte-Carlo Model Describing Organic Crystal Growth from Solution*” The European Physical Journal B, 70 (2009), 403-412.
- Yürüdü C.; Jones M. J.; Ulrich J. “*Modelling of Diffusion for Crystal Growth*“ (in press, Soft Materials, 2010).
- Schmidt C.; Yürüdü C.; Wachsmuth A.; Ulrich J. “*Modelling the Morphology of Benzoic Acid Crystals Grown from Aqueous Solution*“ (submitted to CrystEngComm, 2010).

Vorträge

- Yürüdü C., İsci S., Günister E., Güngör N., “*Investigation of Rheology and Electrokinetic Properties of Hexadecylamine/Montmorillonite Organoclay*“ VIII. National fluid state symposium, Istanbul University, 24–26 September 2004, Istanbul, Türkei.
- Yürüdü C., Ünlü C. H., Atici O., Güngör N., Ece Ö. I., “*Characterization of HDTABr/NaMMT organoclay*“, 12. National Clay Symposium, Yüzüncü Yıl University, 5- 9 September 2005, Van, Türkei.
- Yürüdü C., Jones M. J., Ulrich J. “*Modelling Crystal Morphology under Consideration of the Growth Environment*” DFG Priority Program 1155- Molecular Modelling and Simulation in Process Engineering, 16-17 October 2006, Wien, Österreich.
- Yürüdü C. “*Morphological Calculations for Benzophenone under Consideration of the Growth Environment*“, FA-Sitzung “*Kristallisation*“, 29-30 March 2007, Nürnberg, Deutschland.
- Yürüdü C., Jones M. J., Ulrich J. “*Predicting Crystal Growth using Molecular Modelling Considering the Driving Force*” DFG Priority Program 1155- Molecular Modelling and Simulation in Process Engineering, 21-22 June 2007, Frankfurt, Deutschland.
- Yürüdü C., Ulrich J. “*Determination of the Effect of External Environments on Growth Kinetics Using Molecular Modeling-Calculating Diffusion Coefficients*” DFG Priority Program 1155- Molecular Modelling and Simulation in Process Engineering, 28-29 September 2009, Köln, Deutschland.
- Schmidt C.; Yürüdü C.; Ulrich J. “*What about water in modelling the morphology of crystals?*“ EFCE Working Party on Thermodynamics and Transport Properties, Molecular Modelling and Simulation for Industrial Applications: Physico-Chemical Properties and Processes, EFCE-Event No.687, 22-23 March 2010, Würzburg, Deutschland.